



**Defense University Center  
Spanish Naval Academy**

**FINAL YEAR PROJECT**

*State of the art analysis of Underwater Optical Communications  
and their applications in the military field*

**Mechanical Engineering Bachelor Degree**

**AUTHOR:** María del Rocío Porras de Sola

**SUPERVISOR:** Paula Gómez Pérez

**COURSE:** 2020-2021

**Universida<sub>de</sub>Vigo**





**Defense University Center  
Spanish Naval Academy**

**FINAL YEAR PROJECT**

*State of the art analysis of Underwater Optical Communications  
and their applications in the military field*

**Mechanical Engineering Bachelor Degree**

Naval Technology Specialization

Naval Branch

UniversidadeVigo





# **ABSTRACT**

Underwater optical wireless communication (UOWC) is a developing technology of great interest to the industry, scientific community and military, more specifically to the Navy, who has the operative task of Sea Control. Despite the astounding progress achieved in underwater acoustic communication, its small bandwidth strongly limits its transmission capacity in an era where the amount of information grows exponentially. Therefore, UOWC has attracted considerable attention in recent years, as it offers a much higher transmission bandwidth, thus providing greater data rate. However, UOWC is severely dependent on the properties of the underwater environment, the reason why they must be studied in depth.

This paper analyzes the state of the art of UOWC, providing an exhaustive research on the factors and phenomena affecting the underwater light propagation as well as its main challenges and recent technological advances. Afterwards, a simple UOWC prototype is designed to carry out assorted experiments in order to test the literature and draw meaningful conclusions. Finally, the application of this technology in the military field is discussed in terms of its feasibility, usefulness, main advantages and difficulties of its implementation, opening up a promising future for its development.

# **KEYWORDS**

UOWC, Attenuation, LASER, LED, Military Applications



# RESUMEN DEL TFG

## *Introducción*

Las comunicaciones ópticas submarinas engloban una serie de tecnologías en desarrollo de gran interés para la industria, la ciencia y el ámbito militar, y más concretamente para la Armada, debido a su responsabilidad en el ámbito marítimo. A pesar de los asombrosos avances logrados en este campo, su escaso ancho de banda limita en gran medida su capacidad de transmisión de datos, en una época en la que la cantidad de información a compartir aumenta vertiginosamente. El progreso de los últimos años en las comunicaciones ópticas submarinas trata de subsanar este inconveniente. Estos sistemas dependen en gran medida de las propiedades del entorno subacuático, por lo que deben ser estudiadas en profundidad.

Este trabajo de fin de grado analiza el estado del arte de las comunicaciones ópticas submarinas, sus principales retos y recientes avances tecnológicos, realizando un análisis exhaustivo sobre los factores que afectan a la propagación de la luz bajo el agua. Asimismo, y con el fin de poner a prueba la literatura y extraer conclusiones propias, se ha probado un prototipo sencillo con el que se han realizado diversos experimentos. Por último, se estudia la aplicación de esta tecnología en el ámbito militar en cuanto a su viabilidad, utilidad, principales ventajas y dificultades, abriendo un futuro prometedor para su desarrollo.

## *Análisis del estado del arte*

En este apartado se ha realizado un análisis profuso y detallado sobre la evolución, avances más recientes y principales factores que afectan a la comunicación óptica submarina. Actualmente, las crecientes preocupaciones de los países en materia de defensa y seguridad llevan intrínseco el control completo del mar, incluyendo el dominio submarino. Esto, sumado al crecimiento del número de vehículos submarinos no tripulados y dispositivos submarinos que requieren gran ancho de banda y capacidad, ha desencadenado la atracción científica y militar hacia el campo de las comunicaciones ópticas para la transferencia de información, disparando su desarrollo.

Existen tres sistemas de comunicaciones principales en el entorno submarino: las comunicaciones acústicas, de radiofrecuencia (RF) y las ópticas. Por un lado, las comunicaciones acústicas tienen el mayor alcance (aproximadamente 100 kilómetros) y el menor ancho de banda, mientras que por radiofrecuencia apenas llegan a 10 metros de cobertura, aunque consiguen una mayor velocidad y ancho de banda que las acústicas. Por otro lado, las comunicaciones ópticas tienen el ancho de banda más elevado y un alcance mayor que RF (200 metros en aguas claras), lo que supone una gran ventaja, ya que permite una tasa de transmisión muy superior. No obstante, su principal problema es el alto nivel en que se ven afectadas por el medio.

En este trabajo se analizan los principales factores que afectan a la propagación de la luz bajo el agua. Se describen, por tanto, los dos grupos distintos de propiedades ópticas del agua: las inherentes y las aparentes. Las propiedades ópticas inherentes son aquellas que dependen exclusivamente de la composición de la masa de agua, como el coeficiente de absorción o el de dispersión. Las propiedades aparentes también dependen la incidencia de luz externa, como por ejemplo la irradiación, la reflectancia o la radiancia. Ambos tipos de propiedades tienen sus propias ventajas a la hora de estudiar la propagación de la luz bajo el agua. Mientras que si se conoce el tipo y la composición exacta de la masa de agua se pueden calcular las propiedades ópticas inherentes en dicha masa de agua; en ocasiones es más sencillo medir las propiedades aparentes y calcular las concentraciones y composiciones del cuerpo de agua a partir de ellas.

Posteriormente se describen los principales fenómenos que afectan a la propagación de la luz en el agua, comenzando por la atenuación. La atenuación de la luz es la combinación de la absorción y la dispersión, propiedades indirectamente relacionadas, ya que un fotón absorbido no se dispersa. Ambas

propiedades ópticas son inherentes, por lo que dependen del tipo y la concentración de la materia presentes en el agua analizada. En general, esta materia se clasifica en cuatro categorías distintas en función de sus propiedades ópticas: moléculas de agua, fitoplancton, materia orgánica disuelta y partículas no algales. El nivel de atenuación de un determinado haz de luz depende del tipo y la concentración de estas materias, así como de la longitud de onda de dicho haz. Por lo tanto, la fuente de luz más adecuada dependerá del entorno específico de cada caso. Tras el análisis realizado, se ha observado que para aguas profundas las fuentes de luz azules y verdes son las más adecuadas, ya que son las longitudes de onda menos afectadas. Sin embargo, en aguas costeras, portuarias y poco profundas, se suelen concentrar mayores cantidades de partículas y las longitudes de onda más adecuadas corresponden a la zona verde-amarilla del espectro.

Dependiendo de la fuente de luz empleada, la alineación puede llegar a ser un factor determinante. Además, supone un reto para la aplicación de este tipo de comunicaciones, ya que tanto transmisor como receptor, o incluso ambos, podrían estar en movimiento. La dificultad de alineación depende de la apertura del ancho del haz, así como del área de recepción. Cuanto mayor sean ambos, más fácil será establecer en enlace. Por ello, un LED facilita la alineación en mayor medida que un LÁSER, debido a la mayor divergencia del haz del LED.

Este trabajo detalla igualmente los dos modelos matemáticos que permiten describir el canal óptico submarino, dependiendo de si existe alineación directa o no. Mientras que los canales en los que es posible la alineación directa se describen mediante la ley de Beer Lambert, los demás se encuentran modelados por la ecuación de transferencia radiactiva, cuya compleja resolución se suele realizar a partir del método de Monte Carlo.

Otro factor que afecta notablemente a las comunicaciones ópticas submarinas es la turbulencia, normalmente originada por corrientes, viento u otros factores imprevisibles. Se ha analizado cómo las turbulencias pueden provocar la ruptura e imposibilidad del enlace óptico submarino, además de aumentar la tasa de error de bit (BER). Por lo tanto, las aguas turbulentas suponen un reto significativo para el desarrollo de esta tecnología.

El índice de refracción es otro de los factores a tener en cuenta, ya que su variación provoca la refracción o reflexión de la luz. Estas variaciones están provocadas por cambios en la salinidad, densidad y temperatura, cuyos gradientes son mayores en zonas costeras. Tras investigar cómo varía el índice de refracción en función de estas propiedades y de la longitud de onda de la fuente de luz, se ha podido observar que no altera de forma significativa su propagación porque en las distancias comprendidas dentro del enlace, la masa de agua suele ser relativamente homogénea.

Al igual que en cualquier otra tecnología de comunicación, existe igualmente el ruido de fondo, en este caso, lumínico. Éste procede principalmente de la luz solar, que no penetra en el agua más de trescientos metros. Por tanto, a partir de dicha profundidad, el único ruido de fondo será el procedente de seres vivos bioluminiscentes o de otros sistemas de comunicación óptica submarina, por lo que, en estas situaciones, se podría considerar despreciable. Sin embargo, de día y en aguas poco profundas puede empeorar considerablemente el rendimiento de las comunicaciones ópticas submarinas, por lo que es un factor a tener en cuenta a la hora de diseñar el sistema de comunicaciones.

Por último, y debido a la complejidad del medio de propagación, a día de hoy sigue siendo complejo el modelado de un canal óptico submarino real, por lo que se sigue investigando en este ámbito. A pesar de ello, el gran ancho de banda y tasa de transmisión que puede proporcionar esta tecnología la hacen ofrecer un amplio horizonte de cara a su desarrollo e implementación en el día a día del entorno submarino.

## *Desarrollo y resultados*

Con el fin de poner a prueba los resultados teóricos recopilados de la literatura científica, se desarrolló un prototipo sencillo con el que llevar a cabo diferentes pruebas. El experimento consistió en

un pequeño tanque de agua ubicado en el medio de un enlace óptico básico conformado por una fuente de luz que transmite de forma continua la misma trama de datos, junto con un receptor elemental basado en una placa solar.

En primer lugar, se comparó la influencia de distintas fuentes de alimentación: LÁSER rojo y LEDs de distintas longitudes de onda (colores). Se demostró el resultado esperado con respecto a la alineación, siendo muchos más sencilla con el LED, gracias a la luz difusa emitida.

En cuanto a las longitudes de onda, probando con agua clara, todas las fuentes permitieron que el mensaje fuese recibido sin errores. Sin embargo, al añadir distintas partículas, se comprobó que las longitudes de onda en la zona verde y azul del espectro óptico son las que sufren menor atenuación. A la vista de estos resultados, se midió el efecto óptico de las distintas partículas estudiadas en las distintas longitudes de onda de la fuente. En agua pura se observó que las mayores longitudes de onda (correspondientes al color rojo) sufrían mayor atenuación.

Para analizar el efecto del fitoplancton se simularon las dos especies principales utilizando pigmentos azules y verdes. Con el LED y el LÁSER rojo la señal llegaba a atenuarse mucho más que con los LEDs verdes y azules, si bien el LÁSER rojo sufría menor atenuación que el LED del mismo color. Conforme se aumentaba la concentración de la pigmentación azul, el enlace con el LED verde comenzó a degradarse mucho más rápidamente que con el azul, que demostró ser el más adecuado para este caso. En cuanto a la simulación con la pigmentación verde, el LED verde resultó sufrir mucha menor atenuación que con concentraciones similares del azul.

Se simuló igualmente la concentración de partículas orgánicas disueltas mediante agua turbia con coloración marrón. La turbidez en este caso afectó notablemente a todas las fuentes de transmisión. Reduciendo la turbidez, pero manteniendo la coloración marrón, la única fuente que permitió recibir señal en el receptor fue el LÁSER rojo. Aún así, la señal recibida era muy inferior a la necesaria para realizar la detección de señales binarias, por lo que el enlace no llegó a establecerse. Se demostró por tanto, la sensibilidad de esta tecnología a la turbidez del agua.

Las partículas no algales fueron simuladas con partículas en suspensión (esta vez de color claro), que, al no disolverse fácilmente, quedaron gran parte en suspensión. Todas las fuentes de luz fueron atenuadas en gran medida. Se comprobó su efecto con un LED blanco de alta luminosidad, que no fue suficiente como para recibir el mensaje correctamente. La señal del LED verde fue la que sufrió menor atenuación, y al igual que el LED y el LÁSER rojo permitió la recepción del mensaje. En esta prueba el LÁSER y el LED rojo tuvieron un comportamiento similar.

Como conclusión, se demuestra la elevada dependencia del medio, tanto en su composición como en su concentración, así como la influencia de las distintas longitudes de onda de la fuente.

Se comprobó el efecto de las turbulencias generando corrientes de agua en el tanque, comprobando que éstas aumentaban en gran medida la BER en recepción. Se corrobora así el elevado efecto que tienen las turbulencias en este tipo de comunicaciones, pudiendo llegar a anularlas.

Se hizo un estudio sobre la influencia de la temperatura, cambiando el agua del tanque por fría y caliente. Los resultados fueron similares en ambos casos, como era de esperar. Esto es debido a que lo que varía la propagación es el cambio en el índice de refracción (un gradiente de temperatura) y por lo tanto, un cambio de temperatura en la masa completa de agua no tiene efectos apreciables en la propagación.

Por último, se probó el sistema en la dársena de la Escuela Naval Militar (a 10 cm bajo el agua). De día, el elevado ruido de fondo debido a la luz solar no permitió el establecimiento del enlace. De noche, el mensaje se recibió a una distancia de medio metro, pero con una BER elevada debido a las turbulencias del agua superficial, demostrando estas de nuevo su gran efecto en este tipo de comunicaciones. Dado que las turbulencias son mayores en la capa superficial, el prototipo debería de tener mejor funcionamiento a mayor profundidad, donde, además, el ruido ambiente será menor.

Sin embargo, es importante el conocimiento del canal, pues el agua de la dársena aumenta su turbidez con la profundidad debida al lodo del fondo. Una prueba más exhaustiva requeriría un transmisor y un receptor más sofisticados, que queda fuera del ámbito de este trabajo, pero que se propone en las líneas futuras del mismo.

## *Aplicaciones militares*

Las aplicaciones militares de las comunicaciones ópticas submarinas son amplias y variadas, a pesar de que la mayoría de los avances realizados en este campo son clasificados. No obstante, el hecho de que hace décadas se estableciera un enlace LÁSER entre un submarino sumergido y un satélite, además del conocimiento sobre el desarrollo de redes de sensores submarinas por parte de algunos países, son razones suficientes para considerar que este tipo de comunicaciones puede proporcionar mayor operatividad y capacidad estratégica al entorno militar. En este sentido, los campos en los que se ha considerado la implantación de las comunicaciones ópticas submarinas son el buceo, los vehículos submarinos no tripulados (UUV, *Unmanned Underwater Vehicle*), las redes de sensores submarinas, la guerra submarina y la guerra de minas.

En cuanto a la aplicación en buceadores, se llevó a cabo una encuesta a treinta y cuatro buceadores de la Armada española, de todas las escalas e incluyendo a miembros de la Fuerza de Guerra Naval Especial (FGNE). La gran mayoría de los buceadores normalmente se comunica mediante lenguaje de signos o linterna, y esta comunicación normalmente es de buceador a buceador. Es más, sólo cuatro buceadores de los encuestados utilizan habitualmente sistemas inalámbricos. Las operaciones más habituales para estos buceadores son las búsquedas, rescates y reconocimientos de cascos, exceptuando a los de la FGNE, que suelen realizar incursiones nocturnas. Se les preguntó si alguna vez habían echado de menos estar comunicados durante el tiempo de inmersión y la utilidad de aplicar un sistema de comunicaciones ópticas en su día a día y la gran mayoría respondió que sí, valorando de forma muy positiva la posible implantación de estos sistemas en sus operaciones. De los buceadores encuestados, dos de ellos habían probado sistemas de comunicaciones ópticas, y estos valoraron su utilidad por encima de la media, respondiendo uno de ellos que los aplicaría en todo tipo de operaciones.

Por otro lado, en la Estrategia de Tecnología e Innovación para la Defensa (ETID) 2020 se marcan las metas tecnológicas en el ámbito de la defensa de España, en un marco de 2020-2027. Entre estas metas se encuentra la investigación y desarrollo de los sistemas de comunicaciones ópticas submarinas, así como la creación de una red de sensores submarina. Es por ello que también se considera una de las aplicaciones más realistas de esta tecnología, cuyo funcionamiento óptimo según lo estudiado correspondería a una red híbrida que combinase el mayor alcance de la tecnología acústica con el mayor ancho de banda de la óptica.

Además, es interesante el estudio de las comunicaciones por LÁSER entre un submarino y un satélite, sobre todo cuando se integren los sistemas *Air-Independent-Propulsion* (AIP) en los futuros S-80, de tal manera que puedan pasar mayor tiempo sumergidos pero con comunicaciones disponibles en todo momento.

Otra aplicación atractiva para esta tecnología son los UUVs. Se han estudiado los distintos UUVs de los que dispone la Armada Española. De entre ellos, la aplicación más útil y viable de esta tecnología son los UUVs del buque de salvamento *Neptuno*, ya que se podría retransmitir un vídeo en directo a lo largo de la búsqueda. Cuando se disponga de las redes de vigilancia submarina, sería asimismo una buena aplicación para interconectar los UUVs, submarinos, buceadores y sensores submarinos, mejorando el mando y control y facilitando la toma de decisiones.

En conclusión, se considera que las aplicaciones más factibles y útiles son el buceo y una red de sensores submarina híbrida, que además de proporcionar vigilancia submarina intercomunique a buzos, UUVs, submarinos y satélites.

## *Conclusiones y líneas futuras*

Como conclusión final, este trabajo de fin de grado ha cumplido con creces sus objetivos iniciales. No sólo ha analizado el estado del arte de las comunicaciones ópticas submarinas y sus aplicaciones en el ámbito militar, sino que también ha comprobado las aseveraciones científicas con un sistema real.

En continuidad con este proyecto y ampliándolo, se propone estudiar su viabilidad de un un prototipo más sofisticado para probarlo en aguas portuarias y costeras a diferentes profundidades. En referencia a los objetivos a largo plazo, se propone implementar los sistemas de comunicaciones ópticas submarinas en las fuerzas armadas españolas, donde pueden aportar una gran ventaja estratégica, tal y como se ha visto a lo largo del presente trabajo.





# ACKNOWLEDGMENTS

First, I would like to thank my tutor, Prof. Dr. Paula Gómez Pérez, for all the work and time dedicated to the completion of this work, her help in the laboratory tests, as well as her advice and organization, marking the necessary times to achieve an efficient development of the work. Another special gratitude goes to the Spanish Naval Academy and the Defense University Center for these five years of teaching, instruction and training.

Following, I am grateful to all the people who have helped me in the development of this project as well. To LCDR Rivas Calvar, for helping me in the communications and naval field, and for awakening in me the interest in the underwater environment. To each of the forty-four surveyed divers, especially to the commander of the B.S.R. Neptuno, LCDR Gutiérrez Albert, for his shared opinion on the current interest of this project subject; to my Brigade Commander, LT Mendoza Fernández-Aceytuno, for making the survey known, as well as LT Gallego Casasola; to the LT Rivera Dodero, for his vision on broad experience on the applications of this technology; to LT Llanos Hervella and LTJG Cabello Portela, for all the help and information they have provided me in the field of diver communications. To LT Williams and LT Hue, for the information and research carried out on the current applications of this technology in their countries, the United States and France respectively. To LTJG García Romero, for his insight into the communication systems of the future S-80 submarine. To the companies that have shed some light on the subject with their answers: the Spanish System of Observation and Technological Prospective, SAES, SENER and the Spanish communications company specialized in Defense and Security IDS.

Furthermore, I want to thank Eli for helping me with the night tests in the harbor waters; and to my entire studio: Elena, Ida, Cristina and María; for their cheerfulness and company, making the hours dedicated to this project much more enjoyable.

I would really like to thank my fiancé, Álvaro, for all the support received throughout the realization of this project, these five years of career and for the rest of our lives. Likewise, I am very grateful to my parents, Rocío and Antonio, for the education they have given me and for always supporting me in my decisions, to my grandmother Amparo, for her pleasant daily calls. To each of my siblings, Juan Antonio, Almudena and Santiago, for the privilege of always having them there for me. To the rest of my family, uncles, aunts, cousins, and especially my grandmother Julia and my aunt Maricarmen who have been watching over us from Heaven for a short time. And to all my friends, both those I see daily at the Academy and those who make important efforts to maintain our friendship in spite of the distance.

Last but not least, to Nuestra Señora del Carmen, Our Lady of Mount Carmel, patroness of the Navy and all seafarers, our guiding light who takes us by the hand throughout our lives and will always continue doing so until we reach our Final Port.



## INDEX OF CONTENTS

Index of Contents .....	1
Figure Index .....	5
Table Index.....	11
Acronyms .....	13
1 Introduction and Objectives .....	15
1.1 Introduction.....	15
1.2 Final Degree Project motivation .....	15
1.3 Objectives.....	16
1.4 Memory structure.....	16
2 State of the Art .....	17
2.1 Introduction.....	17
2.1.1 History.....	20
2.2 Underwater wireless communication overview .....	26
2.2.1 RF.....	26
2.2.2 Acoustic .....	28
2.2.3 Optical UWC overview.....	29
2.3 Factors that affect UOWC.....	30
2.3.1 Optical properties of the water.....	30
2.3.1.1 Inherent Optical Properties (IOPs) .....	30
2.3.1.2 Apparent Optical Properties (AOPs) .....	32
2.3.2 Absorption.....	32
2.3.2.1 Water molecules .....	33
2.3.2.2 Phytoplankton .....	34
2.3.2.3 Colored Dissolved Organic Matter .....	37
2.3.2.4 Non-algae particles .....	39
2.3.2.5 Summary.....	41
2.3.3 Scattering .....	43
2.3.3.1 Pure sea water .....	45
2.3.3.2 Phytoplankton .....	47
2.3.3.3 Colored Dissolved Organic Matter .....	49
2.3.3.4 Non-algae particles .....	49
2.3.3.5 Summary.....	51
2.3.4 Spectral beam attenuation .....	53
2.3.5 Beam divergence.....	53

2.3.6	Turbulence .....	54
2.3.7	Turbidity.....	55
2.3.8	Alignment.....	56
2.3.9	Refractive Index Variability.....	61
2.3.10	Background noise.....	65
2.3.11	Radiance.....	65
2.4	Water classification according to its different optical properties. ....	67
3	Benchmarks and Results .....	71
3.1	Simple UOWC prototype.....	71
3.1.1	Light sources under test .....	73
3.1.2	Light sensor under test .....	76
3.2	Experimental setup.....	77
3.2.1	Red LASER without water tank-Free Space Measurement.....	79
3.2.2	Green LED without water tank - Free Space Measurement .....	79
3.2.3	Green LED with water tank (14°C).....	80
3.2.4	Green LED with hot water tank (56°C).....	81
3.2.5	Green LED with blue colored water (2 drops of blue ink) .....	81
3.2.6	Green LED with blue colored water (8 drops of blue ink) .....	82
3.2.7	Green LED with green colored water .....	83
3.2.8	Blue LED with green colored water .....	85
3.2.9	Red LED with green colored water.....	85
3.2.10	Red LASER with green colored water.....	86
3.2.11	Red LASER with green colored water.....	86
3.2.12	Green LED with green colored water .....	87
3.2.13	Blue LED with blue colored water .....	88
3.2.14	Red LASER with water with brown CDOM .....	90
3.2.15	Red LED with water with brown CDOM .....	90
3.2.16	White LED with tap water .....	91
3.2.17	White LED and water with NAP .....	91
3.2.18	Green LED and water with NAP .....	92
3.2.19	Red LASER and water with NAP.....	92
3.2.20	Red LED and water with NAP.....	92
3.2.21	Green LED in harbor waters .....	93
4	Military Applications .....	95
4.1.1	Divers .....	96
4.1.2	Underwater Wireless Sensor Network (UWSN) .....	102

4.1.3	Unmanned Underwater Vehicles (UUVs) .....	104
4.1.4	Submarine Warfare (SW).....	107
4.1.5	Mine Warfare (MW) .....	108
5	Conclusions and Future Developments.....	111
5.1	Conclusions.....	111
5.1.1	Analysis of the state of the art.....	111
5.1.2	IOPs and AOPs .....	111
5.1.3	Underwater light attenuation.....	111
5.1.4	Alignment.....	112
5.1.5	Channel modeling .....	112
5.1.6	Turbulence .....	112
5.1.7	Refractive index effect on underwater propagation.....	112
5.1.8	Background noise.....	112
5.1.9	Prototype design.....	112
5.1.10	Military applications .....	113
5.1.11	Final conclusion .....	113
5.2	Future developments .....	113
5.2.1	Short term.....	113
5.2.2	Long term.....	114
6	References.....	115
	Appendix I: 3D Models .....	127



## FIGURE INDEX

Figure 2-1 Optical visible region of the electromagnetic spectrum [11].	17
Figure 2-2 Simplified example of Optical communication [15].	18
Figure 2-3 Different applications of FSOC according to its range (on a logarithmic scale).	18
Figure 2-4 Submarine cable map [17].	19
Figure 2-5 Greek warriors using beacons [21]. Greeks constructed in 1084 B.C. a 500-km-long line of fire beacons to convey the news of the fall of Troya.	20
Figure 2-6 Flags approved by the Ring Carlos III. On the left, the flag and pennant to be used by warships. On the right, the flag to be used by merchant ships [23].	20
Figure 2-7 Claude Chappe, his coding scheme, and the mechanical device used for making optical telegraphs (licensed under Public Domain via [15]).	21
Figure 2-8 Telegraph prototype [22].	21
Figure 2-9 Henry Mance next to the heliograph prototype (left) [12] and two field heliographs (right) [24].	22
Figure 2-10 Photophone transmitter [26].	22
Figure 2-11 Increase in the BL product during the period 1840–2015. The emergence of new technologies is marked by red squares. Dashed line shows the trend as an aid for the eye. Notice the change in slope around 1977 when optical fibers were first used for optical [15].	23
Figure 2-12 Remarkable historical progresses of UOWC [28].	23
Figure 2-13 Seawater absorption coefficient depending on wavelength. It is shown how blue and green light experience the least absorption in seawater [27].	24
Figure 2-14 Satellite line-of-sight radio and optical propagation [31].	24
Figure 2-15 The BlueComm High Ambient Light (left) and Long Range (right). BlueComm UOWC can achieve 20 Mbps underwater data transmission with a range of 200m [34].	25
Figure 2-16 UOWC in an UWSN with UAVs, divers and submarine.	26
Figure 2-17 RF attenuation in seawater [51].	27
Figure 2-18 Possible multi-path propagation of a RF signal in shallow water [52].	28
Figure 2-19 Different underwater sound propagation paths. The graphic on the left represents the ray trace modeling of underwater sound propagation speed [54].	29
Figure 2-20 Relationship between IOPs and AOPs in Ocean Optics.	31
Figure 2-21 Geometric model for inherent optical properties.	31
Figure 2-22 The three vibrational modes of the water molecule: (a) symmetric stretch, (b) bend and (c) asymmetric stretch [60].	33
Figure 2-23 Absorption spectrum of pure water. It can be seen that peaks in the absorption spectrum correspond to the fundamental frequencies and higher harmonics of the vibration of water molecules [60].	34
Figure 2-24 Absorption coefficient due to pure water as a function of water temperature (°C) for light propagation under water in the visible spectrum [42].	34

Figure 2-25 These two satellite images from NASA images show a phytoplankton bloom that formed east of New Zealand in a fortnight in 2009 [61].	35
Figure 2-26 (a) Absorption spectra for a range of different pigment composition. The difference in the absorption coefficients of diatoms grown in high light compared to those grown in low light can be noted. (b) Generic phytoplankton absorption spectrum for a mixed algae composition [42].	35
Figure 2-27 The absorption spectra major groups of phytoplankton pigments [64].	36
Figure 2-28 Irradiance and absorption of different species of phytoplankton depending of light wavelength. The phytoplankton community was sampled at (g) 120 m depth, in the subtropical Pacific Ocean dominated by low-light adapted <i>Prochlorococcus</i> , (h) 12 m depth in the Baltic Sea, dominated by red-colored <i>Synechococcus</i> strains (i) 75 cm depth in Lake Groote Moost, dominated by green cyanobacteria and green algae [60].	37
Figure 2-29 Sea model-derived CDOM absorption map for 18 October 2005, at 1900 h UT [66].	37
Figure 2-30 Different colors of water depending on ‘gilvin’ concentration. It can be seen how, as turbidity increases, the color of water shifts from blue, via green, towards brownish red [60].	38
Figure 2-31 Map indicating the six sites where absorption properties of CDOM were sampled: LV = Lake Victoria, Uganda; LN = Lake Namtso, Tibet; BS = Bohai Sea, China; SF = Samnangerfjord, Norway, LF = Lysefjord, Norway; RCW = Røst Coastal Water, Norway [67].	38
Figure 2-32 (a) Plots of CDOM absorption spectra for different locations (b) Semi-log plots of the CDOM absorption spectra in (a) [67].	39
Figure 2-33 Generic absorption spectrum of colored dissolved organic matter (CDOM) for mixed composition [42].	39
Figure 2-34 Mass-specific absorption coefficients $a^*(\lambda)$ for four types of mineral. Measured data obtained from [68].	40
Figure 2-35 Absorption spectrum of non-algae particles [58].	40
Figure 2-36 Result of the measurement of the absorption spectrum of non-algae particles in different spots of the artificial Lake Qiandaohu [70]. In can be observed how it follows a seasonal pattern.	41
Figure 2-37 Geometry for defining the volume scattering function. “ $\Phi_i(\lambda)$ ” is the incident power into an area “ $\Delta A$ ”; $\Delta\Phi_a(\lambda)$ is the absorbed power in distance “ $\Delta r$ ”, “ $\Delta 2\Phi_s(\psi, \lambda)$ ” is the power scattered into the annular ring of solid angle “ $\Delta\Omega$ ”. “ $\Delta\Phi_t(\lambda)$ ” is the transmitted power [58].	43
Figure 2-38 Hydrothermal vent. It is an opening on the seafloor that emits hot, mineral-rich solutions. The reason the image blurry in the marked area is because of the scattering induced by temperature fluctuations [73].	44
Figure 2-39 Scattering coefficient of seawater as a function of salinity calculated at 546 nm and 20°C, which is a contribution of two factors: density and concentration fluctuation. The empirical variation is calculated with an equation based on the interpretation of several measurement experiments [74].	45
Figure 2-40 Comparison of Morel model [75] and Zhang [74] pure water scattering coefficient model with experimental data measured in [75].	45
Figure 2-41 (a) The Raman emission functions for four excitation wavelengths [58] and (b) the corresponding wavelengths for the colors of the visible light spectrum.	46
Figure 2-42 Absorption vs. Scattering because of pure seawater [76].	46
Figure 2-43 Results of (A) phytoplankton and (B) non-algae particles scattering coefficients measured in Lake Taihu. Their spectral curves can be compered, and it is clearly shown how the effect of NAP on scattering is remarkably greater than the one corresponding to phytoplankton [82].	47



Figure 2-44 VSFs for the four species of phytoplankton investigated at four different wavelengths in [78]. In order to make the plots of the VSFs distinguishable for each different wavelengths, they have been multiplied by the constant factors of 1000, 100, 10, and 1. ....	48
Figure 2-45 Scattering by different phytoplankton species in comparison with the San-Diego Harbor VSF of [84]. Data from [77] and plots from [58]. ....	49
Figure 2-46 Scattering coefficient spectra from Great Lake (Taihu), China [75]. Data from [82]. ....	50
Figure 2-47 Mass-specific scattering coefficients $b^*(\lambda)$ for four types of mineral. Measured data obtained from [68]. ....	50
Figure 2-48 (a) Measured mass-specific scattering coefficients “ $b^*(\lambda)$ ” of particles for samples of mixed particulate assemblages (top and middle graph) and single-mineral species (bottom graph) and (b) their description, origin, suspended particulate matter (SPM) and particulate organic carbon (POC) [88]. ...	51
Figure 2-49 Beam divergence with a LASER as a light source [91]. ....	53
Figure 2-50 (a) A LASER beam and (b) a LED beam [92]. ....	54
Figure 2-51 VSF measured with turbulence the 26 and 30 of July, and without turbulence the 28 of July [94]. ....	54
Figure 2-52 Capture of an oscilloscope display video in which the water in the tank was turbulent. It can be seen how the received signal is fluctuating and unstable. ....	55
Figure 2-53 (a) Attenuation curve and (b) simulated optical power as a function of the link distance at different values of water turbidity. In (b), the sensitivity is indicated by the straight gray line [33]. ....	55
Figure 2-54 Different direct LOS link configurations: (a) point-to-point, (b) diffuse and (c) boundary [97]. ....	57
Figure 2-55 NLOS link configuration [72]. ....	58
Figure 2-56 (a) Multipath interference in a network in which relay nodes are the blue dots and (b) a plot of the received amplitude of a signal with ISI. ....	59
Figure 2-57 (a) Waveform received at 1 Gb/s at 30m (top) and 50 m (bottom) and (b) waveform received at 100 Mb/s at 30 m (top) and 50 m (bottom) [102]. ....	60
Figure 2-58 Modulating retro-reflector configuration [57]. ....	61
Figure 2-59 (a) Light refraction following Snell’s Law and (b) an example of refractive index variation with depth of an ocean with low turbidity [107]. ....	62
Figure 2-60 Global map of average surface seawater salinity [108]. ....	63
Figure 2-61 Global map of average surface seawater temperature [108]. ....	63
Figure 2-62 Global map of average surface seawater density [108]. ....	64
Figure 2-63 The refractive index as a function of: (a) temperature, (b) salinity and (c) pressure, for different transmission wavelengths in seawater [107]. ....	64
Figure 2-64 Geometry of (a) extended and (b) point source relative to the receiver [57]. ....	65
Figure 2-65 The conceptual process involved in solving (a) the forward radiative transfer problem and (b) remote-sensing inverse radiative transfer problem. ....	66
Figure 2-66 Contributions to the total upwelling radiance above the sea surface [58]. ....	66
Figure 2-67 (a) Diagram of the five layers of the ocean [118] and (b) their characteristics [117]. ....	68
Figure 2-68 Schematic diagram of a vertical layered environment in the ocean [28]. ....	69

Figure 2-69 (a) Typical seawater temperature profile with increasing depth [117] and (b) light penetration across different depths [120].	69
Figure 3-1 Simplified block diagram of the initial prototype.	71
Figure 3-2 Solar panel output current measurement. (a) shows the position of the oscilloscope cables, and (b) the oscilloscope display. The measurement of the output current was 100 mV.	72
Figure 3-3 Operational Amplifier designed with PSIM.	73
Figure 3-4 Optical beam (a) expander and (b) reducer result in different scattering angles result in different beam divergences [42].	74
Figure 3-5 OOK modulation. Logic levels are shown on the top chart, and the transmitted signal is shown on the bottom chart [124].	76
Figure 3-6 Schematic representation of a solar cell. The n-type and p-type layers –the filaments- are shown, with a close-up view of the depletion zone, as well as the electron flow, once they are excited by incident light.	76
Figure 3-7 Different solar cells available at the laboratory. (a) and (b) are small solar cells, while (c) is a bigger one [12].	77
Figure 3-8 Setup for case 1 that shows the distance between the LASER and the solar panel.	78
Figure 3-9 Case 1 oscilloscope display. The yellow signal is measured at the transmitter signal and the green one at the receiver.	79
Figure 3-10 Case 2 (a) setup and (b) illumination of the solar panel by the diffuse light of the green LED.	79
Figure 3-11 Case 2 oscilloscope display.	80
Figure 3-12 (a) Setup for Case 3 and (b) temperature measurement with thermal camera (FLIR).	80
Figure 3-13 Case 3 oscilloscope display.	81
Figure 3-14 Measurement of water temperature in case 5.	81
Figure 3-15 Different perspectives of Case 5: (a) plant view and (b) side view.	82
Figure 3-16 Water tank with turbulence affects UOWC.	82
Figure 3-17 (a) blue ink drops being added and (b) final aspect of the water tank.	83
Figure 3-18 Case 6 oscilloscope display.	83
Figure 3-19 (a) Case 7.1 consists of a green LED with green colored water (2 drops of ink) and (b) its oscilloscope display.	84
Figure 3-20 Different perspectives of 7.2: (a) plant view and (b) side view.	84
Figure 3-21 Case 7.2 oscilloscope display.	84
Figure 3-22 (a) Setup and (b) oscilloscope display for case 8.	85
Figure 3-23 (a) Red LED with a green colored water tank and (b) the oscilloscope display for case 9, which shows that it is not received the LED signal.	85
Figure 3-24 (a) Red LASER with a green colored water tank and (b) the oscilloscope display for case 10.	86
Figure 3-25 Oscilloscope signal display for case 12.	86
Figure 3-26 Green LED tested in green colored water tank dyed with (a) 19, (c) 40, (e) 50 drops of green ink and their respective oscilloscope displays (b),(d) and (f).	87

Figure 3-27 Relationship between the amplitude of the received signal and the increase of ink drops in the green colored water (simulating CDOM). .....	88
Figure 3-28 Picture of the colored water body for different tests and their corresponding oscilloscope display for (a)(b) 2 drops of blue water, (c)(d) 6 drops of blue water and (e)(f) 16 drops of blue ink...88	88
Figure 3-29 Relationship between the amplitude of the received signal and the increase of ink drops in the blue colored water (simulating plankton). .....	89
Figure 3-30 Capture of an oscilloscope display video in which the water in the tank was turbulent. It can be seen how the received signal is fluctuating and unstable. ....	89
Figure 3-31 Water with Brown CDOM and (a) the red LASER and (b) the blue LED. (c) Water body with brown CDOM once in was diluted more. ....	90
Figure 3-32 (a) Red LASER tested with a brown colored water tank and (b) its oscilloscope display..	90
Figure 3-33 (a) Red LED tested with a brown colored water tank and (b) its oscilloscope display. ....	91
Figure 3-34 (a) White LED tested with tap water and (b) its oscilloscope display. ....	91
Figure 3-35 (a) White LED tested in water with white suspension particles and (b) its oscilloscope display. ....	91
Figure 3-36 (a) Green LED tested in water with white suspension particles and (b) its oscilloscope display. ....	92
Figure 3-37 (a) Red LASER tested in water with white suspension particles and (b) its oscilloscope display. ....	92
Figure 3-38 (a) Red LED tested in water with white suspension particles and its oscilloscope display (b) at first and (c) after having been stirred. ....	93
Figure 3-39 Measurement of the maximum range of the prototype teste as a free space system.....	93
Figure 3-1 The prototype being tested in harbor water during the night. ....	94
Figure 4-1 Different applications of UOWC in the military field. ....	95
Figure 4-2 (a) Diving formation of questioned divers and the (b) types of operations they have carried out.....	96
Figure 4-3 (a) Diving communications systems used at least once by the 34 surveyed divers and (b) the most used one for each of the divers.....	97
Figure 4-4 Examples of some communication systems among divers: (a) diving optical manual signals, (b) diver's communication via cable ("umbilical") and example of Acoustic Wireless System, (c) PowerCom 5000D, a Wireless RF system [9] and (d) LUMA X and LUMA 500ER modems from Hydromea, an UOWC system [130]. ....	98
Figure 4-5 Most common diving waters of surveyed divers. ....	99
Figure 4-6 Divers opinion on their most important communication requirements based on different operations. ....	99
Figure 4-7 Most common communication links among surveyed divers. ....	100
Figure 4-8 Diving fields in which UOWC would be more useful according to surveyed divers. ....	100
Figure 4-9 Aqua-Fi would use radio waves to send data from diver's smart phone to a "gateway" device attached to their gear, which would send the data via light beam to a computer at the surface that is connected to the Internet via satellite [127]. ....	101

Figure 4-10 Comparison between Acoustic, optical and hybrid links, regarding their (a) throughput as a function of offered load and (b) energy consumption with varying data size [138].....	103
Figure 4-11 An underwater wireless sensor network with aerospace and terrestrial communication [27]. .....	104
Figure 4-12 (a) An AUV operating in UOWC network scenario [140] and (b) The U.S. Navy's first extra-large UUV, the Boeing Orca [144]. ....	105
Figure 4-13 Different UUVs at the Spanish Navy: (a) Minesniper, (b) Pluto PLUS [149], (c) Scorpio [150] and (d) Navajo [151]. ....	106
Figure 4-14 UUV serving as a data mule to collecting data from seafloor platforms by UWOC [93]. .....	107
Figure 4-15 (a) Interface between submarine, UUV, and data nodes [155] and (b) Echo Voyager and Orca XLUUV [156]. ....	108
Figure 4-16 Mine Detection with a UOWC system [157]. ....	108
Figure A1-1 Two different supporters, those on the front side were printed throughout this Final Project, while the ones at the back are from [12]. ....	127
Figure A1-2 (a) Both transmitter mounts and (b) both receivers mounts. The new one is the shortest in both cases. ....	127
Figure A1-3 (a) General 3D view and (b) (c) (d) different perspectives of the designed transmitter holder. .....	128
Figure A1-4 (a) General 3D view and (b) (c) (d) different perspectives of the designed receiver holder. .....	129

## TABLE INDEX

Table 2-1 Advantages (top) and disadvantages (bottom) of FSOC, fiber-optic communications and UOWC. ....	19
Table 2-2 Remarkable experimental results for UOWC systems since 2016.....	25
Table 2-3 Comparison of underwater wireless communication technologies (with color code for comparison).....	27
Table 2-4 Ideal transmission wavelength for different water types under general conditions [57].....	41
Table 2-5 Summary of absorption characteristics of seawater. Absorption spectra has different scales depending on how much and which wavelengths absorption affects. ....	42
Table 2-6 Cell size “r” is the mean radius and “std” is the standard deviation of the radius), concentration, shape and composition of phytoplankton species investigated in [78]. ....	48
Table 2-7 Summary of scattering characteristics of seawater. Scattering spectra has different scales depending on how much and where it affects absorption. ....	52
Table 2-8 Summary of the causes and consequences of turbulence and turbidity. ....	56
Table 2-9 LOS and NLOS characteristics and channel modeling techniques. ....	61
Table 2-10 General classification of water and the typical values of chlorophyll concentration “C”, absorption “a( $\lambda$ )”, total scattering “b( $\lambda$ )” and spectral beam attenuation “c( $\lambda$ )” for each type.....	67
Table 3-1 Comparison between optical sources for UOWC.....	74
Table 3-2 Wavelengths of the light sources used for the prototype.....	75
Table 3-3 Specifications of HLM1230 5mW red LASER module [123]. ....	75
Table 3-4 Specifications of the chosen solar panel.....	77
Table 3-5 Summary of all different cases and their corresponding light source and water tank. ....	78
Table 4-1 Advantages and disadvantages of the implementation of UOWC systems.....	102
Table 4-2 Advantages and difficulties of the implementation of an UOWC system in UUVs according to its most common missions. ....	106



## ACRONYMS

AIP	Air-Independent-Propulsion
AJEMA	Almirante Jefe del Estado Mayor de la Armada (Chief of Staff of the Navy)
AOP	Apparent Optical Properties
ARQ	Automatic Repeat Request
ASK	Amplitude-Shift Keying
ASW	Anti-Submarine Warfare
AUV	Autonomous Underwater Vehicle
BAM-IS	Buque de Acción Marítima e Intervención Subacuática
BER	Bit Error Rate
BL	Beer Lambert
C2	Command and Control
CDOM	Colored Dissolved Organic Matter
ELF	Extremely Low Frequency
EOD	Explosive Ordnance Disposal
ETID	Estrategia de Tecnología e Innovación para la Defensa
FDP	Final Degree Project
FEC	Forward Error Connection
FGNE	Fuerza de Guerra Naval Especial (Special Naval Warfare Forces)
FLIR	Forward-Looking Infrared
FOC	Field Of View
FSOC	Free Space Optical Communication
GNE	Guerra Naval Especial (Special Naval Warfare)
ID	Identifier
IOP	Inherent Optical Properties
IoUT	Internet of Underwater Things
IR	Infrared
ISI	InterSymbol Interference
JEMAD	Jefe del Estado Mayor de la Defensa (Chief of Defense Staff)
LASER	Light Amplification by Stimulated Emission of Radiation
LD	Laser Diode
LED	Light Emitting Diode
LOS	Line Of Sight
LT	Lieutenant
LCDR	Lieutenant Commander
LTJG	Lieutenant Junior Grade

MW	Mine Warfare
MCM	Mine Counter Measures
NAP	Non Algae Particles
NLOS	Non-Line-Of-Sight
OA	Operational Amplifier
OAP	Optical Access Point
OA-UWSN	Optical-Acoustic Underwater Wireless Sensor Network
OOK	On-Off-Keying
POC	Particulate Organic Carbon
SAES	Specialists in Underwater Acoustics and Electronics
SAR	Search and Rescue
RF	Radio Frequency
ROV	Remotely Operated Vehicle
RSD	Research Skills and Development
R&D	Research and Development
RTE	Radiative Transfer Equation
SLD	Superluminescent Diode
SNR	Signal to Noise Ratio
SONAR	Sound Navigation and Ranging
SOSUS	Sound Surveillance System
SPM	Suspended Particulate Matter
SSK	Space Shifting Key
UAV	Unmanned Aerial Vehicle
UHF	Ultra High Frequency
UOWC	Underwater Optical Communication
USS	United States Ship
UT	Universal Time
UUV	Unmanned Underwater Vehicle
UWSN	Underwater Wireless Sensor Network
VCSEL	Vertical-Cavity Surface Emitting LASER
VHF	Very High Frequency
VLf	Very Low Frequency
VSF	Volume Scattering Function
XLUUV	Extra Large Unmanned Underwater Vehicle
WWI	World War I
WWII	World War II



# 1 INTRODUCTION AND OBJECTIVES

## 1.1 Introduction

The world is undergoing a major technology transformation. This transformation, also known as the 4th industrial revolution, is characterized by sophisticated software systems and sensors, powerful processors and novel telecommunication technologies [1]. The management of much larger amounts of information besides the need of having permanent instant access to it have motivated a research on more efficient means of transferring data, such as optical communication.

Compared to other technologies, optical communication provides a reliable, fast and high transmission bandwidth communication with a low power consumption. Nowadays, instant information can be shared thanks to a massive global network of fiber optic cables laying deep under the oceans [2]. Having said so, the study of *Underwater Optical Wireless Communication* (UOWC) and its potential applications is of great interest to the scientific community, industry, and, of course, the military [3].

## 1.2 Final Degree Project motivation

Focusing on the topic of this project, in the military, a better understanding and knowledge of UOWC could lead to significant advantages. Cyberspace has become the fourth war domain, and it can be affirmed that the electromagnetic spectrum is nowadays battlefield. “*The next war will be won by the side that best exploits the electromagnetic spectrum*” (Soviet Admiral, 1973) [4]. Therefore, military defense forces are focusing their Research, Skills and Development (RSD) on electronic, cyber, spectrum, and information warfare systems, to seize and hold control of communications, radar and other important sensors [5].

The fact about how technological revolution can optimize the overall performance and employment of any organization’s financial, material and human resources also applies to the military fields. As the AJEMA (Chief of Staff of the Navy) once said: “*We should be aware of the risk of falling behind if we do not face these new challenges and do not seize the opportunities we are offered. The Spanish Navy should adapt to changes, in a permanent transformation process, and, though this is one of its hallmarks, now it has speeded up more than ever*” (López Calderón, 2018) [6]. He also highlighted the importance of relying on the fourth industrial revolution recently, when he was promoted to JEMAD (Chief of the Defense Staff), setting himself this goal [7]. Hence, it can be inferred the high interest on military RSD, which is revealed in a series of strategic objectives among which the developing of UOWC can be found [8].

In terms of underwater communications, an astounding progress has been achieved in acoustic systems [9]. Although they can reach long distances, they are strongly limited in bandwidth. Therefore, UOWC has attracted considerable attention in the military, as it offers a higher transmission bandwidth,

thus providing higher data rate. As is often the case, when war comes, it is too late to address adequately the oversights of peace. For that reason, it is now when such advanced systems should be studied, investigated, developed and tested. Not only will they improve nowadays military operability, but also will provide readiness to be up to the task when necessary.

This Final Degree Project gives a detailed view of the state of art of UWOC, regarding its main benefits and challenges. Furthermore, it analyzes how it is affected by water properties and analyzing, which are the best conditions for the development of this technology. Finally, it ends with current and potential applications of the UWOC, focusing on the ones regarding the military.

### **1.3 Objectives**

The initial objectives of this final project were:

- To perform an in-depth study of the State of Art of the UWOC.
- To analyze which are the best conditions for the development of this technology.
- To study the current and potential future applications of the UWOC in the military field.

Although they were not inherent objectives of this project, two more objectives were established and achieved:

- After the state of the art analysis, to develop a basic prototype that demonstrates the capabilities of this technology.
- Analyzing the behavior of light underwater, to compare the theoretical predictions with the experimental results, in order to draw conclusions.

### **1.4 Memory structure**

This final project paper is divided in five distinct parts:

- Introduction and objectives: includes the introduction of this work to contextualize it and describes the objectives to be achieved.
- State of the art: details and analyzes the UOWC technology so far, regarding its history, the benefits of underwater communication, the factors affecting underwater light propagation, and the water classification in terms of its optical properties.
- Benchmarks and results: describes the design and development of a prototype UOWC, as well as several experiments performed to demonstrate the literature.
- Military applications: shows the main current and potential military applications of UOWC, taking into account feasibility, usefulness, type of operation, advantages and challenges.
- Conclusions and future developments: draws conclusions from the project and proposes future lines of research.

## 2 STATE OF THE ART

### 2.1 Introduction

Optical communication are a technology where light propagation is used to transmit information between two points. Light is defined as an electromagnetic radiation within the optical spectrum, which encompasses not only visible light, but also ultraviolet and infrared radiation, as shown in Figure 2-1. Therefore, the optical spectrum involves electromagnetic radiation with wavelengths in the range from 10 nm to  $10^3 \mu\text{m}$ , or frequencies in the range from 300 GHz to 3000 THz [10].

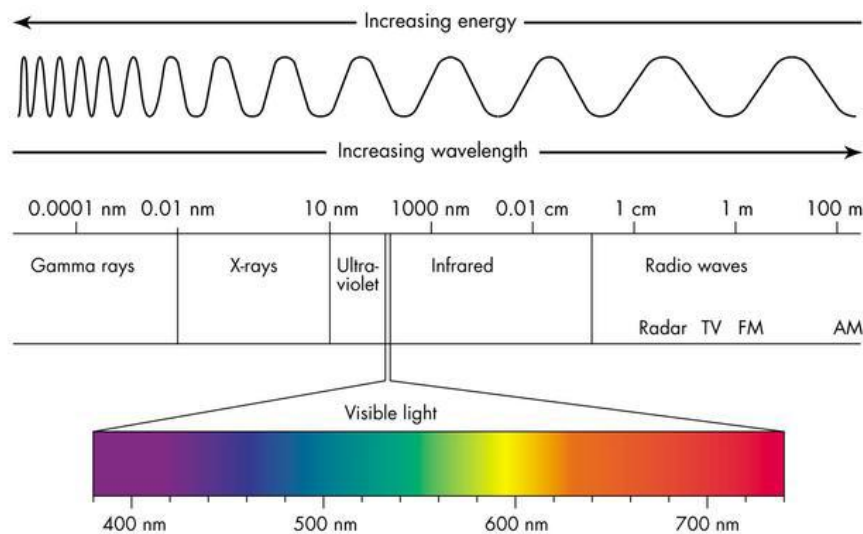


**Figure 2-1 Optical visible region of the electromagnetic spectrum [11].**

The basic components of Optical Communication are (see Figure 2-2):

- **A transmitter.** It converts the electric information to light pulses and emits them. Therefore, it could be any object that emits light, but it is usually a *Light Emitting Diode* (LED) a *Light Amplification by Stimulated Emission of Radiation Diode* (LD) [12].
- **A transparent channel.** A transparent medium is the one that allows light propagation. The more transparent the channel is, the better for the optical communication. If the medium allows only some of the light to pass through it because it scatters some of the light rays, it is a translucent medium. On the opposite, an opaque medium is the one that does not allow any light to go through it [13].

- **An optical receiver.** It converts the light pulses into electric pulses thanks to a light-activated sensor, such as a photodiode or a phototransistor, whose output current is proportional to the light power [14].



Figure 2-2 Simplified example of Optical communication [15].

Depending on the type of channel, optical communication technologies can be classified into:

- **Free Space Optical Communication (FSOC):** where light is wirelessly transmitted through free space, such as air, vacuum, outer space or similar means. Maximum range for FSO is stated in thousands of kilometers, although, in order to provide a telecommunications performance grade, practical application establishes it between 200 and 500 meters. This light performance limitation depends on atmospheric factors such as heat, dust or others. On the other hand, some of the strengths of FSOC are that it is quick and easy to install, and that it operates in an unlicensed spectrum. FSO has many different applications, especially short distance links such as last mile connections between buildings or a television remote control, shown in Figure 2-3 [16].

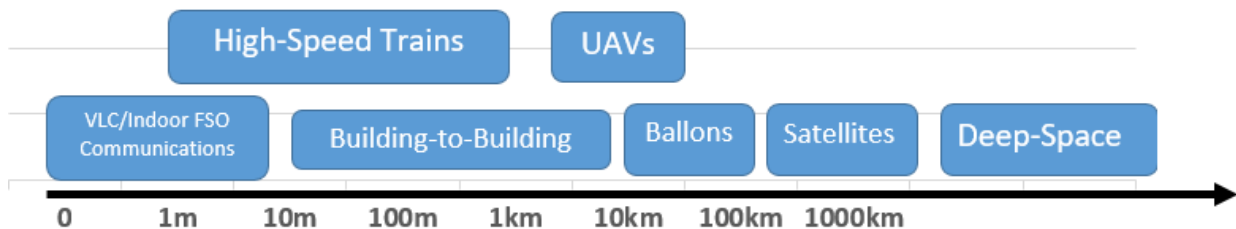


Figure 2-3 Different applications of FSOC according to its range (on a logarithmic scale).

- **Fiber-optic communication:** is an optical communication technology in which light is transmitted through a fiber-optic cable. Its high scope stands out, with a range of up to 10 kilometers between repeaters. In addition, it has a higher bit rate with a low Bit Error Rate (BER). Even though it does not depend on the atmosphere, it does depend on the fiber optic material. This why it is under continuous advancement and development. The main downside of this technology is its dependence on the installation of the fiber, which is expensive and takes long time and big efforts. Nevertheless, there are thousands of cables installed worldwide for high-performance data networking and telecommunications. Some of these cables lay underwater as shown in Figure 2-4, at the bottom of the ocean, allowing instant communication worldwide.

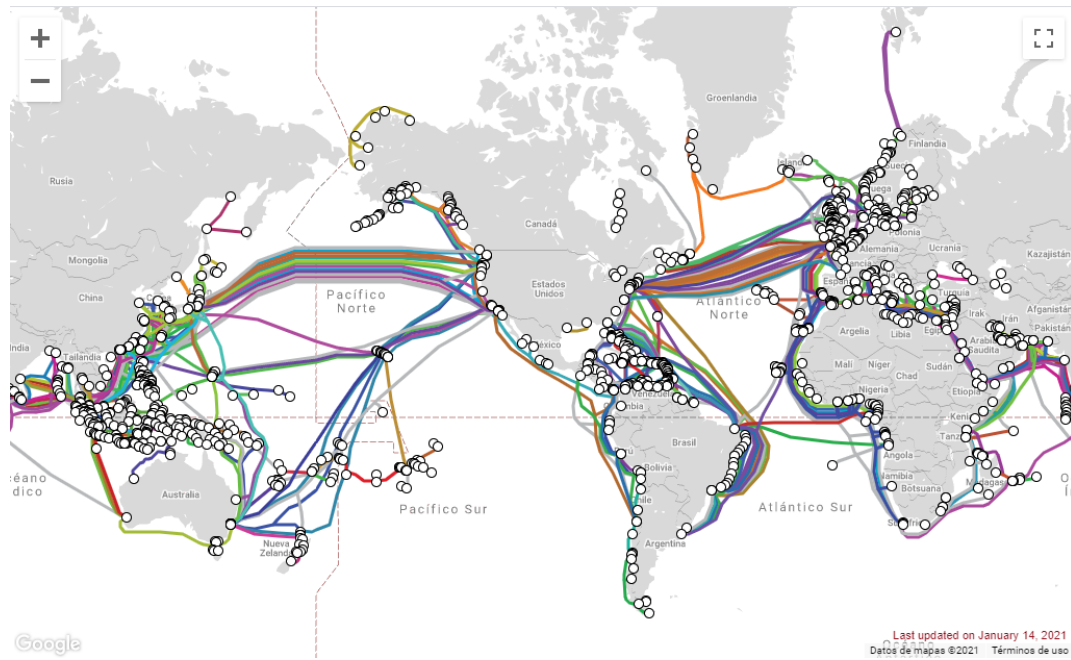


Figure 2-4 Submarine cable map [17].

▪ **Underwater Optical Wireless Communication (UOWC)** is an optical communication technology in which light is wirelessly transmitted through water. Despite not needing cables, the medium propagation properties are considerably different to be set apart.

On the one hand, this newfangled technology has gained interest during the last years as an alternative for broadband inexpensive submarine communications [18]. It has great advantages such as providing secure, discreet, reliable and fluid communication, without the need of installing a cable. On the other hand, the main disadvantages are the significant light absorption and scattering under the water, which results in a short range, up to a hundred meters [19].

It has started up in the technologies market [20], but extensive research is expected in the near future due to interesting feasible applications such as discreet communication with divers, or even an underwater sensor network.

Table 2-1 summarizes the advantages and disadvantages of the different optical communication technologies mentioned above. In addition, they have common advantages and disadvantages (see 2.2), due to being all optical communication technologies.

FSOC	Fiber-optic	UOWC
<ul style="list-style-type: none"> <li>No need of fiber installation (quick and easy).</li> </ul>	<ul style="list-style-type: none"> <li>Transoceanic distances.</li> </ul>	<ul style="list-style-type: none"> <li>No need of fiber installation (quick and easy).</li> </ul>
<ul style="list-style-type: none"> <li>Short distances.</li> <li>Dependence on atmospheric properties.</li> </ul>	<ul style="list-style-type: none"> <li>Need of fiber installation (cost, time and effort).</li> <li>Dependence on the fiber.</li> </ul>	<ul style="list-style-type: none"> <li>Short distances.</li> <li>Dependence on water properties.</li> </ul>

Table 2-1 Advantages (top) and disadvantages (bottom) of FSOC, fiber-optic communications and UOWC.

### 2.1.1 History

History of optical communications dates back to the origins of the human being and it continues nowadays. Most civilizations have used mirrors, smoke signals, sun reflections on the shields or fire beacons to convey information, see Figure 2-5 [12]. Ever since and now, there has been a big interest in developing communication mediums that could provide a more reliable, further and faster information transmission. Attempts to convey more information were made, such as changing the smoke color and turning on and off the beacon signal inside lighthouses, but still, these communication mediums were slow, limited and of a short range [15].



**Figure 2-5** Greek warriors using beacons [21]. Greeks constructed in 1084 B.C. a 500-km-long line of fire beacons to convey the news of the fall of Troya.

Optical communication media predominated on the naval field by virtue of the use of flags and pennants. It was in 1340, during the *Navy of the Crown of Castilla*, when optical signals were imposed in order to give orders to attack the *Crown of Aragon* fleet. This kind of signals had such an impact that in 1785, the king Carlos III approved the flag from whose colors we inherit for the current national flag. Lately, two specific flags were designed for the maritime field, one for the Navy and another for the merchant fleet, see Figure 2-6. This change avoided the existing confusion when identifying the origin of the ships [22]. Although flags and pennants could send more information, range and transmission rate were still very limited even during the 18<sup>th</sup> century.

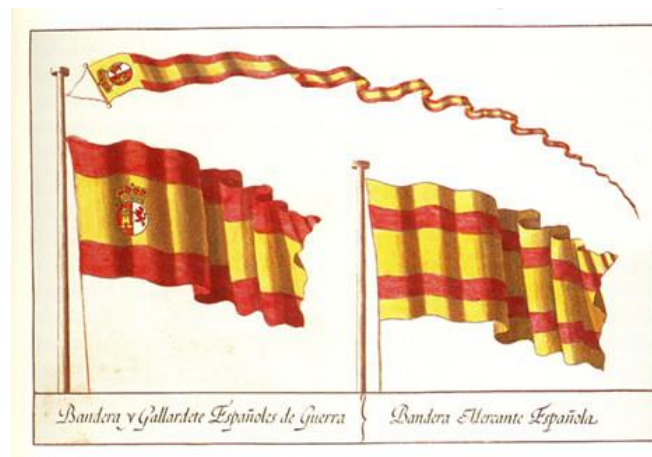


**Figure 2-6** Flags approved by the Ring Carlos III. On the left, the flag and pennant to be used by warships. On the right, the flag to be used by merchant ships [23].

In 1792, Claude Chappe came up with the first system of information transmitter and receiver nodes that allowed the transmission of any kind of information. It was established during the French Revolution, being the first known communication network. Messages were coded using two needles with a coding scheme, and were transmitted over long distances using intermediate relay stations as it is shown in Figure 2-7. Light was only used to make the signals visible. Chappe called his invention optical telegraph [15]. By 1830, it was expanded throughout Europe and it developed to cover up to a range of 5000 km



[22]. Despite the fact that this communication network covered larger distances, it was still so dependent on the medium and limited on transmission rate.

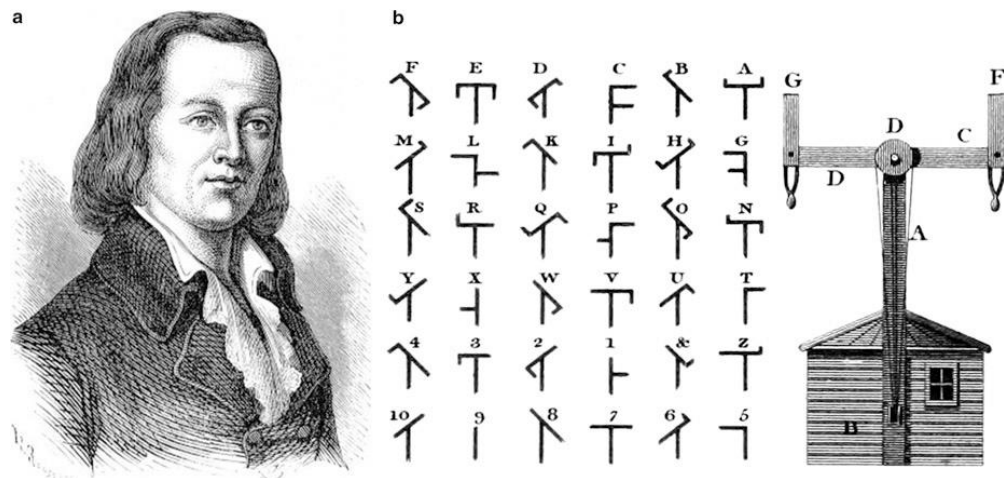


**Figure 2-7 Claude Chappe, his coding scheme, and the mechanical device used for making optical telegraphs (licensed under Public Domain via [15]).**

At the end of the industrial revolution, physicists began to study the fields of electricity and magnetism. After the findings of Oersted, Ampère and Faraday, the era of the electrical communications began with the advent of the electric telegraph in the 1830s, whose father was Joseph Henry [15]. This first model consisted of an electric circuit that marked a paper roll or produced a small noise, see Figure 2-8. Indeed, it was Samuel Morse the first one establishing a telegraphic communication between two cities in 1844 [22]. Afterwards, this became the fastest and most efficient communication at the time, although optical communications continued developing.



**Figure 2-8 Telegraph prototype [22].**

It has been said that Romans, Greeks and other past civilizations used their war shields to reflect the sunlight, but it wasn't until 1869 that Henry Christopher Mance developed the first widely accepted heliograph. A heliograph provides wireless optical communication, but it is permanently dependent on the solar light. Nevertheless, it was the most powerful visual signaling known and was used in war by different countries [24]. Two heliographs could achieve a range of thirty-five miles and a line of heliographs much more. Some of the reasons it survived while coexisting with the telegraph were the low probability of interception and the no need of any cable installation.



**Figure 2-9 Henry Mance next to the heliograph prototype (left) [12] and two field heliographs (right) [24].**

Lately, in 1876, telephone was patented by well known scientific and engineer Alexander Graham Bell, resulting on a great success. Surprisingly, what Bell believed his most important invention wasn't the telephone, but the photophone, invented in 1880 [25]. This device allowed a voice transmission in a visible light ray at a distance of 200 meters. Hence, he established the foundations of optical communications, even though it was not until much later that the first applications derived from his photophone appeared, initially only in the military field [12].

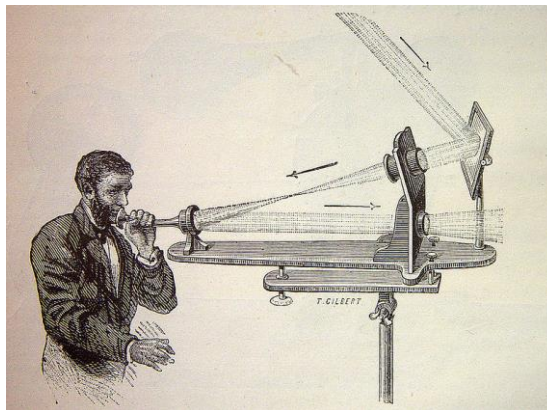


**Figure 2-10 Photophone transmitter [26].**

In 1940, coaxial cables were put into service, increasing bandwidth and speeding up telecommunications. Still, cable losses limited the bandwidth through this medium, which led to development of microwave communication systems. By 1950, the scientific interest on providing solutions for enhancing the capacity of telecommunications led them to look towards optics, although neither coherent optical source nor convenient transmission medium was yet available [15]. This changed in 1960, with the invention of the LASER (Light Amplification by Stimulated Emission of Radiation). Many military organizations were especially interested, and encouraged its development and in-depth investigation. However, those investigations in FSO systems were partially overshadowed by the increasing interest in fiber technologies [12].

Since the invention of the LASER, multiple terrestrial optical communication applications appeared [27]. In addition, the development of optical fiber greatly enhanced the capacity of telecommunications. LASER was improved as well, in order to get further through the optical fiber. In 1975 the first generation of commercial optical fiber was developed, with bit rates of 45 Mbps and signal repeaters every 10 kilometers [12]. Figure 2-11 shows bit rate exponential evolution since 1840.



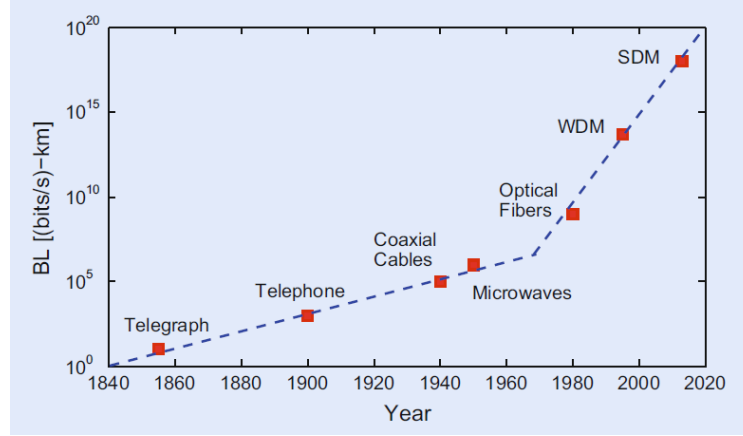


**Figure 2-11 Increase in the BL product during the period 1840–2015. The emergence of new technologies is marked by red squares. Dashed line shows the trend as an aid for the eye. Notice the change in slope around 1977 when optical fibers were first used for optical [15].**

Overall, these discoveries refer to terrestrial communications while two thirds of the earth surface are covered with water. Despite ocean exploration attraction, the early development of UOWC was far behind the terrestrial free-space optical (FSO) communications, due to the severe attenuation effects of seawater to visible light and the limited knowledge of aquatic optics [27]. Therefore, underwater wireless communication through radio frequency (RF) and acoustics were developed and implemented before underwater optical communications. Nevertheless, optical communications have many advantages over RF and acoustic ones regarding bit rate, bandwidth, discreteness and reduced aquatic environment contamination (as shown in section 2.2).

These outstanding characteristics of optical communication have led to growing research activity in UOWC in the recent years. Figure 2-12 presents a time line with some of the most substantial historical advances over UOWC.

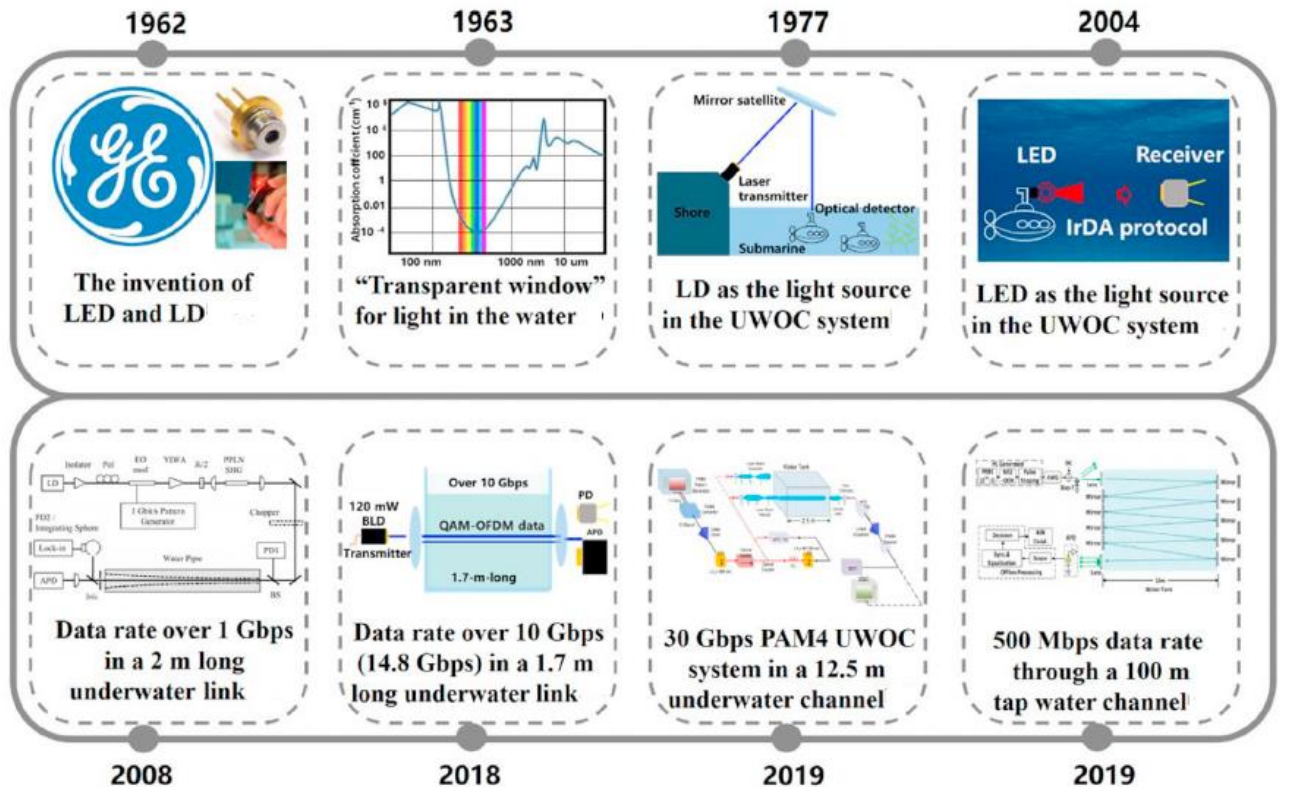


**Figure 2-12 Remarkable historical progresses of UOWC [28].**

In 1963, after almost 20 years of theoretical and experimental studies of light propagation in the sea, Duntley proposed that seawater shows a relatively low attenuation property to blue and green light, which corresponds to light with wavelengths from 450 nm to 550 nm [27], shown in Figure 2-13. This postulation was then experimentally confirmed by Gilbert [29]. The existence of this “transparent window” for aquatic attenuation [11] provided a foundation for the development of future UOWC.

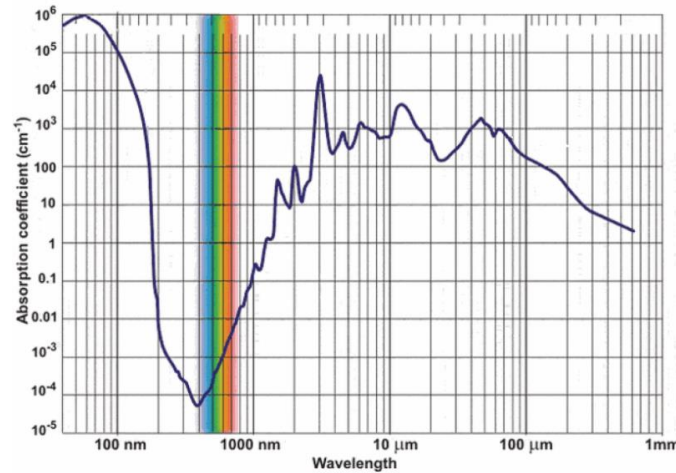


**Figure 2-13 Seawater absorption coefficient depending on wavelength. It is shown how blue and green light experience the least absorption in seawater [27].**

The first applications of UWOC were mainly for military purposes, especially for submarine communications. For example, in 1976, Karp studied the feasibility of optical wireless communications between an underwater terminal and a satellite [30]. The year after, researchers from the University of California proposed a half-duplex optical communication system from shore to submarine (Figure 2-14). The transmitter employed a blue-green LASER source with a compact architecture to generate the light pulses. Through this system, a submarine would be able to communicate at deeper positions than through a RF system, in which only very long wavelength radio waves would be able to penetrate the ocean at considerable depths [31]. In the early 1990s, the U.S. Navy tested other UOWC topologies such as full duplex and plane-to-submarine.

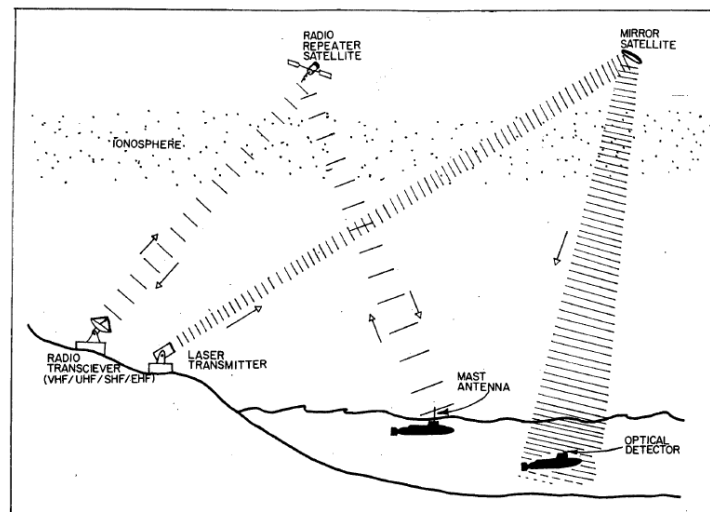


**Figure 2-14 Satellite line-of-sight radio and optical propagation [31].**

Nevertheless, interest in UOWC has been limited to military applications for decades [32]. UOWC have not achieved the massive market yet. However, in the early 2010s, a few limited products were commercialized, such the *BlueComm* UOWC (Figure 2-15) and the *Ambalux* UOWC. The *Ambalux* UOWC system provides a 10 Mbps data transmission over a distance of 40 meters [27]. In 2016, a

numerical study was published, showing the possibility of achieving LED-based visible light communication over a link distance of 500m in pure seawater by employing a single photon avalanche diode [3]. These discoveries boosted bit-rate and range, which awoke researcher's interest on UOWCs and its potential applications [33].



**Figure 2-15 The BlueComm High Ambient Light (left) and Long Range (right). BlueComm UOWC can achieve 20 Mbps underwater data transmission with a range of 200m [34].**

Therefore, many experiments were carried out in the UOWC field in order to have a better understanding of the propagation of light under the water. Table 2-2 shows the result of some remarkable experimental achievements of UOWC systems since 2016. It can be seen that is a promising evolving technology that can be very successful for specific applications if studied in depth.

Year	Bit Rate (Mbit/s)	Distance (m)	Water	Optical Source	$\lambda$ (nm)	Test	Modulation Format	Ref
2016	1500	20	Clean	LD	450	Water tank	OOK-NRZ	[35]
2016	200	5,4	Clean	$\mu$ LED	440	Water tank	OOK-NRZ	[36]
2016	125	4,8	Turbid	Laser	515	Harbor	OOK-NRZ	[37]
2017	3	N.A.	N.A.	LED	N.A.	Water tank	N.A.	[38]
2017	2700	34,5	Clean	LD	520	Water tank	OOK-NRZ	[39]
2018	10	10	Turbid	LED	470	Harbor	Manchester	[40]
2018	9700	2,3	Clean	LD	RGB	Water tank	OOK-NRZ	[41]
2019	30000	12,5	Clean	LD	487	Water tank	PAM4	[42]
2019	3000	1,2	Clean	LED	Blue	Water tank	64-QAM	[43]
2019	500	100	Clean	LD	520	Water tank	OOK-NRZ	[44]
2019	30	14,7	Clean	LD	450	Water tank	OOK-NRZ	[45]
2019	50	3	Clean	LD	450	Water tank	16-QAM	[46]
2020	20000	1,2	Clean	Led array	Multi chromatic	Water tank	PS-bitloading-DMT	[47]
2020	2	117	Clean	LD	450	Water tank	OOK	[48]
	0,0005	144						

**Table 2-2 Remarkable experimental results for UOWC systems since 2016.**

Nowadays, there has been a growing interest in ocean exploration systems with the depletion of resources due to global climate change. Therefore, researchers have proposed a new concept: Underwater Wireless Sensor Networks (UWSN). In order to achieve efficient high bandwidth data transmission in these networks, the market of UOWC seems very promising.

A UWSN consists of distributed nodes with the capability of maintaining the collaborative monitoring to the underwater environment through processing, sensing and communicating transmit via acoustic or optical links (see Figure 2-16). These nodes can be *Autonomous Underwater Vehicles* (AUVs), *Remotely Operated Vehicles* (ROVs), seabed sensors or relay buoys, which relay signals to ships, submarines and other underwater vehicles [49]. Above the sea surface, the onshore data center processes data and communicates with satellite besides ships through RF or FSO links [27]. These applications of UOWC are very interesting for military applications and will be detailed later in section 4.

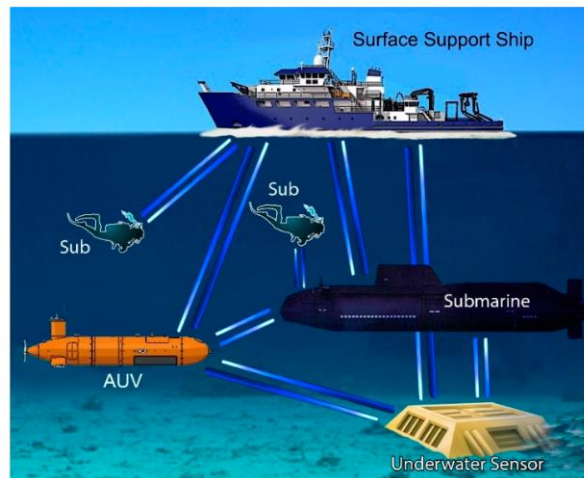


Figure 2-16 UOWC in an UWSN with UAVs, divers and submarine.

## 2.2 Underwater wireless communication overview

The world is a water planet, two thirds of which are covered by water. As a result of rapid developments in technology, the scientific community, the industry and the military have a growing interest on underwater wireless communication. This is not only for the increasing exploitation of natural resources under water, but also for the potential technology advances in the domains of warfare, environmental monitoring, oil and gas exploration, and oceanography research. Nevertheless, underwater communication technology presents a new challenge: the water itself, which makes every technology work very different from how they do through the atmosphere. Despite this fact, three different technologies for underwater communication have been developed: radio frequency, acoustic and optical. Each of them presents its advantages and disadvantages, detailed in this FDP, and summarized in Table 2-3.

### 2.2.1 RF

Radio-frequency waves are the most common and extended technique used on terrestrial communications, but they are strongly attenuated under water due to its conductivity, suffering high absorption and scattering [20]. The propagation of the RF signal depends on environmental conditions, such as temperature and salinity, as well as its frequency. Given the relevance of the salinity in conductivity, the attenuation of RF signal is higher in seawater than in fresh water. From the physics viewpoint, for VHF and UHF ranges, the seawater is also very conductive, resulting in being hard to establish links for distances beyond 10 meters in the ocean [27].

On the other hand, at lower frequencies such as ELF and VLF, the attenuation can be considered low enough to allow for reliable communications over several kilometers. Unfortunately, their bandwidth is too narrow to enable transmissions at high data rates. In addition, communication in these frequency ranges has financial and operational difficulties, since the equipment is expensive, large and requires high power [50].

Parameter	Acoustic	RF	Optical
Attenuation	Distance and frequency dependent (0,1–4 dB/km)	Frequency and conductivity dependent (3,5-5 dB/m)	0,39 dB/m (ocean) 11dB/m (turbid) Dependent on light and water properties.
Speed	1500 ms <sup>-1</sup>	2,3 * 10 <sup>8</sup> ms <sup>-1</sup>	2,3 * 10 <sup>8</sup> ms <sup>-1</sup>
Data Rate	Kbps	Mbps (fresh water) Kbps (sea water)	Gbps
Latency	High	Moderate	Low
Distance	More than 100 km	≤ 10 m	10-150 m (500 m potential)
Bandwidth	1kHz-100kHz	MHz	150 MHz
Frequency Band	10-15 kHz	30-300 MHz	5 * 10 <sup>14</sup> Hz
Transmission Power	10 W	mW-W	mW-W
Cost	High	High	Low

**Table 2-3 Comparison of underwater wireless communication technologies (with color code for comparison).**

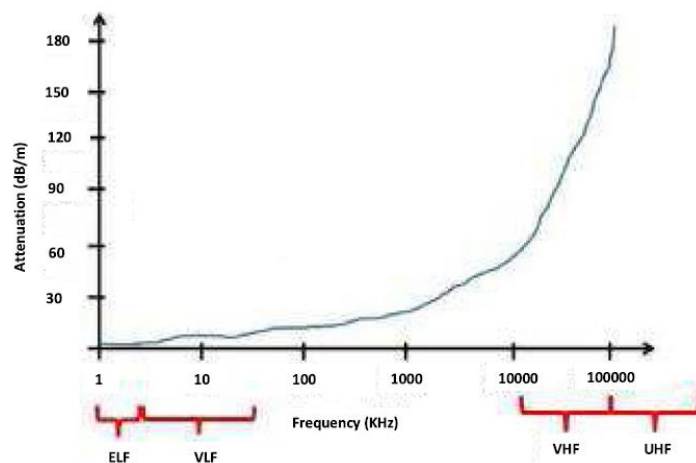


**Figure 2-17 RF attenuation in seawater [51].**



Despite the weaknesses mentioned above, underwater RF signals can travel through several paths, crossing easily water-to-air or water-to-earth boundaries following the least resistance path. This advantage can be used to increase the signal propagation distance (Figure 2-18), and could contribute to network design implementation. Other benefits are the tolerance to turbulence, pressure gradients, low visibility, and acoustic noise, as well as the less known effects on marine life than acoustic signals [52].

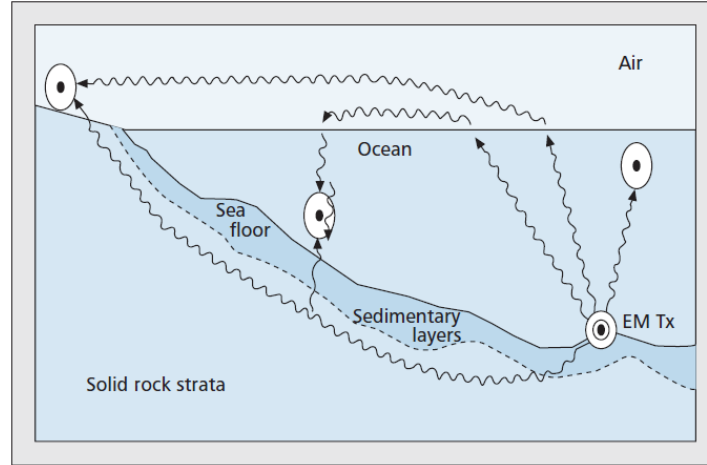


**Figure 2-18 Possible multi-path propagation of a RF signal in shallow water [52].**

Nevertheless, regardless of all mentioned advantages. This technology has still much to evolve in order to meet up to high expectations of speed, bit-rate and underwater distance due to its very short range and very low bandwidths for ELF and VLF. Hence, it has few and specific applications, such as sensor networks for monitoring seabed sediments in order to control coastal erosion.

### 2.2.2 Acoustic

Acoustic underwater communications are the best alternative to reach higher distances in underwater wireless communications and it is also the dominant one. In fact, the first example of this technology dates back from the Renaissance, when Da Vinci designed the first passive SONAR (*Sound Navigation and Ranging*) prototype [53]. Since then, it has continued developing until now.

With underwater acoustic technology, very long propagation distances can be reached. The range can exceed 200 kilometers [50], depending on the transmitter power, frequency and bathymetry of the zone. Power loss occurs due to three main phenomena: spreading loss, absorption loss, and scattering loss. Spreading depends on the distance, while absorption and scattering depend on the frequency [53]. Therefore, the further you want to communicate, the greater the power you need. This fact has the side effect of producing more acoustic pollution, which is harmful for the marine environment, especially for cetaceans.

However, underwater acoustic communication has other inherent disadvantages, such as big propagation delay, low transmission rate and high power consumption. The speed of propagation of waveforms depends on the electromagnetic and mechanical properties of the medium, which are temperature, salinity and depth [53]. These properties must be known in order to establish an acoustic link; given they determine the propagation path. In order to calculate it, the ray trace modelling of underwater sound propagation speed must be plotted, see Figure 2-19 [54]. An additional constraint is the latency of the acoustic waves, which hampers the signal processing solution utilized in these systems [50].

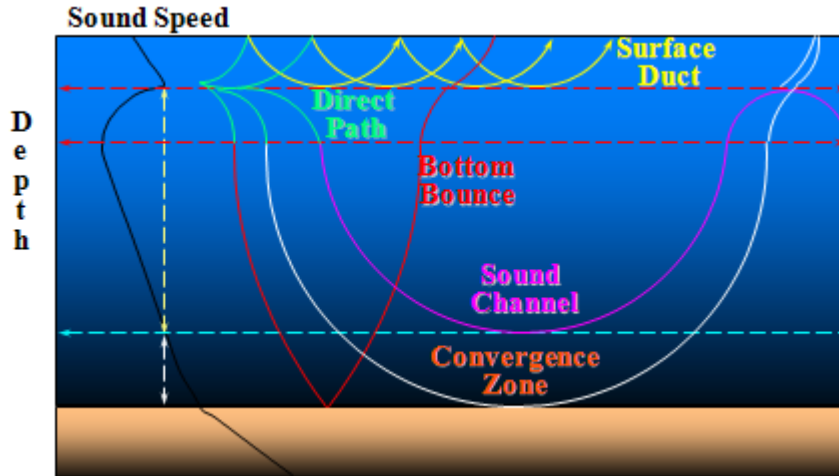


**Figure 2-19 Different underwater sound propagation paths. The graphic on the left represents the ray trace modeling of underwater sound propagation speed [54].**

On the one hand, this kind of network can only be used for small capacity data transmission, not being suitable for transmitting large-capacity and high-speed data, such as video or image [55]. Moreover, regarding military applications, research and development of acoustic systems benefit warfighters of the submarine force, the land force, and the sea mine countermeasures force. One of its most widespread and well-known applications is the SONAR. Nowadays, acoustics play a crucial role in operational systems and they will continue doing so, with new sensing technologies, signal processing and data fusion methods being developed [56].

### 2.2.3 Optical UWC overview

Although tremendous progress has been made in the field of underwater acoustic communication, it is still limited by bandwidth. It has been stated how acoustic wave transmission is restricted to several hundreds of kbps, supports slow data rate, and distresses marine mammals. It has also been explained how RF waves are strongly attenuated in water due to absorption and scattering. Therefore, they can only be used for relatively short-range real-time applications up to a range of a few meters [18]. All these effects have led to an increasing interest in underwater wireless communications because it provides large bandwidth communications at longer distances than RF.

Underwater Optical Wireless Communications (UOWC) are relatively less explored than RF and acoustic and far more challenging. Underwater optical waves undergo a wide range of physical processes depending on numerous types of underwater environments, resulting in profuse behaviors [57]. While in RF communication, the water acts as a conductor, in optical communication it acts as a dielectric and thus, can provide higher rates and range than RF [50].

Despite the high latency, low bandwidth, slow data rate and Doppler spread of acoustic channel, the optical channel can support large bandwidth data rate up to Gbps, at a distance of few hundreds of meters. The main limitation of UOWC is the severe water absorption at optical frequency bands, and the strong backscatter from suspended particles. However, there is an optical window at blue-green wavelengths where the underwater attenuation is relatively low, as shown before in Figure 2-13 [57].

Therefore, interest in UOWC is soaring, as it could be a better alternative to the existing underwater communication systems or a complement for their performance improvement. This work deepens in underwater optical properties, and the characteristics of water that affect them. A detailed insight is given in the field of UOWC, including current and potential applications, as well as the development of a UOWC model to demonstrate the results of this research with a basic prototype.

## 2.3 Factors that affect UOWC

Optical underwater communication could provide fluid, safe and reliable communications, being a very appealing alternative to current underwater technologies. The main challenge for optical underwater communication is underwater light behavior, especially when it is absorbed and/or scattered. These factors depend on the optical properties of the water.

### 2.3.1 Optical properties of the water

In ocean optics, water properties can be classified into *inherent* (depending on the medium) and *apparent* (depending on the combination of the medium and the light source).

*Inherent Optical Properties* (IOP) are used to determine the absorption coefficient, scattering coefficient, the attenuation coefficient and the volume scattering function, whereas *Apparent Optical Properties* (AOP) are used to evaluate the underwater ambient light levels near the surface, and can only be formed from regular and stable light sources. They depend on both IOP and the light source, defining the directional property of the optical beam, such as irradiance, radiance and reflectance [57].

The inherent optical properties (IOPs) of the water body, along with the boundary conditions that specify the incident radiance and how it is transmitted and reflected, are the inputs to the *Radiative Transfer Equation* (RTE), shown in Figure 2-20. The result of the RTE equation is radiance distribution, used to compute all other radiometric variables and AOPs. The main difference between a radiometric variable and an AOP is that the former is not stable, whereas AOPs are stable enough to be a useful description of the water body [58].

#### 2.3.1.1 Inherent Optical Properties (IOPs)

IOPs are properties of the medium and are independent of the ambient light field. They describe the absorption and scattering properties of a medium such as seawater despite the amount of light. These properties depend on the composition, morphology, and concentration of the particles and dissolved substances in the ocean. Therefore, it does not matter where IOPs are measured, whether in the laboratory on a water sample or in situ, results should be the same [58].

The two fundamental IOPs are absorption coefficient and volume scattering function, which describe how a medium absorbs and scatters light respectively. Knowing these two IOPs, everything about the interaction between non-polarized light and the medium can be analyzed. Moreover, any other IOP can be defined once the absorption and scattering coefficients are known [58].

IOPs are defined using the geometric model shown in Figure 2-21, where a water body of small volume “ $\Delta V$ ” and thickness “ $\Delta r$ ”, is being illuminated by a collimated beam of monochromatic light of spectral radiant power “ $\Phi_i(\lambda)$ ” (in  $Wnm^{-1}$ ) at wavelength “ $\lambda$ ”. Some of the incident power is absorbed within the water body “ $\Phi_a(\lambda)$ ”, and some is scattered out of the beam “ $\Phi_s(\lambda)$ ”. More specifically, “ $\Phi_s(\lambda, \psi)$ ” stands for the scattered power when it is referred to a specific angle “ $\psi$ ”. The remaining power “ $\Phi_t(\lambda)$ ” is transmitted through the volume with no change in direction.



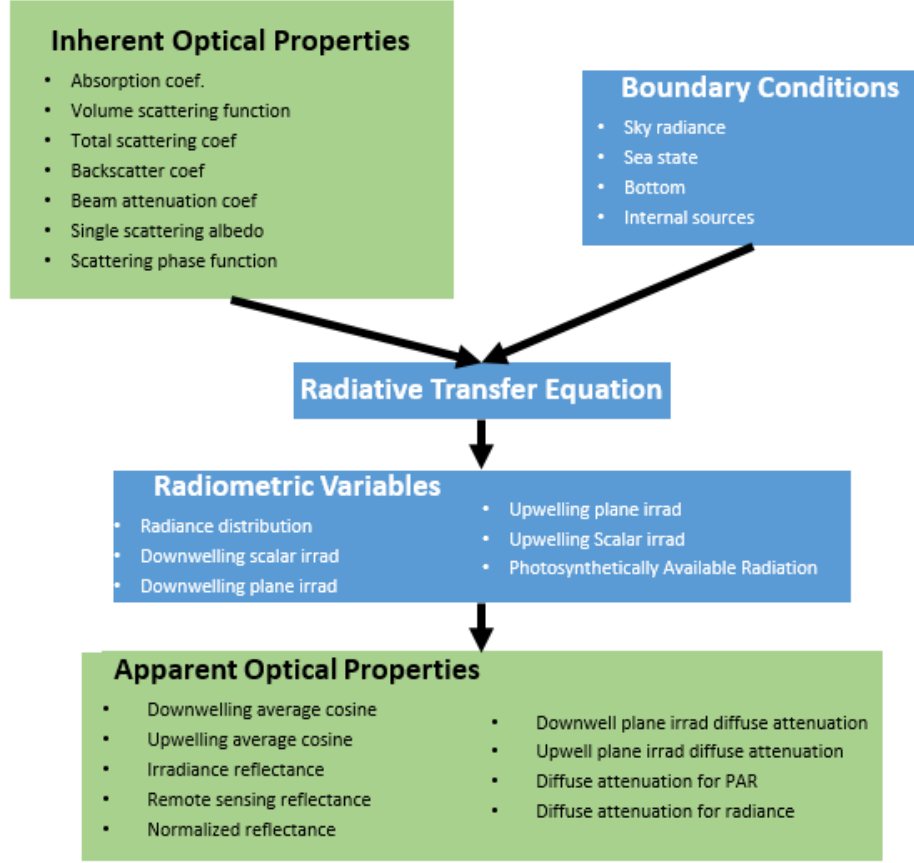


Figure 2-20 Relationship between IOPs and AOPs in Ocean Optics.

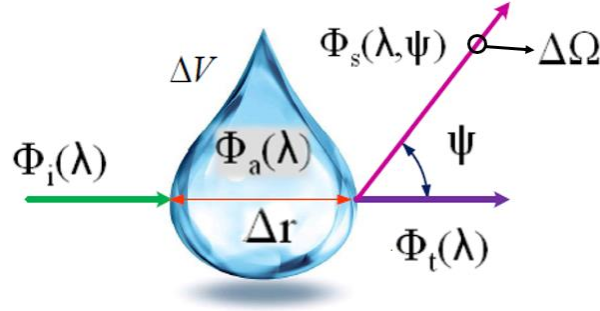


Figure 2-21 Geometric model for inherent optical properties.

Assuming that the light wavelength remains constant during the scattering process, Eq.(1) can be obtained by the conservation of energy law.

$$\Phi_i(\lambda) = \Phi_a(\lambda) + \Phi_s(\lambda) + \Phi_t(\lambda) \quad (1)$$

Besides, absorptance “ $A(\lambda)$ ”, scatterance “ $B(\lambda)$ ” and transmittance “ $T(\lambda)$ ” are the fraction of incident power, which is absorbed, scattered out and remains unaltered respectively, as shown in Eq. (2), (3) and (4). Evidently,  $A(\lambda) + B(\lambda) + T(\lambda) = 1$ .

$$A(\lambda) = \frac{\Phi_a(\lambda)}{\Phi_i(\lambda)} \quad (2)$$

$$B(\lambda) = \frac{\Phi_s(\lambda)}{\Phi_i(\lambda)} \quad (3)$$

$$T(\lambda) = \frac{\Phi_t(\lambda)}{\Phi_i(\lambda)} \quad (4)$$

The absorption and scattering coefficients are the absorbance and scatterance per unit distance. They are calculated as shown in Eq. (5) y (6).

$$a(\lambda) \equiv \lim_{\Delta r \rightarrow 0} \frac{\Delta A(\lambda)}{\Delta r} = \frac{dA(\lambda)}{dr} \quad (m^{-1}) \quad (5)$$

$$b(\lambda) \equiv \lim_{\Delta r \rightarrow 0} \frac{\Delta B(\lambda)}{\Delta r} = \frac{dB(\lambda)}{dr} \quad (m^{-1}) \quad (6)$$

The beam attenuation coefficient  $c(\lambda)$  is calculated by adding the absorption coefficient and the scattering coefficient, as shown in Eq. (7).

$$c(\lambda) \equiv a(\lambda) + b(\lambda) \quad (m^{-1}) \quad (7)$$

Optical properties of water mentioned before (in Figure 2-20) enable the numerical calculation of the other factors that affect the UOWC [58], which will be defined and detailed along this section.

### 2.3.1.2 Apparent Optical Properties (AOPs)

AOPs are those properties that do not only depend on the medium as the IOPs, but also on the radiance distribution. Consequently, as they show enough regular features and stability, they are beneficial descriptors of a water body [58]. They are very useful in optical oceanography because, while it can be difficult to measure in situ IOPs apart from the beam attenuation coefficient, it is relatively easy to measure radiometric variables such as the upwelling and downwelling plane irradiances. This is the reason why AOPs started to be used to describe the bulk optical properties of water bodies instead of IOPs. Examples of AOPs are radiance in any direction " $L(\Theta, \Phi)$ ", upwelling radiance " $L_u$ ", downwelling irradiance " $E_d$ ", upwelling irradiance " $E_u$ ", scalar irradiance " $E_o$ ", irradiance reflectance or remote-sensing reflectance.

### 2.3.2 Absorption

Absorption is one of the main phenomena impairing the propagation of light in water, which is referred to the loss of light photons due to water molecules, as well as dissolved organic and inorganic materials. The electromagnetic radiation is captured by the aforementioned matter, converting the energy of photons into other forms such as internal energy or heat.

The absorption can be quantified by the absorption coefficient at a wavelength " $a(\lambda)$ ", measured in  $m^{-1}$ . As explained before, it is an IOP, so it remains invariant with changes in radiance distribution. Besides, it obeys simple additive laws [59]. Therefore, the total absorption coefficient is calculated by a

weighted sum of the absorption coefficients of all optically active substances present on a water body following Eq.(8).

$$a(\lambda) = a_w(\lambda) + C_{phyt} * a_{phyt}(\lambda) + C_{CDOM} * a_{CDOM}(\lambda) + C_{NAP} * a_{NAP}(\lambda) \quad (8)$$

Where:

- $a_w(\lambda)$  : Absorption coefficient of pure seawater.
- $C_{phyt}$  : Concentration of phytoplankton.
- $a_{phyt}(\lambda)$  : Absorption coefficient of phytoplankton.
- $C_{CDOM}$ : Concentration of yellow substances (Colored Dissolved Organic Matter).
- $a_{CDOM}(\lambda)$  : Absorption coefficient of yellow substances.
- $C_{NAP}$  : Concentration of Non-Algae Particles (NAP).
- $a_{NAP}(\lambda)$  : Absorption coefficient of non-algae particles.

As it is shown in Eq.(8), substances that are optically active in seawater are generally categorized in three groups, (i) Phytoplankton and associated detrital matter, (ii) dissolved organic matter and (iii) suspended material not belonging to group (i), such as sediments in suspension (non-algae particles) [59]. Consequently, the factors that affect underwater light absorption will be the ones described below in detail.

### 2.3.2.1 Water molecules

Water molecules are in constant movement, given they rotate and vibrate continuously. As Figure 2-22 shows, there are three different modes for vibration of water molecules: symmetric stretching ( $\nu_1 = 3280 \text{ cm}^{-1}$ ), bending ( $\nu_2 = 3490 \text{ cm}^{-1}$ ) and asymmetric stretching ( $\nu_3 = 1654 \text{ cm}^{-1}$ ). The energy needed for these vibrations is obtained by absorption of radiation, the reason why the vibrations are most intense at wavelengths matching the energy requirements of these motions [60].

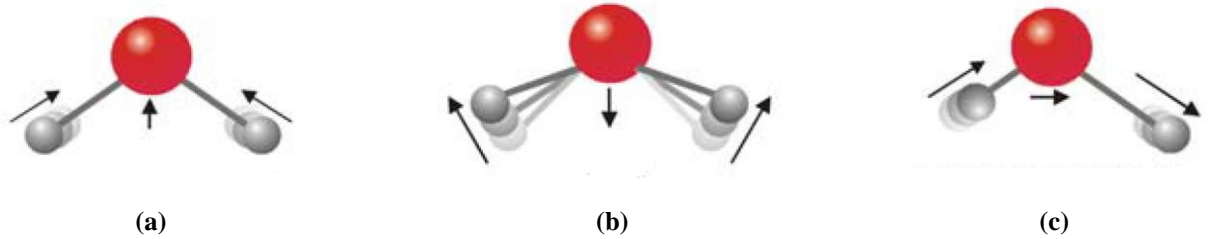


**Figure 2-22 The three vibrational modes of the water molecule: (a) symmetric stretch, (b) bend and (c) asymmetric stretch [60].**

Absorption peaks coalesce into a large absorption peak at around 3000 nm for symmetric and asymmetric stretching, while absorption peak for bending vibrations occurs at a lower energy level, at around 6000 nm. Figure 2-1 shows the subtle shoulders in the absorption spectrum of pure water, which correspond with vibration harmonics of water molecules [60].

Temperature alter molecules vibration, so the absorption coefficient is modified as well. Figure 2-24 shows the absorption coefficient in pure water with respect of the temperature. In the optical spectrum, it can be observed that temperature affects more at larger wavelengths (lower frequencies, such as red) while its effect is almost negligible at the shortest, in the blue region.

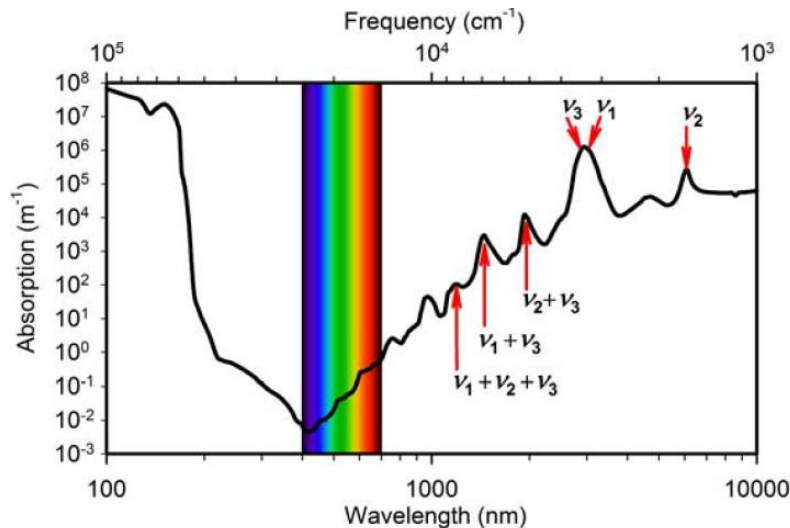


Figure 2-23 Absorption spectrum of pure water. It can be seen that peaks in the absorption spectrum correspond to the fundamental frequencies and higher harmonics of the vibration of water molecules [60].

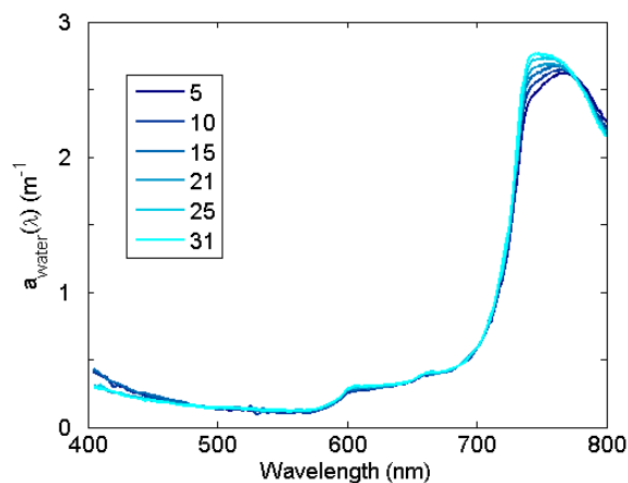
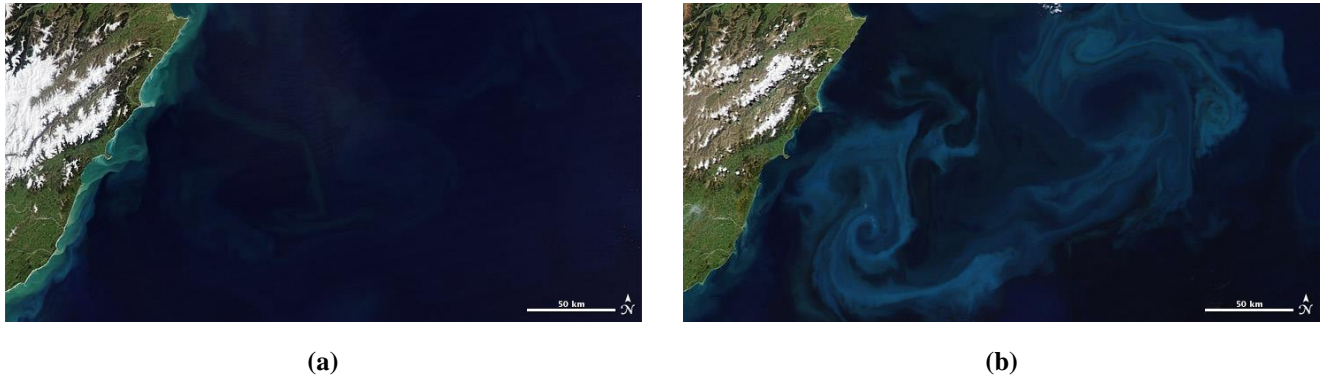


Figure 2-24 Absorption coefficient due to pure water as a function of water temperature (°C) for light propagation under water in the visible spectrum [42].

### 2.3.2.2 Phytoplankton

This category includes both, phytoplankton and its detrital matter<sup>1</sup>. Phytoplankton are microscopic organisms that live in watery environments, both salty and fresh. They have chlorophyll to capture sunlight, and they use photosynthesis to turn it into chemical energy, consuming carbon dioxide, and releasing oxygen. Therefore, their growth depends on the availability of carbon dioxide, sunlight, and nutrients, such as nitrate, phosphate, silicate, and calcium. Besides predators, their growth rates are influenced by water temperature and salinity, water depth or wind. Another characteristic is that their concentration can grow explosively or suddenly plummet, as it is shown in Figure 2-25 [61].

<sup>1</sup> Detrital matter associated to phytoplankton refers to dead particulate organic material, as distinguished from dissolved organic material.



**Figure 2-25** These two satellite images from NASA images show a phytoplankton bloom that formed east of New Zealand in a fortnight in 2009 [61].

Since phytoplankton concentration depends on sunlight, among others factors, it is strongly related to light absorption. The more availability of light will result in an increase on phytoplankton population, and therefore, in greater light absorption. The steady state is reached when the phytoplankton growth is attenuated by its own shadow [60]. As a result, the phytoplankton concentration through the water column descends with increasing depth, simply because the deeper the water, the less available sunlight. At a depth of more than 200 meters, it is very unusual to discover phytoplankton species, in contrast with the existence many zooplankton species [62].

Figure 2-26 (a) shows the absorption spectra for a range of different pigment composition, which were grown at the laboratory, illustrating their light dependence. It can be notice that the absorption coefficient of the *diatom* plankton exposed to high light outranges the one of the other diatom, which was exposed, to low light. Figure 2-26 (b) shows the generic phytoplankton absorption spectrum for a mixed algae composition [58].

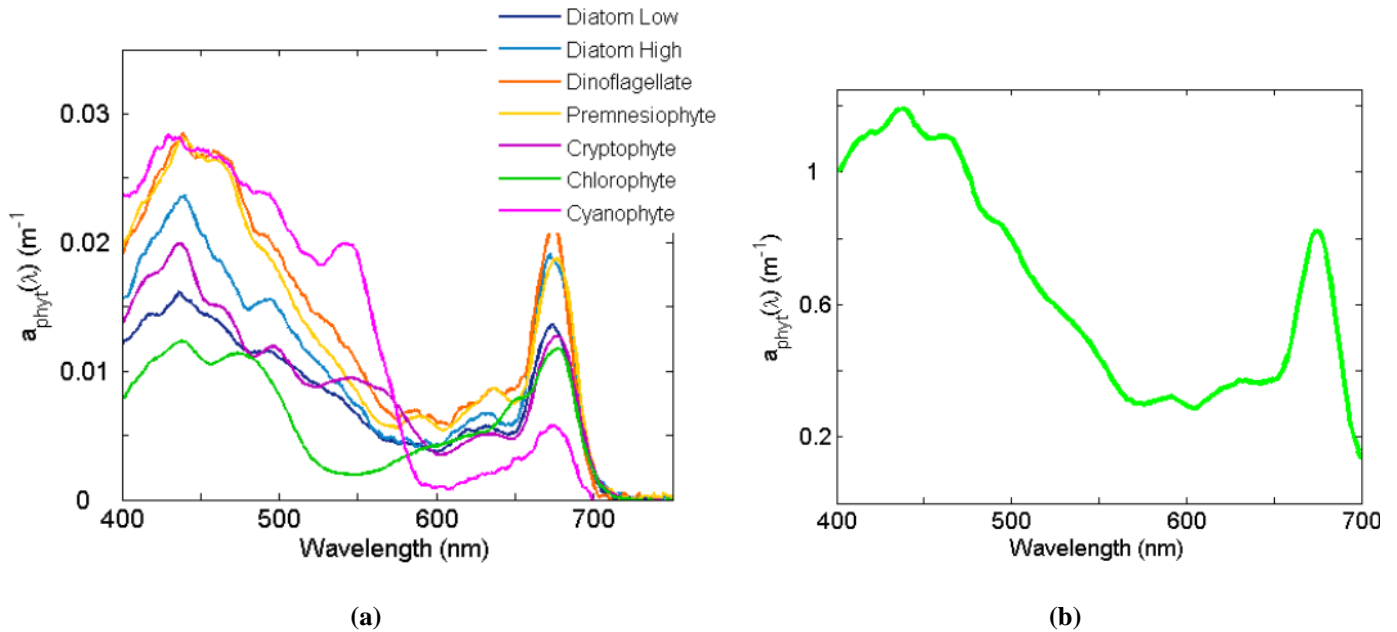


**Figure 2-26 (a)** Absorption spectra for a range of different pigment composition. The difference in the absorption coefficients of diatoms grown in high light compared to those grown in low light can be noted. **(b)** Generic phytoplankton absorption spectrum for a mixed algae composition [42].

The diversity of phytoplankton species is extremely rich, ranging from some 10,000 to 20,000 different species in the world's oceans. Although many species of phytoplankton have been identified, why and where they occur is largely unexplored, representing a serious knowledge gap. Apart from being a key element of ocean ecosystems and serving as the fundamental basis of the marine food chain,

they produce more oxygen than all the world rainforests thanks to its photosynthetic pigments. These pigments determine the part of the light spectrum the species can harvest for photosynthesis [63]. Pigments have unique absorption spectra, which lend a range of colors to phytoplankton, as well as spectral shapes to the respective absorption coefficients (Figure 2-27).

There are three major groups of pigments:

- The *Chlorophylls*, which are structurally a tetrapyrrole ring and carbon chain tail, typically have two absorption peaks, one in the blue and one in the red (shown as the green absorption spectrum in Figure 2-27).
- The *Carotenoids* (beta carotene), which are structurally long double-bonded carbon chains with broad single peaked absorption spectra in the blue-green wavelength range (shown as the black and red absorption spectra in Figure 2-27).
- The *Phycobilipigments* (*phycoerithrobin*), which are structurally in between with chains of pyrrole rings and have broad absorption peaks in the yellow to orange wavelength range (shown as the blue absorption spectrum in Figure 2-27).

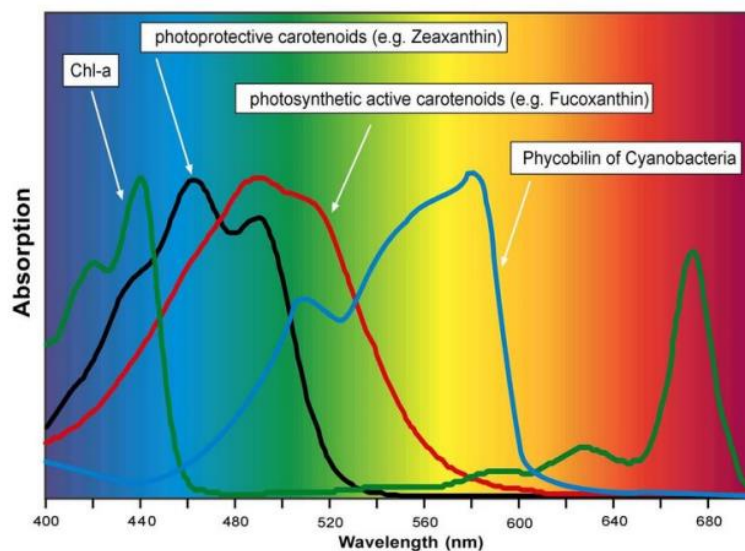


Figure 2-27 The absorption spectra major groups of phytoplankton pigments [64].

These pigments can also be found in phytoplankton bacteria, such as red-colored picocyanobacteria, which absorb the available green light with their pigment phycoerythrin effectively (Figure 2-28), and green-colored phytoplankton species (like green cyanobacteria and green algae) which absorb the available red light with pigments such as phycocyanin and chlorophylls (Figure 2-28).

On the other hand, low-light adapted *Prochlorococcus* strongly absorbs the available blue light using the pigments divinyl-chlorophyll (Figure 2-28) [60].

As a conclusion, in order to calculate the light absorption coefficient due to phytoplankton, the type, as well as its concentration must be known. Nevertheless, if the kind of plankton is unknown, an approximated value can be calculated with the absorption spectrum shown in Figure 2-26 (b).



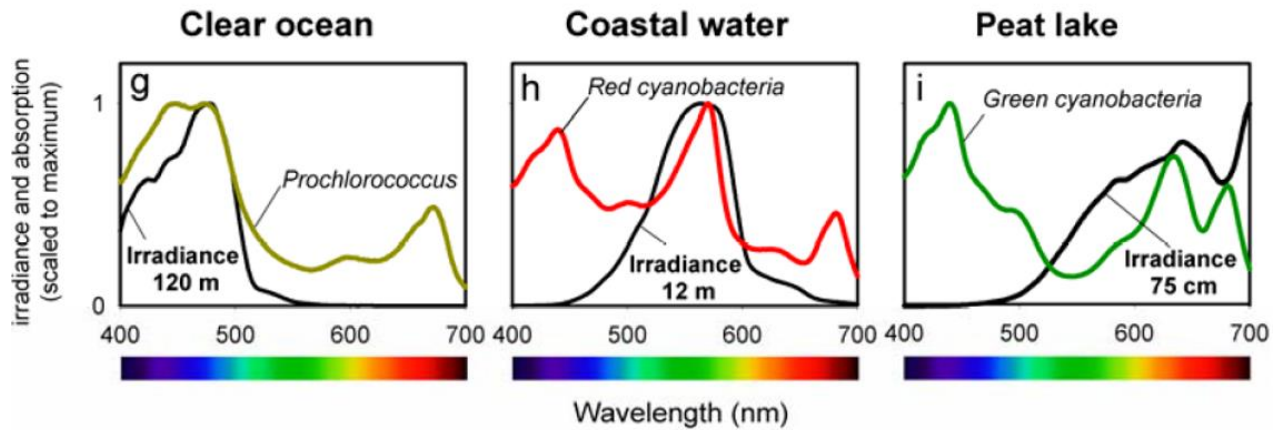


Figure 2-28 Irradiance and absorption of different species of phytoplankton depending of light wavelength. The phytoplankton community was sampled at (g) 120 m depth, in the subtropical Pacific Ocean dominated by low-light adapted *Prochlorococcus*, (h) 12 m depth in the Baltic Sea, dominated by red-colored *Synechococcus* strains (i) 75 cm depth in Lake Groote Moost, dominated by green cyanobacteria and green algae [60].

### 2.3.2.3 Colored Dissolved Organic Matter

Colored Dissolved Organic Matter (CDOM), also known as *yellow substances* and as ‘*gilvin*’ or ‘*gelbstoff*’ in the optics literature [57] [60] [65] are mainly dominated by terrestrial sources. This is the reason why their concentrations are lower on open ocean waters than in coastal, where land drainage is considerable. In [66], a study carried out in the northern region of the Gulf of Mexico, encompassing Mississippi, Louisiana, and parts of Texas coast. The study used field and satellite ocean color data along with the outputs from a numerical model. Figure 2-29 shows how the coastal and confined waters experiment more light absorption due to CDOM concentration than open waters.

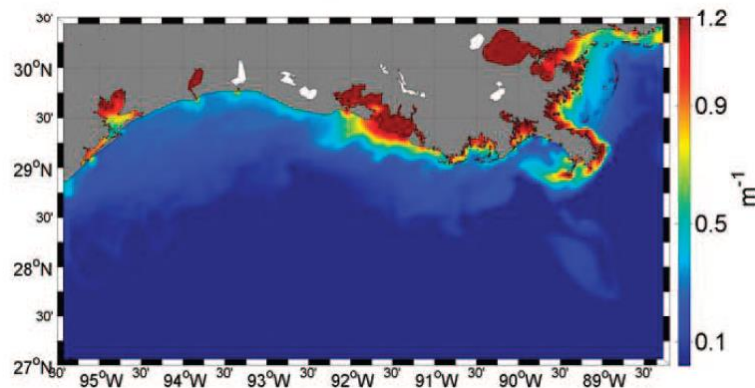
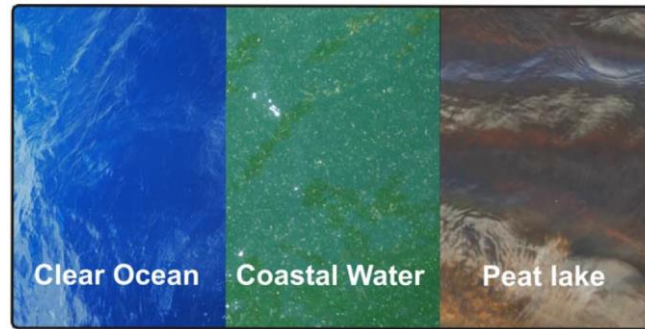


Figure 2-29 Sea model-derived CDOM absorption map for 18 October 2005, at 1900 h UT [66].

In addition, CDOM concentration increases because of global warming [44]. The higher the concentration of *gilvin* in a water body, the more turbid the water is, and thus, the more light it absorbs. With increasing turbidity the color of water shifts from blue (clear oceans), via green (coastal water), towards brownish red (peat lakes), sees Figure 2-30.



**Figure 2-30** Different colors of water depending on 'gelvin' concentration. It can be seen how, as turbidity increases, the color of water shifts from blue, via green, towards brownish red [60].

Several investigations indicate that CDOM absorption increases exponentially towards shorter wavelengths [59]. In [67], absorption properties of colored dissolved organic matter (CDOM) are presented, sampled in six different water bodies along extreme altitudinal, latitudinal, and trophic state gradients. These sites are in Norway: the mesotrophic Lysefjord (LF), Samnangerfjord (SF), and Røst Coastal Water (RCW); in China: the oligotrophic Lake Namtso (LN) and the eutrophic Bohai Sea (BS); and in Uganda: the eutrophic Lake Victoria (LV), shown in Figure 2-31.

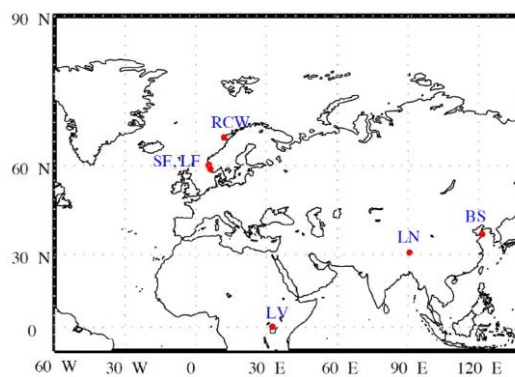


**Figure 2-31** Map indicating the six sites where absorption properties of CDOM were sampled: LV = Lake Victoria, Uganda; LN = Lake Namtso, Tibet; BS = Bohai Sea, China; SF = Samnangerfjord, Norway, LF = Lysefjord, Norway; RCW = Røst Coastal Water, Norway [67].

The results of the measurement of the absorption properties of CDOM are shown in Figure 2-32. It can be concluded, that light absorption due to CDOM is exponentially higher at smaller wavelengths, no matter where you are. It can also be noticed that, CDOM seems to be originated from terrestrial sources in LF, SF, BS, and LV, resulting in higher absorption than in RCW and LN, where CDOM has an autochthonous origin [67].

To calculate CDOM absorption, the type and its concentration must be known as well, in a similar way to how phytoplankton absorption coefficient is calculated. Nevertheless, if that information might not be available, an approximated value can be calculated with the absorption spectrum shown in Figure 2-33.

It is worth bearing in mind that CDOM concentration is also related to the phytoplankton composition, given the available light changes from green to red. Thus, in addition to the strong positive effect of global warming, promotes the dominance of green cyanobacteria, affecting light absorption as well [60].



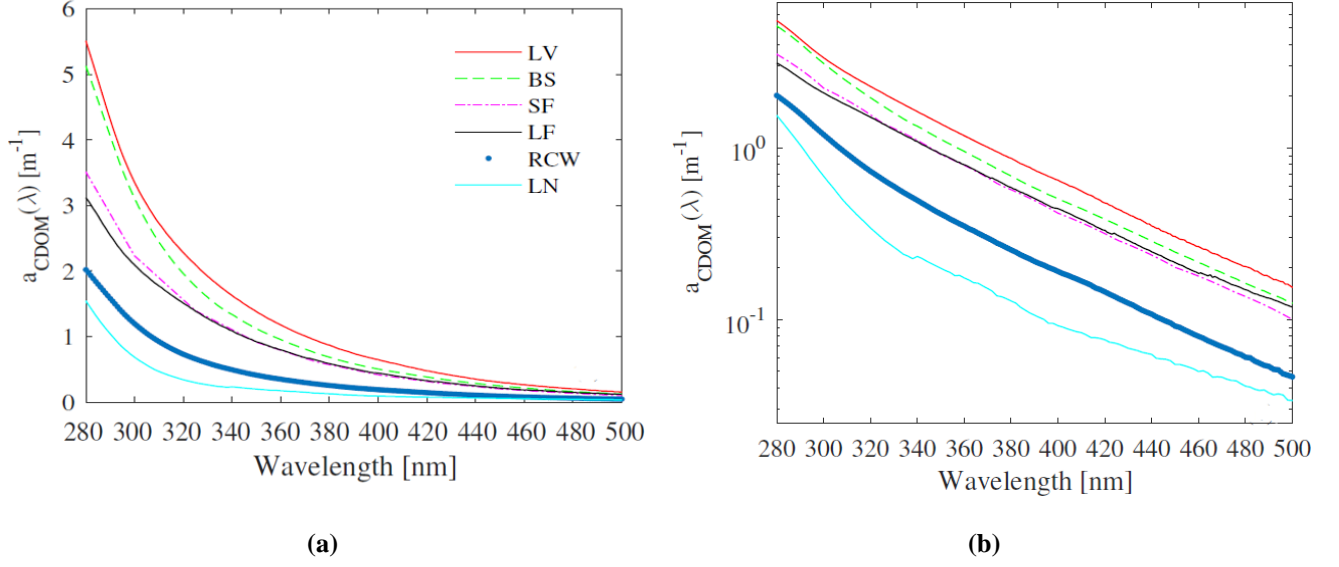


Figure 2-32 (a) Plots of CDOM absorption spectra for different locations (b) Semi-log plots of the CDOM absorption spectra in (a) [67].

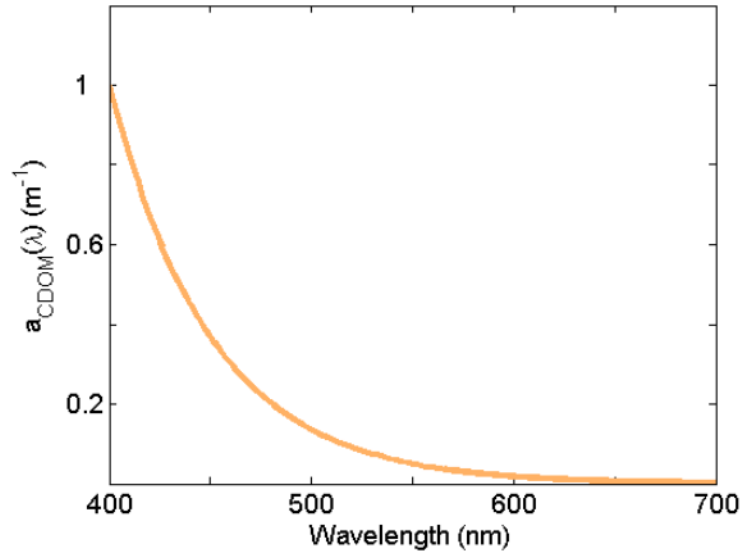


Figure 2-33 Generic absorption spectrum of colored dissolved organic matter (CDOM) for mixed composition [42].

#### 2.3.2.4 Non-algae particles

*Non-algae Particles* (NAP) are also known as ‘tripton’ or as non-chlorophyllous particles [57] [60] [65]. This category englobes suspended material that is neither phytoplankton nor its associated detrital matter, such as sediments in suspension detritus or mineral particles. Therefore, NAP could be studied as a composition of detritus or mineral particles. Detritus particles are non-living particles of organic matter, including dead cells, fecal pellets, dead bacterial and shell, among others. They constitute an important fraction of the total IOPs of a water body, regarding absorption and scattering [58].

Mineral particles may come from external sources such as erosion, sediment suspension, atmosphere dust, coastal erosion, or river discharge. They have as many different and important properties as biological particles, even though there are few studies on this field. The results of one of these few studies on mineral’s scattering and absorption properties is shown in Figure 2-34. There is widespread agreement that absorption by minerals can range from highly absorbing in the blue through exponential decrease with increasing wavelength, to almost non-absorbing and spectrally flat [58].

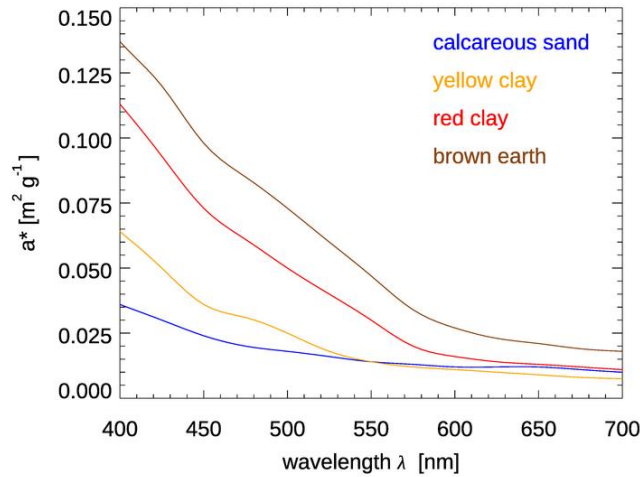


Figure 2-34 Mass-specific absorption coefficients  $a^*(\lambda)$  for four types of mineral. Measured data obtained from [68].

Nevertheless, this division between organic and inorganic particles is not always made. Many researches study non-pigment suspension absorption as a whole, such as [69], where it is concluded that NAP spectrum characteristics are relatively stable. Figure 2-35 shows the absorption spectrum of non-algae particles, where the highest absorption level is reached at lowest wavelengths.

As stated before, different investigations have illustrated that NAP has relatively stable absorption characteristics [70], so light absorption is mainly going to depend on its concentration. In [70], a study on the natural variability of absorption coefficients was conducted in a deep artificial lake (Lake Qiandaohu, China). This study showed that non-chlorophyllous particles absorption coefficient near the surface exceeds the one in deep waters, given the concentration of inorganic compounds in the superficial water is higher due to runoff inlet. The main reason for this variation on concentration is that these areas are most affected by other external sources [70]. As a result, it was demonstrated that concentrations of the principal inorganic constituents of the oceans vary primarily in response to an exchange of water (precipitation and evaporation), following a seasonal pattern [70], with relative concentrations remaining nearly constant [71].

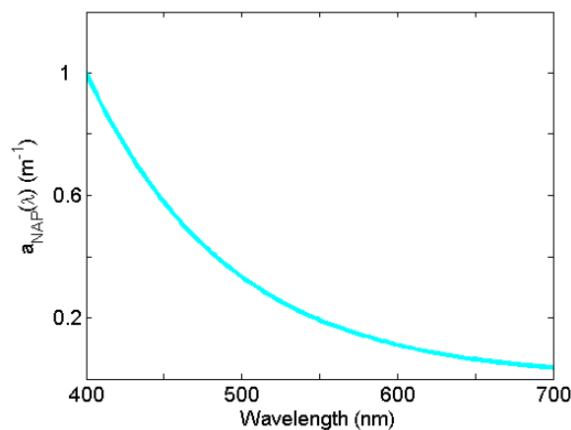
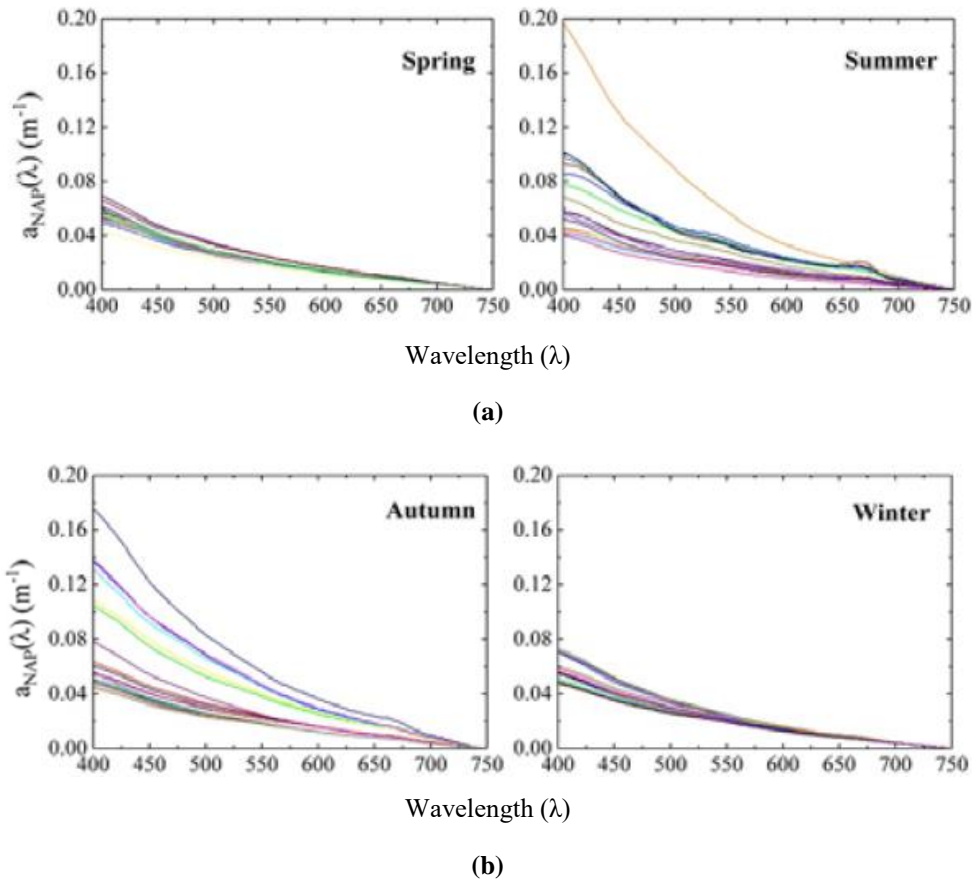


Figure 2-35 Absorption spectrum of non-algae particles [58].



**Figure 2-36 Result of the measurement of the absorption spectrum of non-algae particles in different spots of the artificial Lake Qiandaohu [70]. In can be observed how it follows a seasonal pattern.**

Regarding overall absorption, it can be inferred that it depends on many specific and changing factors. Therefore, the minimum attenuation window is not the same for every water type. Table 2-4 shows the ideal transmission wavelengths for different water types on a general line [57].

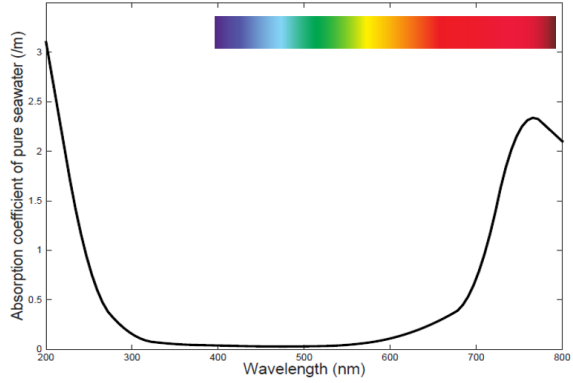
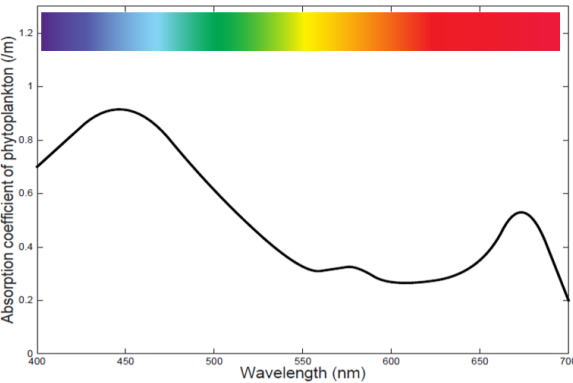
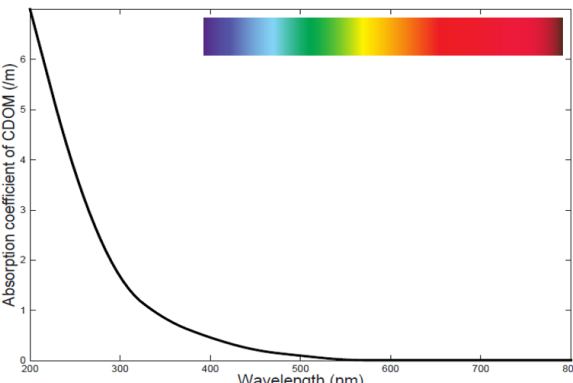
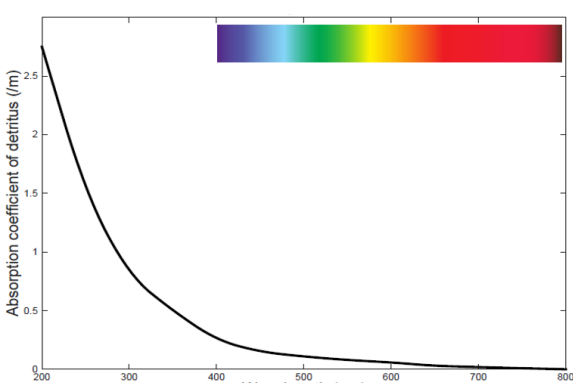
Water Type	Chlorophyll concentration	Operating wavelength
Pure sea/clear ocean	Less	400-500 nm (blue-green)
Coastal ocean	High	520-570 nm (yellow-green)
Turbid harbor	Very high	520-570 nm (yellow-green) <sup>2</sup>

**Table 2-4 Ideal transmission wavelength for different water types under general conditions [57].**

### 2.3.2.5 Summary

Table 2-5 summarizes the effects of different compositions on absorption coefficient. Depending on the concentration of each of them, a different wavelength will be optimal for UOWC. For example, although as a general guideline in ocean waters blue light is absorbed the least, if the concentration of phytoplankton results in a greater absorption in the blue region than seawater in the red, then, a red light source will be the most appropriate choice. This reflects the complexity of a versatile and functional UOWC system.

<sup>2</sup> Implies performance limited by absorption and scattering coefficients.

Composition	Absorption coefficient	Absorption spectra
Pure Water	<p>Depends on <math>\lambda</math>.</p> <p>At different constant temperature and pressure, it changes at a negligible manner.</p>	
Phytoplankton	<p>Depends its type and concentration, which can quickly changes depending on the availability of carbon dioxide, sunlight and nutrients.</p> <p>Due to its dependence on sunlight, it decreases with depth and it is very unusual to be found deeper than 200 m.</p> <p>Its color indicates the light <math>\lambda</math> they absorb the least.</p>	
CDOM	<p>Depends on its type and concentration.</p> <p>Mainly dominated by land-based sources, so their concentrations are lower in deep oceans than in coastal waters.</p>	
NAP	<p>Depends on their type and concentration, which vary in response to exchange of water and following a seasonal pattern, with relative concentrations remaining almost constant.</p> <p>Its concentration is very high in turbid harbors, high in coastal oceans and less in clear oceans.</p>	

**Table 2-5 Summary of absorption characteristics of seawater. Absorption spectra has different scales depending on how much and which wavelengths absorption affects.**

### 2.3.3 Scattering

Both absorption and scattering are equally important to the prediction and understanding of underwater light propagation [58]. Scattering is a phenomenon consisting on the deviation of light photons, which significantly impairs the propagation of light under water. Photons are spread toward random directions so that some of them are not received, and others may be delayed due to following different propagation paths. Thus, it leads to multi-path fading, time-jitter, and inter-symbol interference phenomena [72].

Scattering can be *elastic* or *inelastic*. It is elastic when the kinetic energy of incident photons is conserved, whereas it is inelastic when both kinetic energy and wavelength change. This section will explain elastic scattering in detail, which refers to light direction changes with constant wavelength. It can be graphically seen in Figure 2-37, which shows the geometry for defining the *Volume Scattering Function* (VSF).

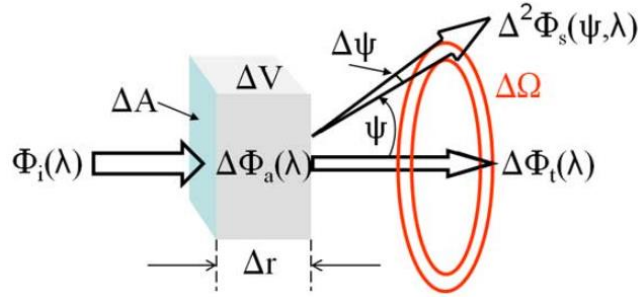


**Figure 2-37** Geometry for defining the volume scattering function. “ $\Phi_i(\lambda)$ ” is the incident power into an area “ $\Delta A$ ”; “ $\Delta\Phi_a(\lambda)$ ” is the absorbed power in distance “ $\Delta r$ ”, “ $\Delta^2\Phi_s(\psi, \lambda)$ ” is the power scattered into the annular ring of solid angle “ $\Delta\Omega$ ”. “ $\Delta\Phi_t(\lambda)$ ” is the transmitted power [58].

Scattering is described by the VSF that calculates the angular distribution of non-polarized light scattered from its initial direction into another, at a wavelength “ $\lambda$ ”. In order to calculate the VSF in seawater, two assumptions must be made. First, the medium is considered isotropic<sup>3</sup>, so its influence on light is the same in all directions. In second place, particles are supposed to be randomly oriented by turbulence and incident light is assumed non-polarized [58].

When the medium is isotropic, scattering does only depend on the angle “ $\psi$ ” between the incident and final direction, given it is an azimuthally symmetric process. This symmetry is found in all processes consistent with the previous assumptions. Some examples are spherical or randomly oriented non-spherical particles with non-polarized incident irradiance, as well as most cases of the turbulent aquatic environment. In these cases, the VSF “ $\beta(\psi, \lambda)$ ” can be defined as the radiant intensity “ $dI(\psi, \lambda)$ ”, emanating with an angle “ $\psi$ ” from an infinitesimal volume “ $dV$ ” element for a given incident irradiance “ $E(0, \lambda)$ ”, which is calculated with Eq.(9) [58].

$$\beta(\psi, \lambda) = \frac{1}{E(0, \lambda)} \frac{dI(\psi, \lambda)}{dV} (m^{-1}sr^{-1}) \quad (9)$$

Where:

- $\beta(\psi, \lambda)$ , measured in  $(m^{-1}sr^{-1})$ : Volume scattering function
- $dI(\psi, \lambda)$ , measured in  $(Wsr^{-1}nm^{-1})$ : Radiant intensity.
- $E(0, \lambda)$ , measured in  $(Wm^2nm^{-1})$ : Incident irradiance.
- $dV$ , measured in  $(m^3)$  : Infinitesimal volume element.
- $\psi$ : Angle between transmitted power and scattered power.

<sup>3</sup> A medium whose electromagnetic properties such as the refractive index are the same in all directions.

The scattering coefficient “ $b(\lambda)$ ” is calculated by integrating the VSF over all angles, as it measures the overall magnitude of scattered light regardless of its angular distribution. Eq.(10) shows a simplification of this integration.

$$b(\lambda) \equiv 2\pi \int_0^\pi \beta(\psi) \sin\psi d\psi \quad (10)$$

Another characteristic parameter is the backscattering coefficient, defined as the total light scattered into the hemisphere from which light has originated, as shown in Eq.(11).

$$b_b \equiv 2\pi \int_{\frac{\pi}{2}}^\pi \beta(\psi) \sin\psi d\psi \quad (m^{-1}) \quad (11)$$

Usually, elastic scattering occurs when the refraction index changes from one spatial location to another, as it happens with irregular particles, pure water (because of its molecules) and turbulence. In Figure 2-38, it can be noticed how the turbulence induced by fluctuations in temperature causes the light to scatter.



**Figure 2-38 Hydrothermal vent.** It is an opening on the seafloor that emits hot, mineral-rich solutions. The reason the image blurry in the marked area is because of the scattering induced by temperature fluctuations [73].

As commented before, scattering is an IOP because it does only depend on the water body nature. Therefore, the scattering coefficient “ $b(\lambda)$ ” is calculated by adding the absorption coefficients of all optically active substances present on a water body in an equivalent proportion to its concentration, as it is shown in Eq.(12). As these optically active particles are more abundant in shallow waters, their effect in scattering is more pronounced in coastal areas than in open oceans [57].

$$b(\lambda) = b_w(\lambda) + C_{phyt} * b_{phyt}(\lambda) + C_{NAP} * b_{NAP}(\lambda) \quad (12)$$

Where:

- $b_w(\lambda)$  : Scattering coefficient of pure seawater.
- $C_{phyt}$  : Concentration of phytoplankton.
- $b_{phyt}(\lambda)$  : Scattering coefficient of phytoplankton.
- $C_{NAP}$  : Concentration of non-algae particles.
- $b_{NAP}(\lambda)$  : Scattering coefficient of non-algae particles.

For Eq.(12), all the optically active constituents of the Ocean that affect scattering have been accounted. Each of them is addressed in turn along this subsection.



### 2.3.3.1 Pure sea water

The elastic scattering of light in pure seawater is due to a change in the dielectric constant, which can be caused by random motion of water molecules besides changes in salinity, temperature, and, to a lesser extent, pressure. An empirical model for the calculation of seawater scattering coefficient because of salinity fluctuations is shown in Figure 2-39 [74].

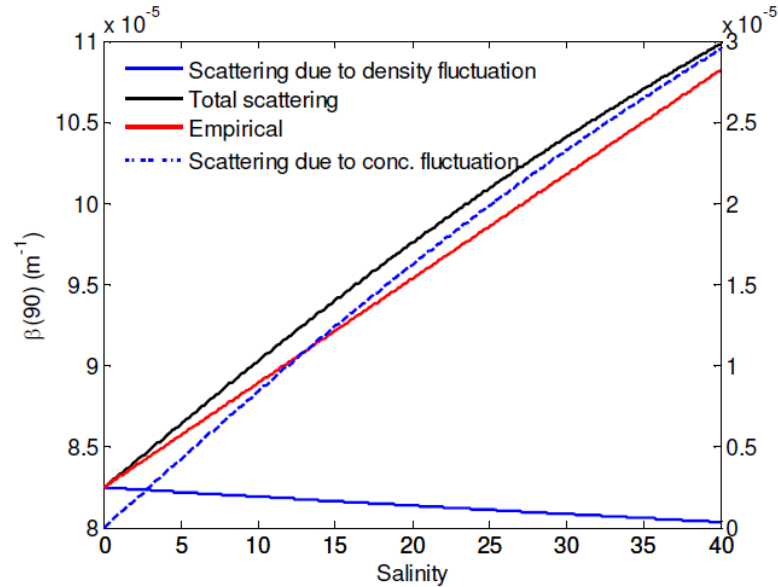


Figure 2-39 Scattering coefficient of seawater as a function of salinity calculated at 546 nm and 20°C, which is a contribution of two factors: density and concentration fluctuation. The empirical variation is calculated with an equation based on the interpretation of several measurement experiments [74].

Different models have been developed to estimate pure water scattering coefficient, such as the Morel model in [75] and the Zhang model in [74], which are shown in Figure 2-40.

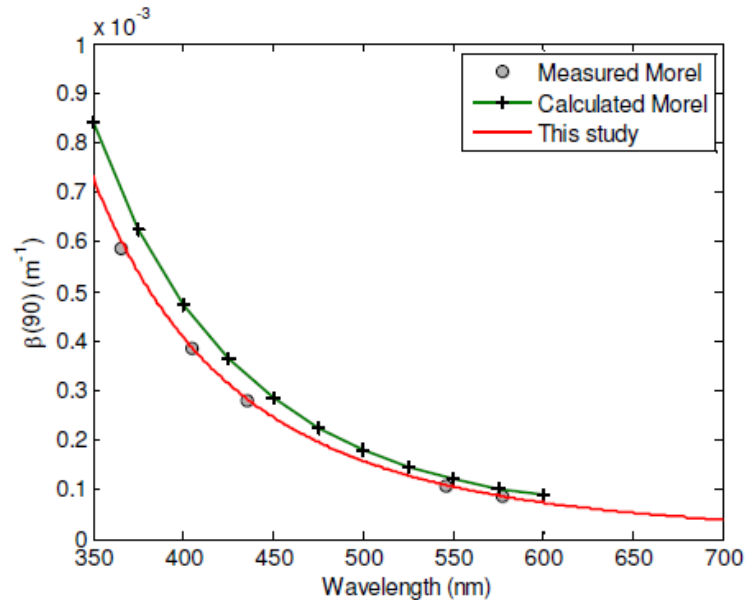
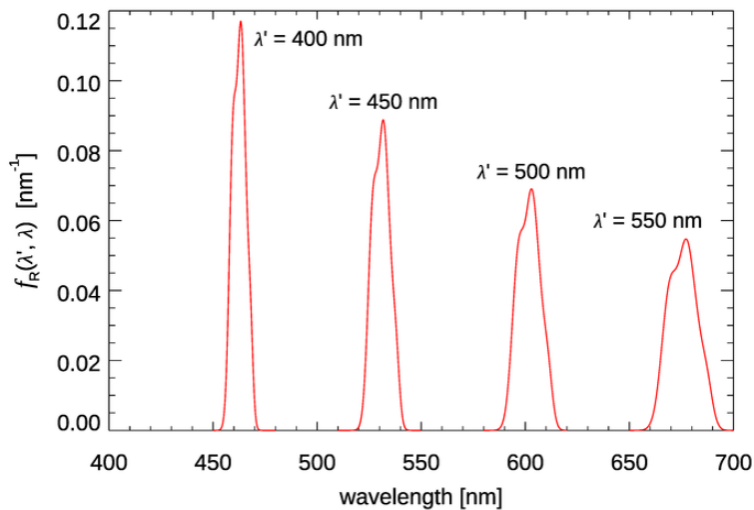


Figure 2-40 Comparison of Morel model [75] and Zhang [74] pure water scattering coefficient model with experimental data measured in [75].

Pure water molecules also scatter light inelastically, which is known as *Raman scattering*. On the one hand, in elastic scattering (also known as *Rayleigh scattering*) light excites a molecule in its ground state to a higher “virtual” energy level, and immediately afterwards, light of the same wavelength is emitted decaying back to its initial state. On the other hand, under inelastic scattering, the emitted light

has a longer wavelength (lower energy) than the incident light, so the molecule's final energy level is greater than the initial [58].

Figure 2-41 shows the Raman emission functions “ $f_R(\lambda', \lambda)$ ” for four incident wavelengths “ $\lambda'$ ”. As the incident wavelength  $\lambda'$  increases, the emission band becomes broader and the wavelength shift becomes larger. It can be noticed that excitation at 400 nm emits light centered at round 460 nm, a shift of 160 nm; while excitation at 550 nm results in an emission centered at about 680 nm, a shift of 130 nm.



(a)

The colors of the visible light spectrum		
color	wavelength interval	frequency interval
red	~ 625–740 nm	~ 480–405 THz
orange	~ 590–625 nm	~ 510–480 THz
yellow	~ 565–590 nm	~ 530–510 THz
green	~ 500–565 nm	~ 600–530 THz
cyan	~ 485–500 nm	~ 620–600 THz
blue	~ 440–485 nm	~ 680–620 THz
violet	~ 380–440 nm	~ 790–680 THz

(b)

Figure 2-41 (a) The Raman emission functions for four excitation wavelengths [58] and (b) the corresponding wavelengths for the colors of the visible light spectrum.

If pure water molecules influence on scattering is compared to theirs on absorption, it can be easily concluded that they have a much more significant effect on absorption than they do on scattering (it is showed in Figure 2-42).

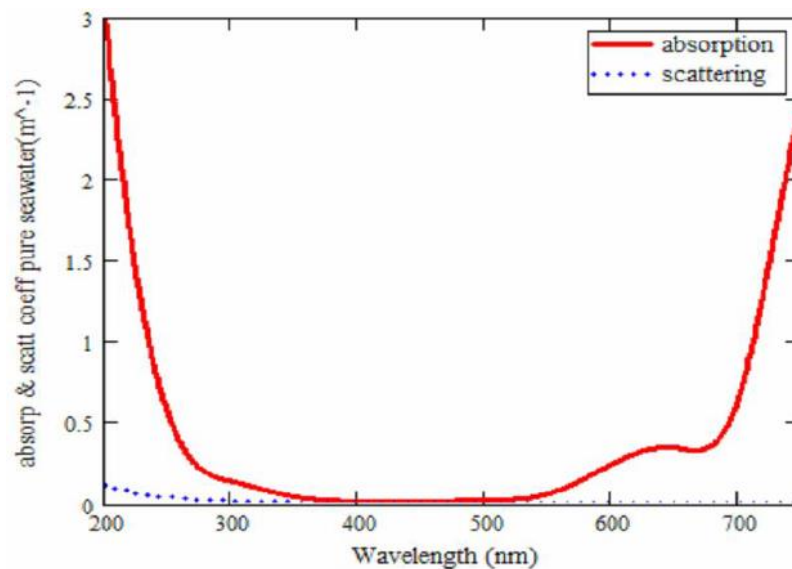
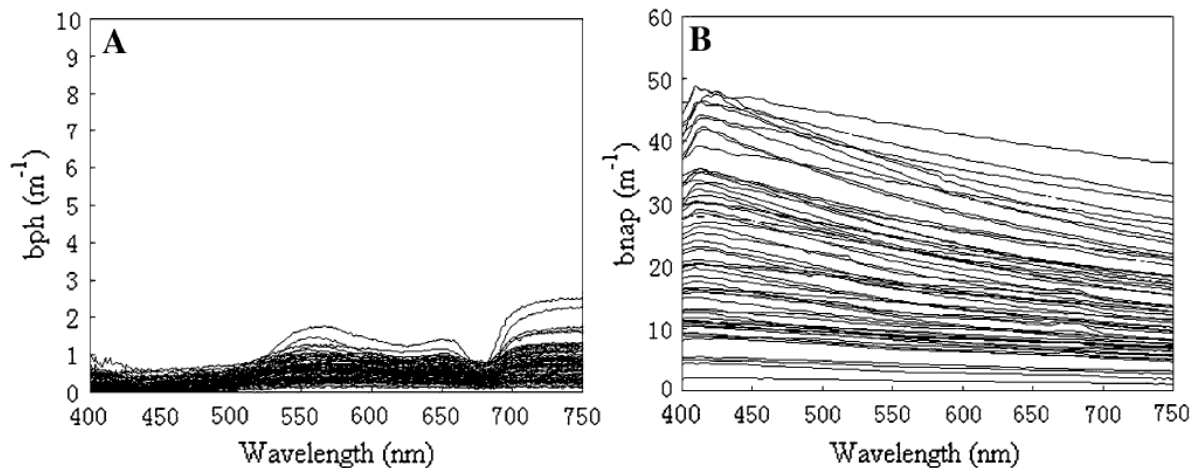


Figure 2-42 Absorption vs. Scattering because of pure seawater [76].



### 2.3.3.2 Phytoplankton

Phytoplankton scattering properties depend on the size, shape and refractive index of all components of its cell. Scattering and backscattering coefficients, as well as the volume scattering function of phytoplankton can be directly measured, as it has been done in [77] [78] [79]; or calculated from theoretical models, like the Mie Scattering Theory [80]. When compared to other particles, phytoplankton scatters relatively little light (Figure 2-43), given its strong absorptive properties and high water content. Nevertheless, there are some exceptions such as coccolithophores<sup>4</sup>, which are so remarkable scatters that their blooms can be seen from the space [81].



**Figure 2-43 Results of (A) phytoplankton and (B) non-algae particles scattering coefficients measured in Lake Taihu. Their spectral curves can be compared, and it is clearly shown how the effect of NAP on scattering is remarkably greater than the one corresponding to phytoplankton [82].**

Since beam attenuation is the result of absorption and scattering, scattering is the difference between attenuation and absorption of the light, because an absorbed photon is not scattered. Therefore, the absorptive properties of the cell give shape to the spectral scattering. Consequently, the scattering spectra of the same species will generally be an inverse picture of its absorption spectra. Besides, this can also be observed in backscattering [83].

Few researches have been conducted in order to calculate the angular distribution of scattering for phytoplankton, such as [84], [85] and [86]. In [78], four different phytoplankton (whose characteristics are described in

Table 2-6) species were studied using a new effective measuring method that included adding spectral information, a novel optical design of the sample container, and two new ways of eliminating unwanted reflections. The VSF spectra are plotted Figure 2-44.

From this study, it can be concluded that the new measuring method is very effective despite the noticeable noise in the angular range from 90° to 171°, due to not having an accurate sensitivity. As each VSF has a characteristic shape for each type of alga, it could be a valuable database for future phytoplankton recognition and classification. It can be observed that the VSFs for *Chaetoceros Calcitrans* and *Phaeodactylum tricornutum* show less wavelength dependence than the *Synechococcus*. This dependence, although there is not enough evidence to be corroborated, could be because the size parameter of a given phytoplankton species increases as the wavelength decreased. Moreover, the shoulders of the VSF depend on the wavelength being is more forward peaked at shorter wavelengths. As a matter of fact, despite the *Chaetoceros calcitrans*'s cylindrical shape and the *Phaeodactylum*

<sup>4</sup> Phytoplankton that secretes small calcium carbonate scales.

tricornutum's needle shape, their VSFs are very alike, and have similar extent in all directions [78]. Therefore, the only clear conclusion is that each phytoplankton specie has a unique VSF spectra.

Name	r [ $\mu\text{m}$ ]	std [ $\mu\text{m}$ ]	Concentration [ $\mu\text{m}$ ]	Cell wall	Vacuoles	Shape
Chaetoceros calcitrans	1,82	0,22	$1,7 \cdot 10^4$ /ml	$\text{SiO}_2$	Liquid	Cylindrical
Phaeodactylum tricornutum	1,72	0,23	$5,9 \cdot 10^4$ /ml	$\text{SiO}_2$	Liquid	Needle
Protoceratium reticulatum	12,1	2,7	$5,7 \cdot 10^4$ /ml	Cellulose	Not present	Spheroidal
Synechococcus sp.	0,85	0,12	$2,2 \cdot 10^4$ /ml	Murein, lipopolysaccharides	Not present	Spherical

**Table 2-6** Cell size “r” is the mean radius and “std” is the standard deviation of the radius), concentration, shape and composition of phytoplankton species investigated in [78].

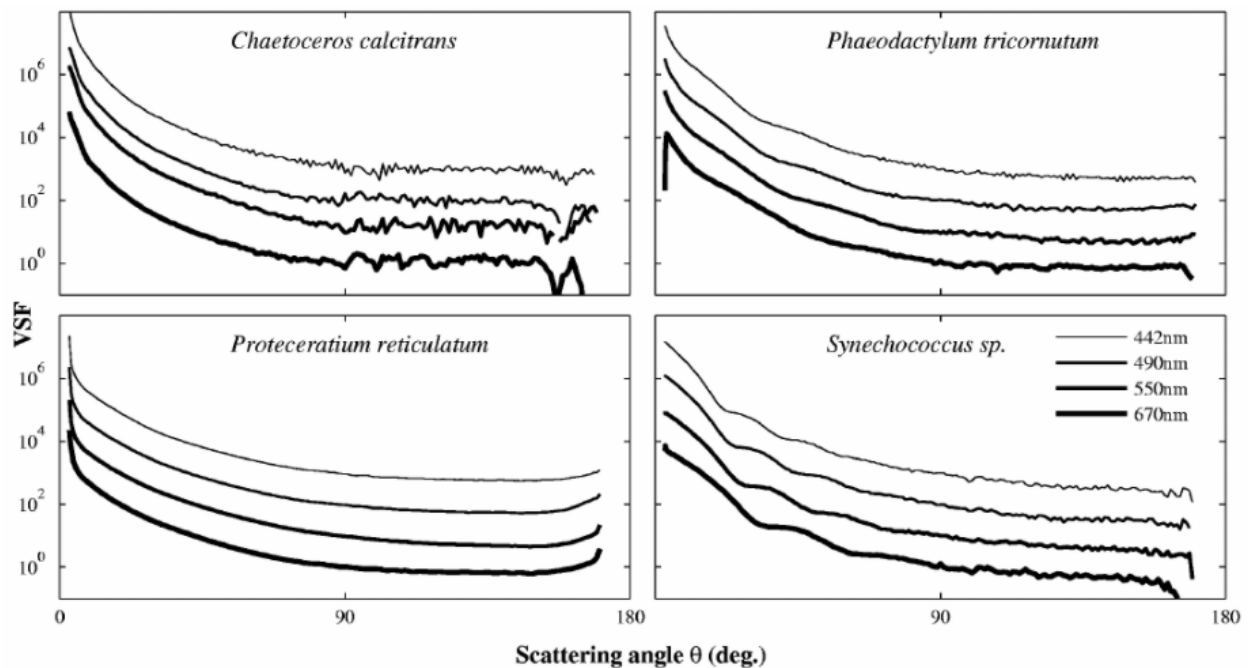


**Figure 2-44** VSFs for the four species of phytoplankton investigated at four different wavelengths in [78]. In order to make the plots of the VSFs distinguishable for each different wavelengths, they have been multiplied by the constant factors of 1000, 100, 10, and 1.

Figure 2-45 shows another research conducted in [77] on other different phytoplankton species, where more scattering results for different phytoplankton species. From this study, it is concluded that scattering is not easily predicted from the morphology of the particles, given spherically and cylindrically species could produce similar results, while two spherical species may yield quite different results. In general, cylindrically celled species have a higher probability of oscillations in scattering function, probably because of their narrower size distribution compared to other cell shapes. Besides, internal structural features, such as gas vacuoles, play an important role in the scattering behavior [77].

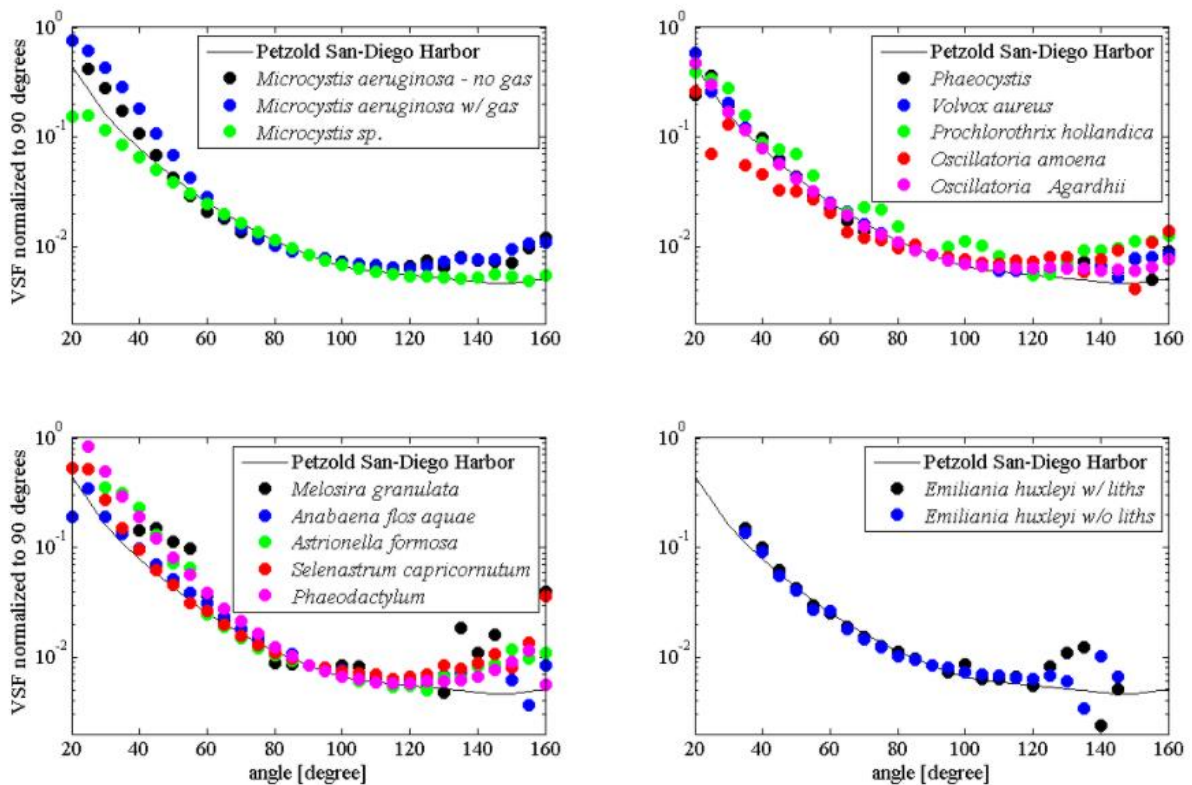


Figure 2-45 Scattering by different phytoplankton species in comparison with the San-Diego Harbor VSF of [84]. Data from [77] and plots from [58].

To sum up, it has been demonstrated how the scatter produced by phytoplankton depends on each specie, and may affect all wavelengths. It can also be noticed that most of the light is scattered forward, with an angle less than  $90^\circ$ , while only a small part of the photons is scattered backward.

### 2.3.3.3 Colored Dissolved Organic Matter

Despite all research and studies conducted on scattering, CDOM contribution to scattering is controversial. Although theory suggest that if CDOM is abundant enough it could contribute to scattering, especially to backscattering, experimental measurements do not demonstrate this fact. Given there is no observational evidence about the contribution of CDOM to scattering [87], it is usually neglected [58].

### 2.3.3.4 Non-algae particles

As stated before, NAP includes detritus and minerals. Even though NAP and CDOM absorption coefficients are very similar, scattering spectra are very different. Figure 2-46 shows the different scattering coefficient for different types of NAP found in the investigated water body in Great Lake, China [58]. It can be observed how in specific non-algae particles, scattering decreases from blue to red, although with a couple of notable exceptions where it shows featureless dependence on wavelength. This graphic shows the same data as the one shown in Figure 2-43 (b), regardless each type of NAP is represented by a different color, when it was mentioned that NAP has a more notorious effect on scattering than phytoplankton.

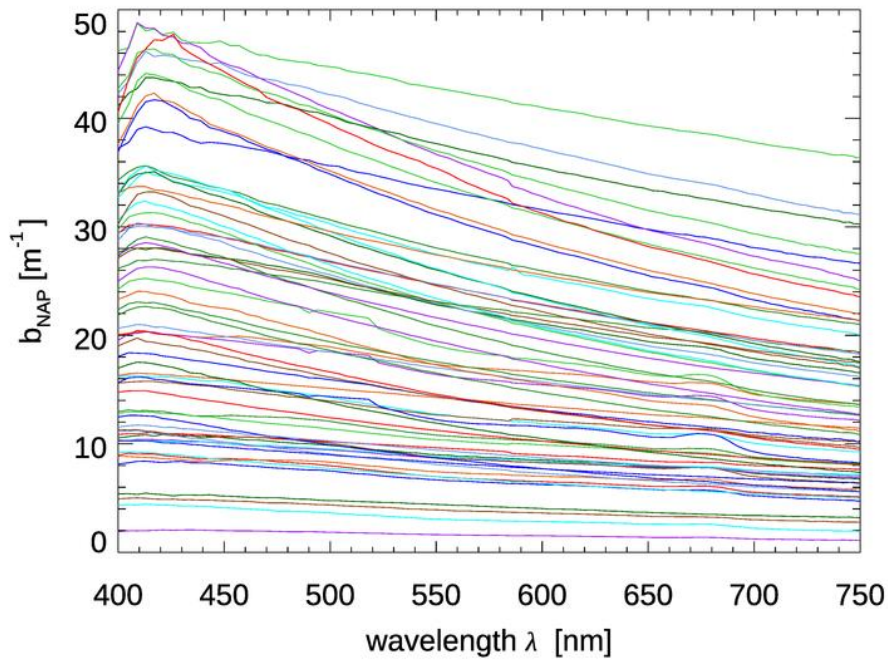


Figure 2-46 Scattering coefficient spectra from Great Lake (Taihu), China [75]. Data from [82].

Research conducted on minerals have measured the scattering coefficients “ $b^*(\lambda)$ ”, the results of and are in shown in Figure 2-47 and Figure 2-48 respectively. It can be observed how scattering decreases while wavelength increases, even though there are notable exceptions such as brown earth, which has its peak values at green wavelengths. Now that their characteristic spectrum is known, it should be accounted that scattering coefficients could be modeled with different functions.

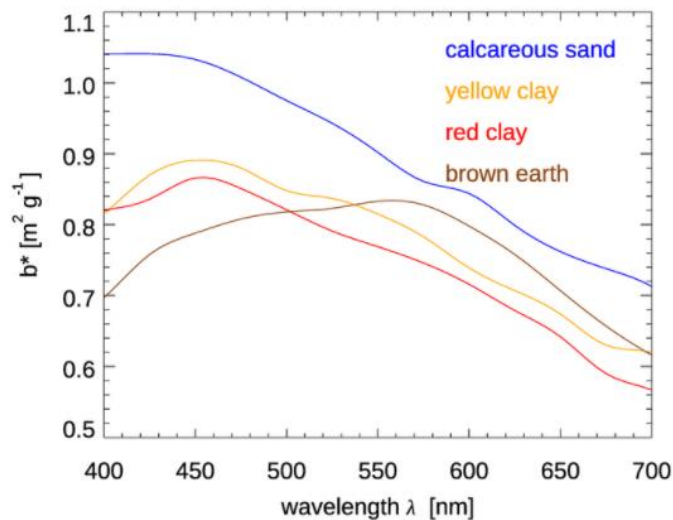
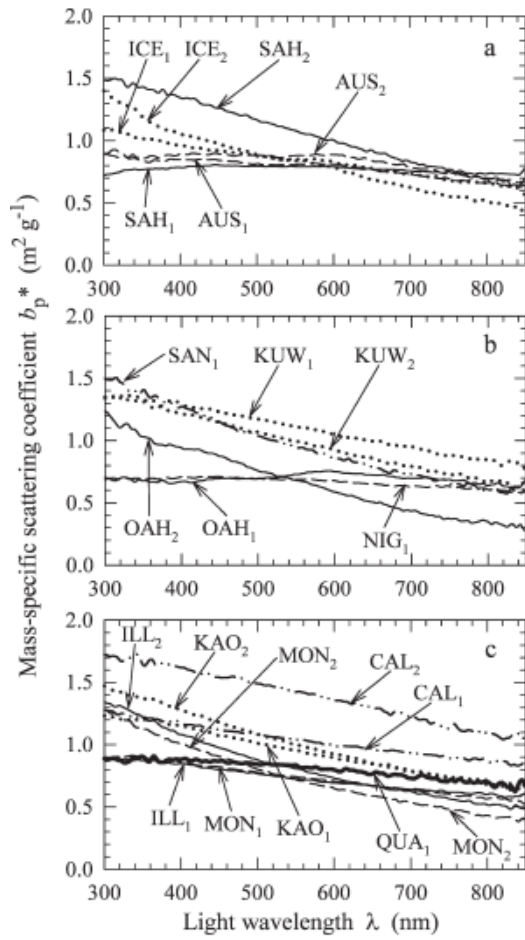


Figure 2-47 Mass-specific scattering coefficients  $b^*(\lambda)$  for four types of mineral. Measured data obtained from [68].

Minerals analyzed in the laboratory [88] were made with two different particle size distributions, indicated with subscripts “1” and “2” in the sample identifier (ID). Figure 2-48(b) gives the values for the concentration of suspended particulate matter (SPM), and, in some cases, the particulate organic carbon (POC) concentration of the particle samples. Figure 2-48(a) shows the mass-specific scattering coefficients “ $b^*(\lambda)$ ” of the measured particles.



(a)

ID	Description	Origin	SPM (g m <sup>-3</sup> )	POC (g m <sup>-3</sup> )
ICE <sub>1</sub>	Ice-rafted particles	Glacier runoff, Kongsfjord, Spitsbergen, Norway	28,51	0,44
ICE <sub>2</sub>			22,37	0,44
SAH <sub>1</sub>	Atmospheric dust from Sahara	Red rain event, Villefranche-sur-Mer, France, Nov 1996	43,43	1,28
SAH <sub>2</sub>			19,47	1,28
AUS <sub>1</sub>	Surface Soil Dust	Cliff shore, Palm Beach north of Sydney, Australia	32,03	0,87
AUS <sub>2</sub>			24,05	0,64
SAN <sub>1</sub>	Atmospheric dust	San Diego, California	17,08	2,73
KUW <sub>1</sub>	Surface Soil Dust	Kuwait (eastern part, close to ocean)	23,36	6,27
KUW <sub>2</sub>			23,10	6,27
OAH <sub>1</sub>	Surface Soil Dust	Oahu Hawaii Islands	31,67	1,12
OAH <sub>2</sub>			18,05	0,62
NIG <sub>1</sub>	Surface Soil Dust	San Diego, California	17,08	2,73
ILL <sub>1</sub>	Illite	Source Clay Minerals Repository, University of Missouri	37,71	0,86
ILL <sub>2</sub>			26,53	0,86
MON <sub>1</sub>	Ca-montmorillonite	Source Clay Minerals Repository, University of Missouri	38,48	0,73
MON <sub>2</sub>			28,52	0,73
CAL <sub>1</sub>	Calcite	Natural crystal	26,48	1,28
CAL <sub>2</sub>			12,6	1,28
KAO <sub>1</sub>	Kaolinite (poorly crystallized)	Source Clay Minerals Repository, University of Missouri	28,34	0,73
KAO <sub>2</sub>			23,3	0,73
QUA <sub>1</sub>	Quartz	Natural crystal	14,17	1,28

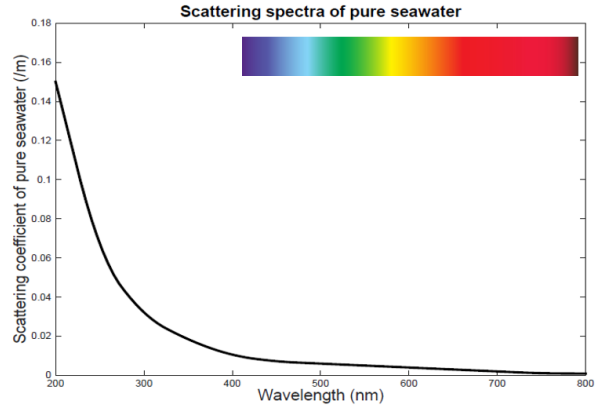
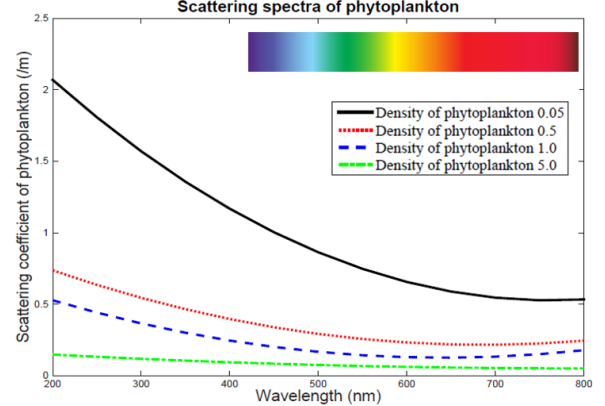
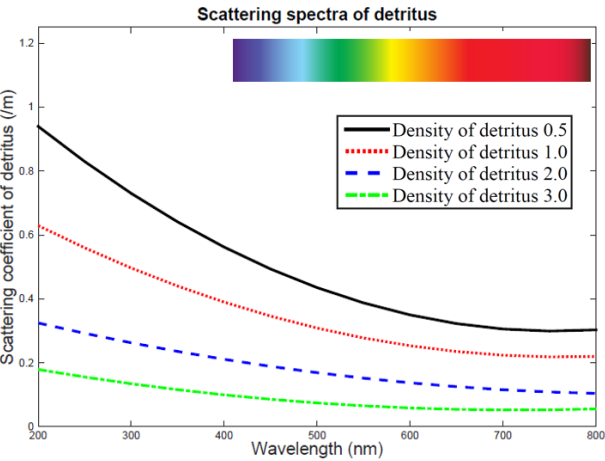
(b)

**Figure 2-48 (a) Measured mass-specific scattering coefficients “ $b^*(\lambda)$ ” of particles for samples of mixed particulate assemblages (top and middle graph) and single-mineral species (bottom graph) and (b) their description, origin, suspended particulate matter (SPM) and particulate organic carbon (POC) [88].**

The magnitude of the mass-specific scattering coefficients in Figure 2-48(a) is relatively high compared with other estimates [89]. It can be noticed that most spectra for the mixed samples scatter near the IR region. Theoretical modeling predicts as well that the increased proportion of large particles, high-density mineral particles, or both will reduce the magnitude of “ $b^*(\lambda)$ ” [89] [90]. The highest values of the measured scattering in Figure 2-48 seem to be due to larger size distribution. Several samples showed, however, weak spectral dependence [74], such as “AUS” or “NIG”. Besides, data for the mixed samples and single-mineral species follow a similar pattern, with some exception such as “MON1” and “MON2”. Nevertheless, further generalizations about the variability of “ $b^*(\lambda)$ ” are hard to make, because of the complexity of their unique patterns [88].

### 2.3.3.5 Summary

Table 2-5 summarizes characteristics of scattering because of the different compositions of ocean water already mentioned. Scattering is most affected by high phytoplankton concentrations. As forward scattering outcomes backward scattering in Phytoplankton and NAP, Mie scattering model can be used to approximate these two types of scattering. It is important bearing in mind that when light suffers Rayleigh scattering its wavelength changes. In addition, as a photon absorbed is not scattered, absorption and scattering are indirectly related.

Compositions	Scattering coefficient	Scattering spectra
Pure Water	<p>Depends on <math>\lambda</math>.</p> <p>Due to changes refractive index.</p> <p>There is inelastic scattering and elastic scattering (Rayleigh scattering)</p> <p>Small effect compared with absorption.</p>	
Phytoplankton	<p>Depends on its size, shape and refractive index of all components of its cell.</p> <p>Due to its dependence on sunlight, it decreases with depth and it is very unusual to be found deeper than 200 meters.</p> <p>Most of the light is scattered forward and only a small part is scattered backward.</p>	
CDOM	Negligible.	-
NAP	<p>Depending on the type and concentration of detritus and minerals.</p> <p>Usually decreases while wavelength increases, although there are some exceptions such as brown earth, whose peak scattering values are at green wavelengths.</p>	

**Table 2-7 Summary of scattering characteristics of seawater. Scattering spectra has different scales depending on how much and where it affects absorption.**



### 2.3.4 Spectral beam attenuation

Generally, to describe optical propagation in water of collimated light under low scattering regimes, the spectral beam attenuation is used. Absorption and scattering are the two most important phenomenon impairing the propagation of light in water and they both depend on the frequency and thus, on the wavelength. Spectral beam attenuation refers to the combination of the loss and deviation of light photons. Therefore, it is calculated as the sum of the absorption and scattering coefficients (Eq.(13)):

$$c(\lambda) = a(\lambda) + b(\lambda) \quad (13)$$

After having described how light attenuation depends on the type and composition of the water body as well as the wavelength, it can be concluded which wavelengths are going to be most suitable depending on the water body. On the one hand, in deep pure waters blue and green lights are the most appropriate light source, as it is they suffer the least attenuation by water molecules. On the other hand, in coastal, harbor and shallow waters, as the concentration of phytoplankton, CDOM and NAP increases, the most convenient wavelength shifts to the green-yellow spectrum.

### 2.3.5 Beam divergence

Beam divergence is an optical regime characteristic for electronic beams, which is especially used when the aperture of the beam is very large with respect to the wavelength. It also known as the angular spread or beam spreading, and is measured as the increase in beam diameter or radius with distance from the aperture from which the beam emerges (shown in Figure 2-49).

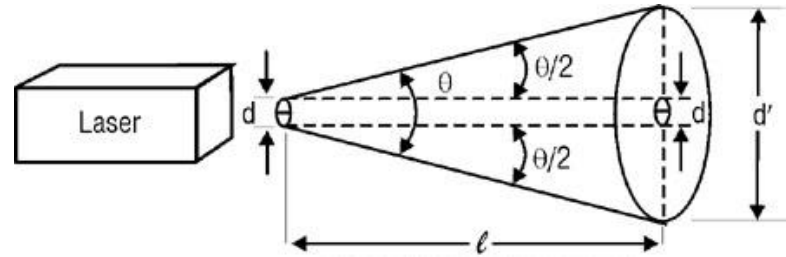


Figure 2-49 Beam divergence with a LASER as a light source [91].

Because of beam divergence, the spread becomes less uniform as the distance from the source increases. The maximum intensity center's diameter “d” does also change as it is drifted away. Consequently, it is hard to measure as it depends on observer [91].

Beam divergence results from light scattering, as a small scattering angle result in small beam divergence and more intense light in the receiver, while a large scattering angle results in large beam divergence and less intense light in the receiver [42]. In addition, it is also related to the light source, as shown in Figure 2-50. A LED has a greater beam divergence than a LASER because of being an incoherent beam<sup>5</sup>. On the other hand, LASER beam is formed by coherent light<sup>6</sup>; therefore, it will not spread and diffuse because of its source. The advantages and disadvantages of these two light sources are discussed later in 3.1.1.

<sup>5</sup> Incoherent light contains photons whose wavelengths are not in phase with one another, which results in diffuse light.

<sup>6</sup> Coherent light is a beam of photons that have the same wavelength and are identical in phase.

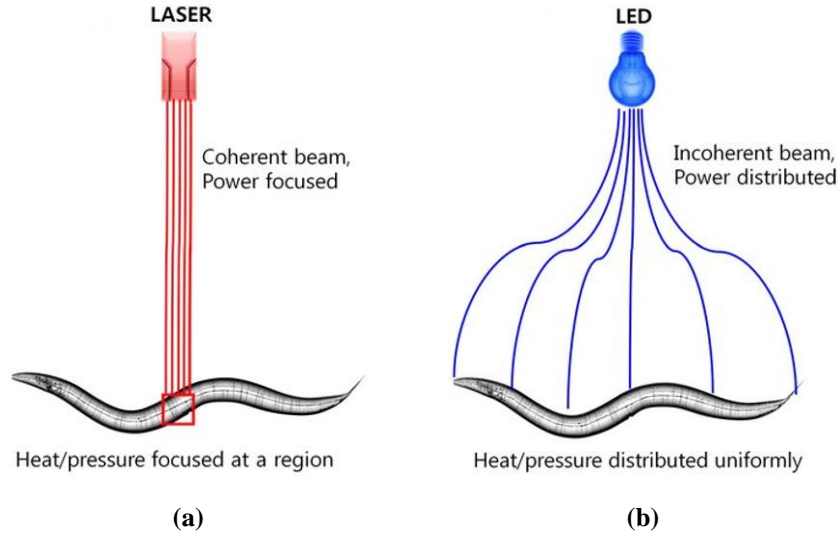


Figure 2-50 (a) A LASER beam and (b) a LED beam [92].

### 2.3.6 Turbulence

Turbulence is a phenomenon in which a fluid goes through several stages of self-mixing, from ordered, laminar, to complete irregular and/or chaotic. In the ocean, it is generated at an interface such as where freshwater flows into ocean water [107], or where warm and salty seawater in the surface layer mixes with fresh and cold rainwater. It can also be formed deeper as a result of melting ice, currents, thermoclines or rivers flowing in among others [93].

Ocean turbulence has a remarkable effect on UOWC, which is one of the reasons why the optical signal is severely affected by the underwater environment. The effect of turbulence is demonstrated in Figure 2-51, where it is seen that scattering increases with high wind. The VSF was measured two high windy days (26 and 30 July) and a low wind day (28 July), being much higher on a high wind day [94]. Turbulent water does also increase BER and *InterSymbol Interference* (ISI), given it makes the signal fluctuate.

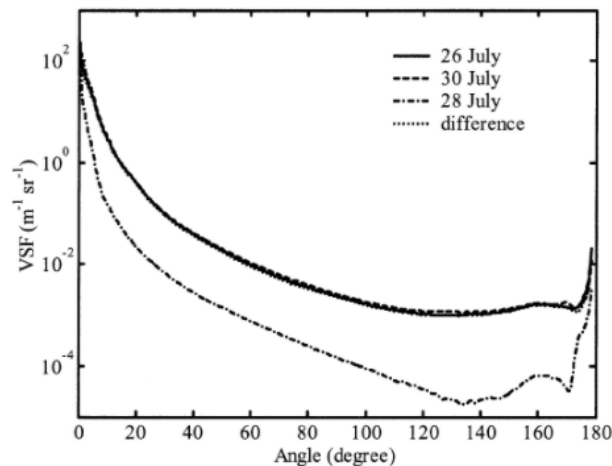
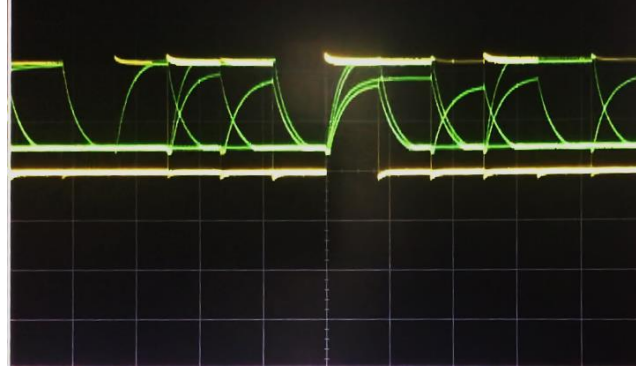


Figure 2-51 VSF measured with turbulence the 26 and 30 of July, and without turbulence the 28 of July [94].

While working with the prototype, it could be observed how the turbulence caused by stirring the water strongly affected the signal, which was received with errors and little delays. In the oscilloscope, the signal plot interestingly bounced up and down while the water continued moving, as illustrated in Figure 2-52.





**Figure 2-52** Capture of an oscilloscope display video in which the water in the tank was turbulent. It can be seen how the received signal is fluctuating and unstable.

### 2.3.7 Turbidity

Another phenomenon that affects UOWC is turbidity, which measures its clarity and transparency loss because of the presence of suspended particles. The more turbid the water is, the more light it attenuates and the less distance for the water link (Figure 2-53).

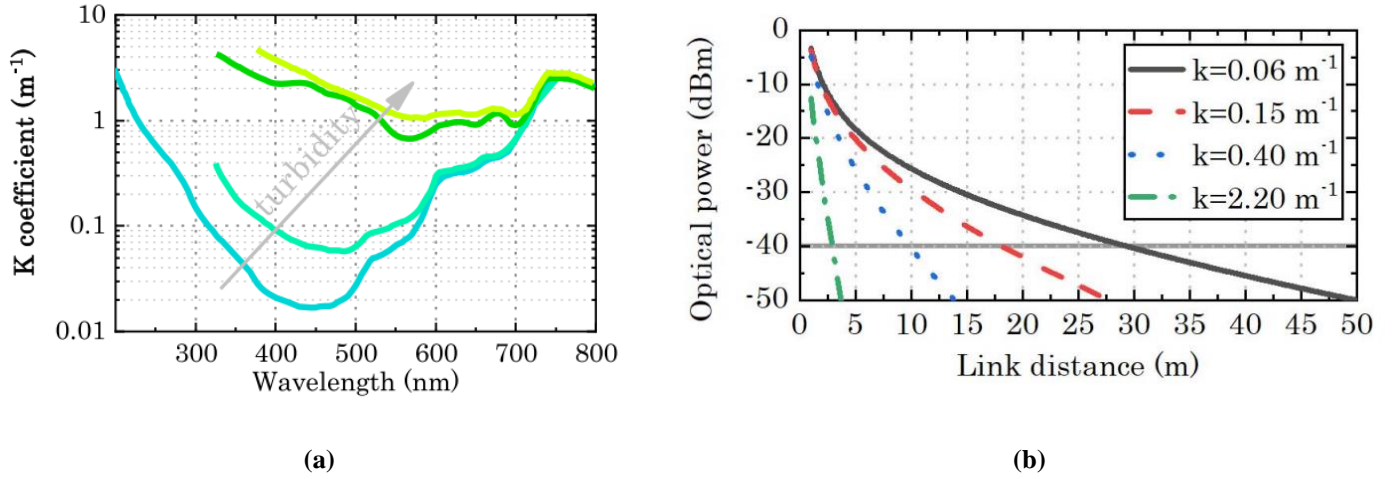


**Figure 2-53** (a) Attenuation curve and (b) simulated optical power as a function of the link distance at different values of water turbidity. In (b), the sensitivity is indicated by the straight gray line [33].

It can be noticed that turbidity, as well as turbulence, represents a crucial challenge in UOWC.

Table 2-8 summarizes the causes and consequences of both of them. Specific zones such as coastal and harbor waters are often turbid, representing a threat for establishing a UOWC link that may explain why it is still a developing technology.

Nevertheless, divers usually go underwater in such zones, which is one of the reasons why the prototype was tested in a harbor. It was observed that surface water was not very turbid, as turbidity increased with depth, reaching its peak at the bottom, which is covered with sludge.

Phenomenon	Cause	Consequences
Turbulence	Surface interference: warm and salty water mixes with fresh and cold rainwater, winds.	Attenuation increase.
	Water currents.	Fluctuation of the signal.
	River mouths.	Increase of the BER and ISI.
	Underwater life.	
Turbidity	Increase of suspended and dissolved particles.	
	It tends to be higher in coastal zones than in deep oceans.	Attenuation increase.
	Underwater life debris.	

**Table 2-8 Summary of the causes and consequences of turbulence and turbidity.**

### 2.3.8 Alignment

An optical beam is characterized by high directivity, with scattering peaked in the forward direction, especially in clear waters where dispersion is low [95]. Maintaining the LOS is critical in UWOC, given the optical beam is very narrow. In order to maintain a permanent reliable link, uninterrupted tracking between transceivers is essential to overcome ocean turbulence caused by currents, underwater vehicles or other sources [57].

Diffuse light enhances alignment in UOWC, as it means the beam is wider and the photons come from different directions. In practice, it is difficult to establish a perfect lining up, which impacts on the received intensity. Increasing the transmitter beam divergence diminishes the alignment requirement between the transmitter and the receiver. This is the reason why LEDs are easier to align with the receiver than LASERS. In deep seas, exact node positioning is very complicated, but its impact can be reduced by changing the receiver inclination to receive the maximum signal intensity. Other solutions for reducing the alignment challenge are using an array of photodetectors that allows a wide detection surface [83] and using a signal amplifier in case the signal is so diffuse that it doesn't reach the receivers sensibility.

There are different optical link configurations:

- **Direct Line-Of-Sight (LOS).**

Direct LOS link is an unobstructed underwater connection between the transmitter and the receiver [57]. There are different types of direct LOS configurations, as can be seen in Figure 2-54.

Firstly, point-to-point LOS configuration (shown in Figure 2-54(a)) is the most common and simple link configuration used in UOWC [57]. In this arrangement, the transmitter fixes the direction in which the receiver is placed in order to detect the light beam directly. Nevertheless, these systems require precise pointing, strongly limiting the performance of UOWC systems in case of turbid and turbulent water environments [20]. In addition, they can cause heavy problems when the nodes move, for example, if they are AUVs, ROVs, submarines or divers.

Secondly, diffuse light sources such as high-power or highly efficient LEDs are used for a diffused LOS configuration (shown in Figure 2-54(b)). Their larger divergence angles permit broadcasting UOWC to different receiver nodes positioned within the angle covered by the beam. Nevertheless, this configuration is very sensitive to the attenuation caused by the water because of the large volume of light-water interaction. Consequently, shorter communication distances and low transmission data rates can be reached [20].

Thirdly, LOS boundary configuration refers to the communication link between a satellite and an underwater object (Figure 2-54(c)). This link is very hard to establish using a LASER due to its high directionality, but it is even harder using a LED because of its high divergence and attenuation in such long distance. Therefore, a requirement for LOS boundary configuration would be to know the exact position of both transmitter and receiver, which is a great challenge but not impossible as it has already been done (like in [31] [96]).

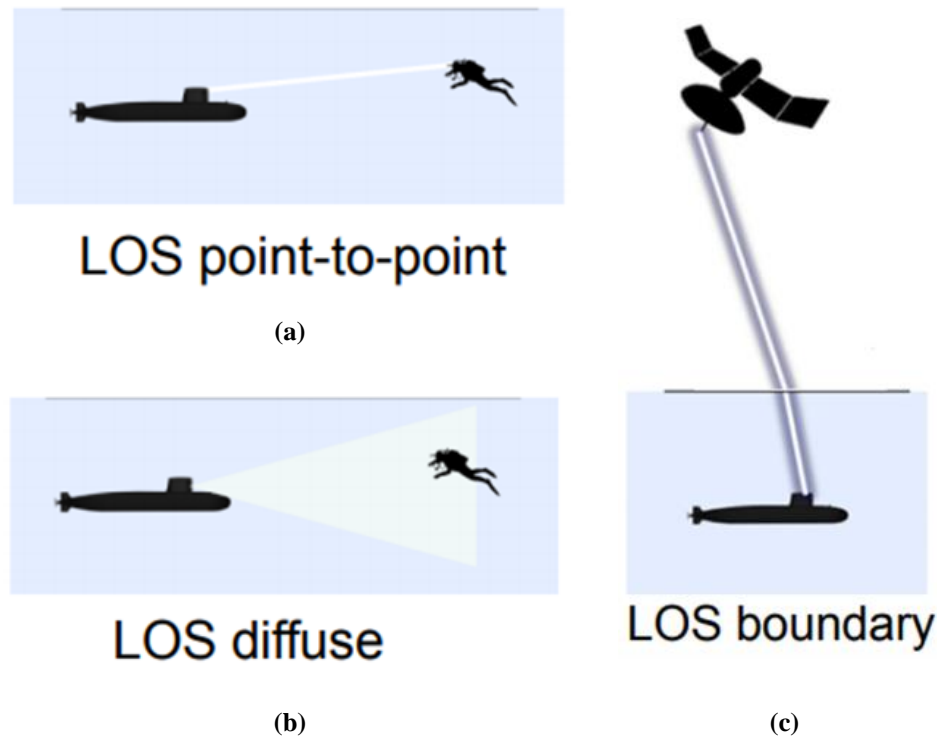


**Figure 2-54 Different direct LOS link configurations: (a) point-to-point, (b) diffuse and (c) boundary [97].**

Generally, LOS UOWC link is modeled by Beer Lambert's (BL) law, which estimates propagation losses due to absorption and scattering in a simple underwater channel. BL expression is given by Eq.(14) and is used to describe the light attenuation effect [98]:

$$I = I_0 e^{-c(\lambda)z} \quad (14)$$

Where:

- $I$ : Power of the received light.
- $I_0$ : Power of the transmitted light.
- $c(\lambda)$ : Attenuation coefficient.
- $z$ : Distance of the light transmission.

However, when photons undergo multiple scattering resulting in a Non-LOS link, the channel is more accurately described by the *Radiative Transfer Equation* (RTE), detailed in the following section.

- **Non-Line-Of-Sight (NLOS)**

As it has been stated, a LOS link is hard to establish and sometimes, it can be impossible in practical systems because of underwater marine life, bubbles and suspended particles (Figure 2-55). Such interferences can lock the beam and hinder the LOS tight pointing and tracking system. Therefore, a NLOS underwater communication link was proposed [99] and it resulted feasible [99] [100]. In a NLOS configuration the optical link achieved by using the reflection of the ocean surface [100], complex sensor network [28] and minute particles in the water [101] and to reflect the beam. These types of links are also called reflective links [57].

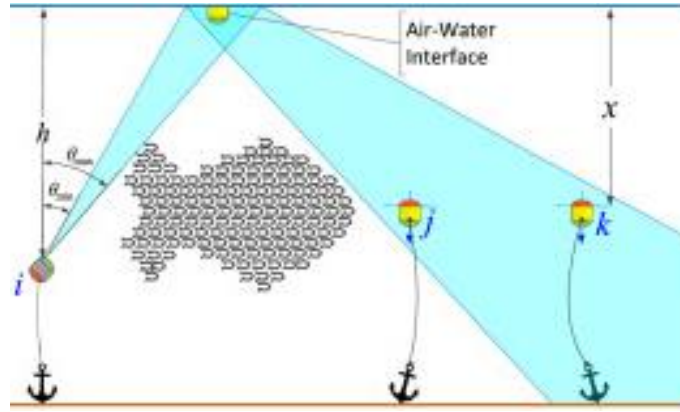


Figure 2-55 NLOS link configuration [72].

In [100], numerical results show that the wind induces random surface slopes that may strongly corrupt the received signal. Nevertheless, this detrimental effect can be dismissed if scattering light dominates over the reflected one in the received signal. Apart from indicating the feasibility of the NLOS UWOC network concept, simulation results showed the BER of this type of link configuration increases with a larger node distance [100].

Although the NLOS UWOC model has been developing rapidly in recent years, it is not mature and accurate enough [101]. This is because despite water characteristics quality and random fluctuations of the sea level affect NLOS UOWC links, the existing model mainly considers the slope of the sea level and pays little attention to other important factors [28], such as dissolved particles or fluctuations in salinity, temperature and density [97]. A longer NLOS UOWC link (40 m) in turbid water was envisaged by reporting a simulation study and considering experimental results. This study is believed to open a new research paradigm complementing the LOS counterpart by accomplishing high-speed UOWC in challenging water environments [101].

The most widely used model for a NLOS UOWC link is the RTE, which describes the propagation of light through the medium coming from energy conservation law. The two-dimensional RTE is expressed by Eq.(15), which is more accurate because it takes into account multiple scattering and light polarization, but has been simplified not taking into account time dispersion of light [28].

$$\vec{n} * \nabla(\lambda, \vec{r}, \vec{n}) = -cL(\lambda, \vec{r}, \vec{n}) + \int_{2\pi} \beta(\lambda, \vec{r}, \vec{n})L(\lambda, \vec{r}, \vec{n})d\vec{n} + E(\lambda, \vec{r}, \vec{n}) \quad (15)$$

Where:

- $\vec{n}$ : Direction vector.
- $\vec{r}$ : Position vector.
- $c$ : attenuation coefficient.
- $\nabla$ : Divergence operator.
- $L$ : Optical radiance (see 2.3.11).
- $\beta$ : VSF.

There are different numerical solutions methods for the RTE [98], such as *Monte-Carlo*, *Discrete Ordinate*, *Invariant Imbedding* and the *Stochastic Model*. While Monte-Carlo is easy to program, offers accurate solution and high flexibility, the other three methods have high simulation efficiency but are difficult to program [28]. Some factors give even greater importance to NLOS link as they can impede LOS configuration. Some of these factors are multipath interference and physical obstruction.

○ **Multipath interference**

Multipath interference is produced when an optical signal reaches the receiver after encountering multiple scattering objects or having been reflected multiple times (Figure 2-56(a)). Consequently, it depends upon the propagation environment as well as system specifications. For example, while in shallow waters multiple signals at the detector reflections from surface or bottom, in deep oceans these reflections can be disregarded [57]. Therefore, multipath interference affects shallow waters to a greater extent than deep oceans.

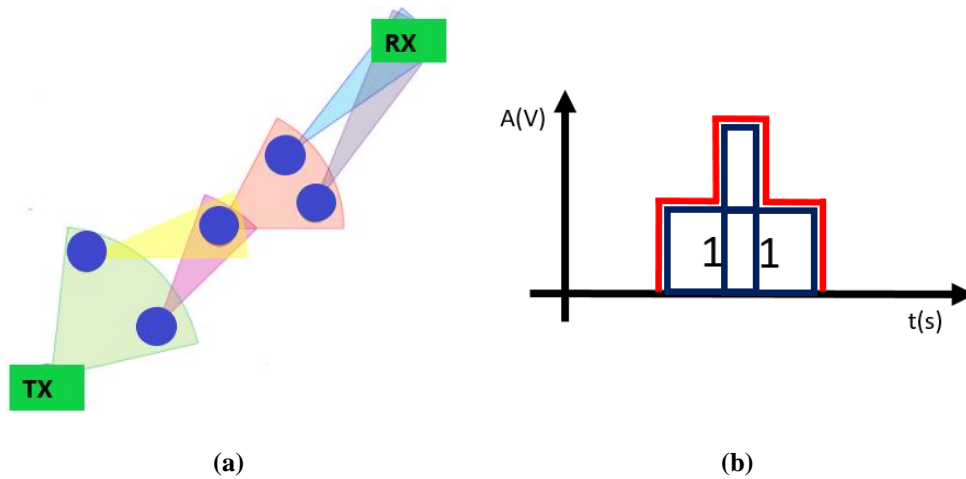


**Figure 2-56 (a) Multipath interference in a network in which relay nodes are the blue dots and (b) a plot of the received amplitude of a signal with ISI.**

The combination of scattered and reflected optical waves eventually leads to time dispersion<sup>7</sup> and decreases the data rate due to ISI (graphically shown in Figure 2-56(b)). In order to suppress this interference, sophisticated signal processing techniques such as channel equalization and adaptive optics can be used at the detector. In addition, accurate characterization of underwater optical channel helps to design the most convenient system for reliable and high quality optical link besides minimizing the challenge of channel equalization for rapidly changing underwater channel [57].

Multipath interference results in greater ISI in long-range communication high data rate [102], as it is shown in Figure 2-57. On the one hand, the narrower the source beam is, the less temporal broadening and greater bandwidth despite the most critical pointing and tracking. On the other hand, the temporal broadening will be increased if the detector is misaligned and receives more scattered photons [103]. In addition, another inconvenient of a multipath link would be the temporal dispersion due to the light that is been re-scattered back towards the receiver [88].

Using Monte Carlo Simulation<sup>8</sup> method [104] it was concluded that the channel time dispersion could be neglected when working over limited distances except for highly turbid water. Consequently, a UOWC system is able to support high data rates at moderate distances [57]. It can also be observed that multipath interference decreases when ISI degradation is compensated with spatial diversity, although it rises at higher data rates and *Signal to Noise Ratio* (SNR) [57].

<sup>7</sup> Time dispersion occurs when multipath components of a symbol are received beyond the duration of the symbol.

<sup>8</sup> Monte Carlo Simulation is a type of computational algorithm that uses repeated random sampling to obtain the likelihood of a range of results of occurring.

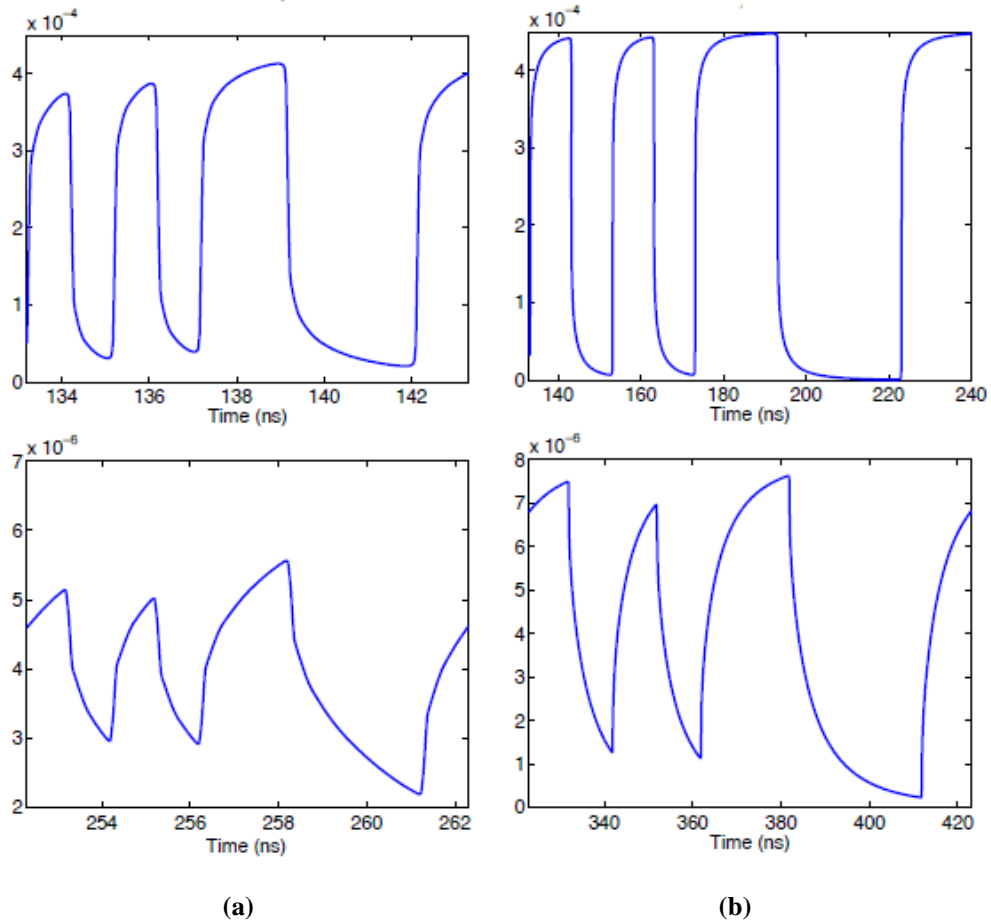


Figure 2-57 (a) Waveform received at 1 Gb/s at 30m (top) and 50 m (bottom) and (b) waveform received at 100 Mb/s at 30 m (top) and 50 m (bottom) [102].

#### ○ Physical obstruction

In the ocean water, any living organism will cause temporary loss of signal at the detector. In order to avoid the consequences of temporary signal lost, appropriate error correction techniques, signal processing techniques and redundancy measures can be used. These error correction techniques are also known as protocols, and the two most widely used ones in underwater environment are *Automatic Repeat Request* (ARQ) and *Forward Error Correction* (FEC). ARQ tolerates the re-transmission of lost data after the obstruction, although it is not effective with high BER, as it does not provide constant throughput. In FEC, the source coding is carried out again if needed, boosting the UOWC link. Nevertheless, it should be taken into account that it increases transmission payload [57].

In addition, there are other techniques to improve the quality of the optical link and enhance the system against physical obstruction, such as advanced signal processing capabilities [42] that allow larger distances links and approaching hop-to-hop or multipath communication [105].

#### ● Retro-reflector links

In retro-reflector links, the transmitted signal is reflected back to the source that originated it, where there is also an optical receiver (Figure 2-58). It is useful for limited duplex communication, it works in photon, and contrast limited scenarios. For example, clear ocean water and lakes are photon-limited scenarios as the link range and capacity is limited by the amount of photons falling on the detector due to absorption. Otherwise, turbid harbors are contrast limited scenarios where link range and capacity are limited by scattering, affecting underwater LASER imaging [57]. Nevertheless, the backscatter component can be remarkably reduced by using polarization discrimination [106].

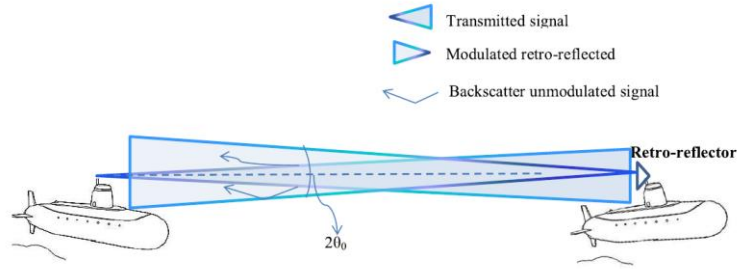


**Figure 2-58 Modulating retro-reflector configuration [57].**

Table 2-9 summarizes the characteristics and channel modeling techniques of the LOS and NLOS alignments.

Alignment	Channel model	Characteristics
LOS	Beer Lambert's law	<p>Easier alignment with diffuse light on detriment of its maximum range.</p> <p>Usually difficult to establish due to alignment requirement.</p> <p>Types: point-to-point, diffuse, boundary.</p>
NLOS	RTE equation.	<p>It is the only possible alignment with physical obstruction and multipath interference.</p> <p>Feasible, but hard to design. The modelling is actually developing to complement LOS links accomplish high-speed UOWC.</p> <p>It has greater BER and ISI than LOS, which increase with bit rate and distance.</p> <p>Greater temporal broadening and dispersion.</p> <p>These drawbacks can be overcome with proper channel equalization, correction and signal processing techniques.</p>

**Table 2-9 LOS and NLOS characteristics and channel modeling techniques.**

### 2.3.9 Refractive Index Variability

The Refractive Index “n” is the value calculated from the ratio of speed of light in a vacuum “c” to that in a second medium “v” (Eq.(16)). When light passes through two media with different refractive indexes, it refracts following Snell's Law (Eq. (17)), as it is shown in Figure 2-1.

$$n = \frac{c}{v} \quad (16)$$

$$n_i * \sin(\theta_i) = n_r * \sin(\theta_r) \quad (17)$$



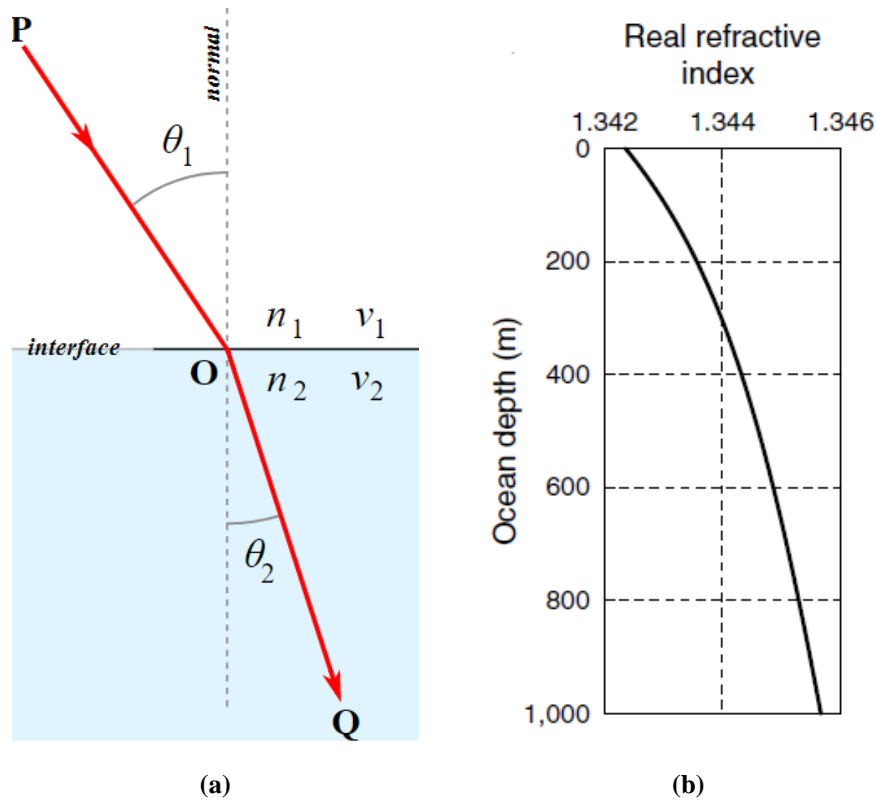


**Figure 2-59 (a) Light refraction following Snell's Law and (b) an example of refractive index variation with depth of an ocean with low turbidity [107].**

The variations in the refractive index changes the path light follows and increases amount of scattering. The refractive index can change on a small or large scale. On the one hand, it varies to a little extent when photons interact with dissolved particles depending on its composition [88]. Therefore, in ocean zones with different types and concentrations of particles, such as coastal or harbor water, the refractive index will change resulting in a NLOS UOWC system (previously detailed in section 2.3.8) [101]. On the other hand, changes in density, pressure, temperature and salinity cause large-scale fluctuations in the refractive index, leading to turbulence, which conclusively causes scintillation in an optical beam. Indeed, turbulence can slightly and continuously change the propagation direction of photons (2.3.6) [107].

Large-scale fluctuations of global sea surface salinity, temperature and density around global ocean water can be observed in Figure 2-60, Figure 2-61 and Figure 2-62 respectively. The larger the gradient in any of these three properties, which can be seen by contrasting colors, the more it affects the refractivity index. In these cases, photons will be refracted further from their initial direction, making UOWC link alignment harder to achieve.



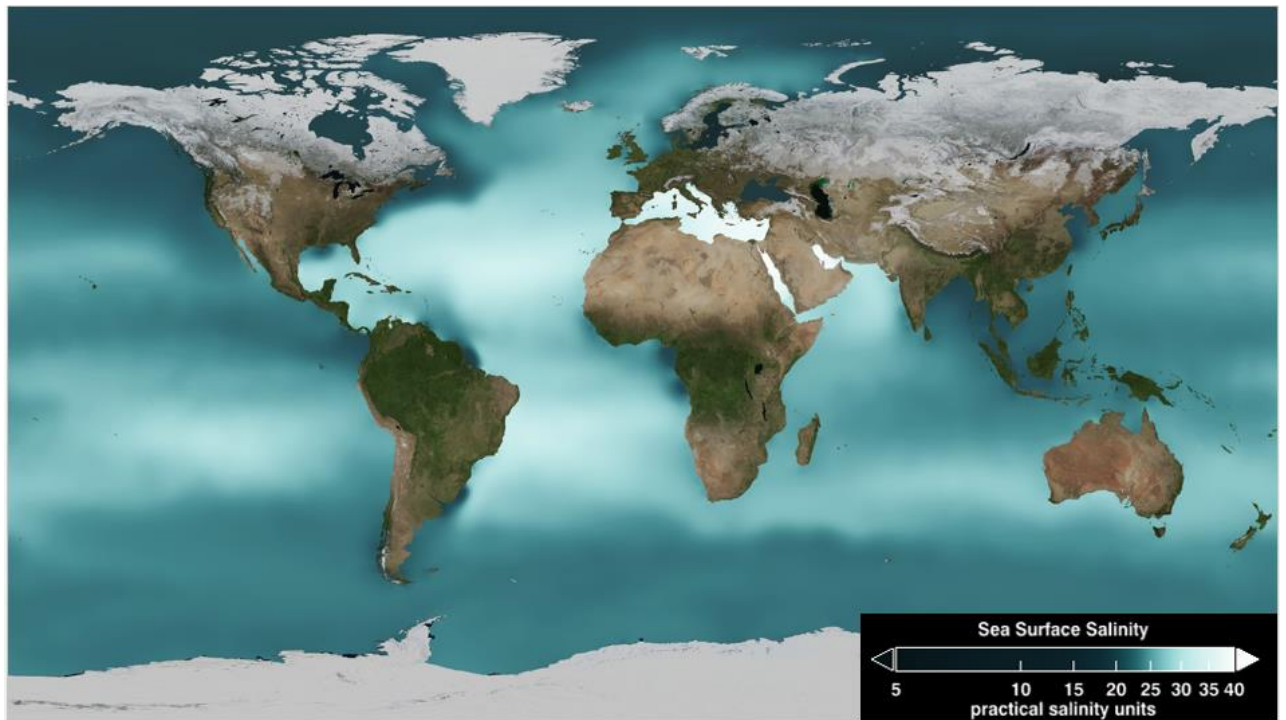


Figure 2-60 Global map of average surface seawater salinity [108].

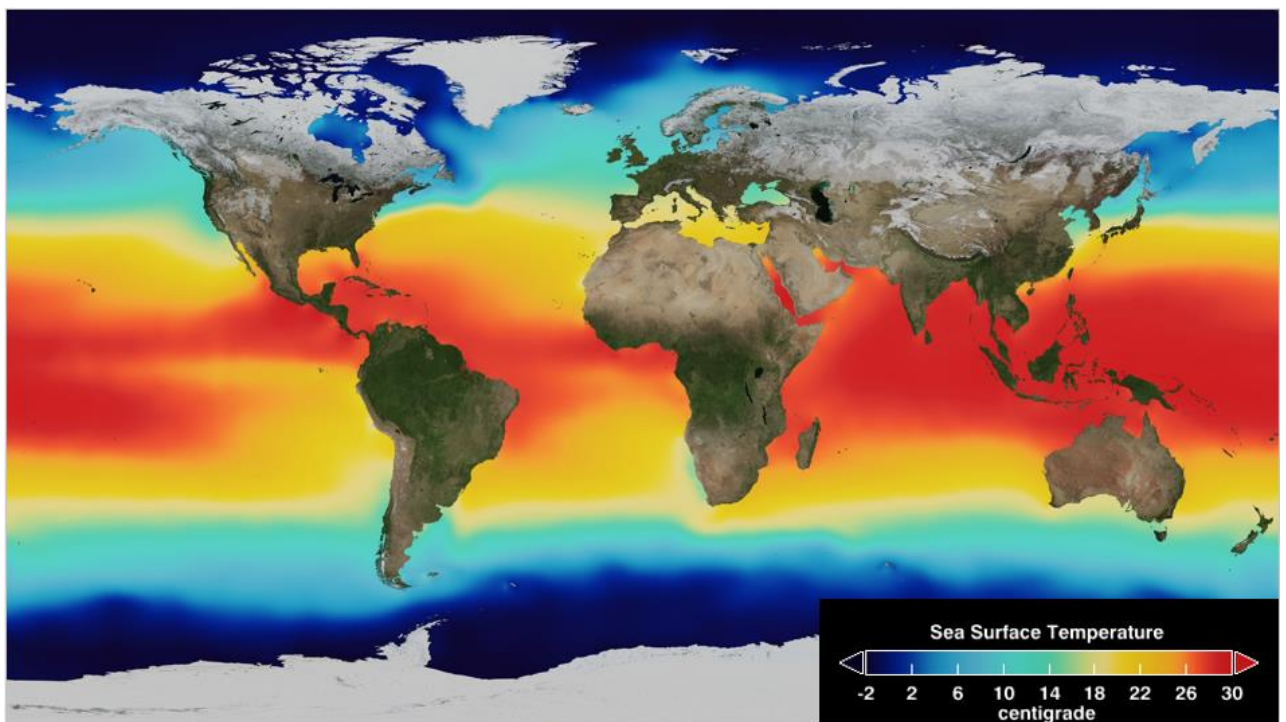


Figure 2-61 Global map of average surface seawater temperature [108].

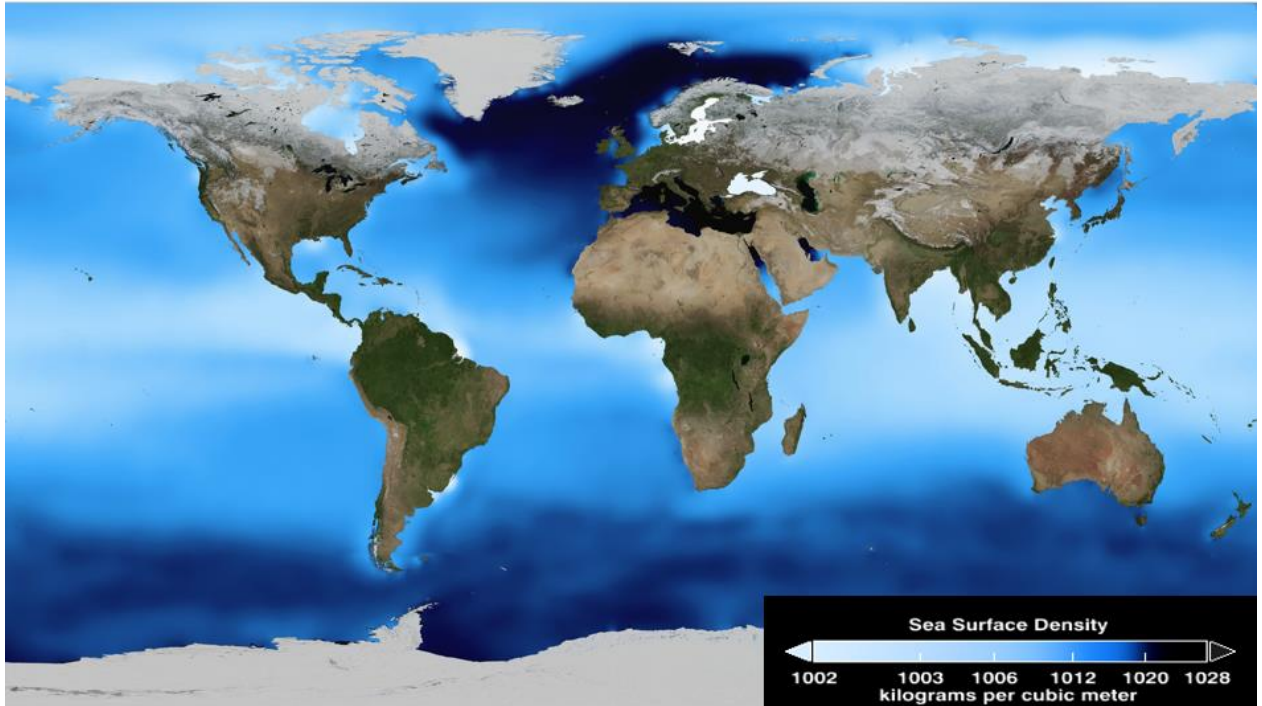


Figure 2-62 Global map of average surface seawater density [108].

In addition to mentioned large-scale fluctuations, there are also gradual changes in the refractive index [109]. Nevertheless, these gradual changes are larger in shallow and surface waters, given deep ocean waters are more homogeneous. Consequently, in deep ocean waters, the effect of temperature, salinity and pressure variations is usually neglected because of its little effect on UOWC [31]. However, it is specifically significant for long ranged communications as it may cause the light beam to bend away from the receiver [109]. Figure 2-63 shows the gradual changes of the refractivity index depending on temperature, salinity and pressure. It can be observed how it is also a function of the wavelength. It can be noticed as well how the salinity gradients have a greater effect than temperature, and temperature than pressure. Nevertheless, salinity is usually constant, while temperature and pressure change more. Temperature especially varies near the surface following a seasonal pattern and pressure rises gradually as depth increases.

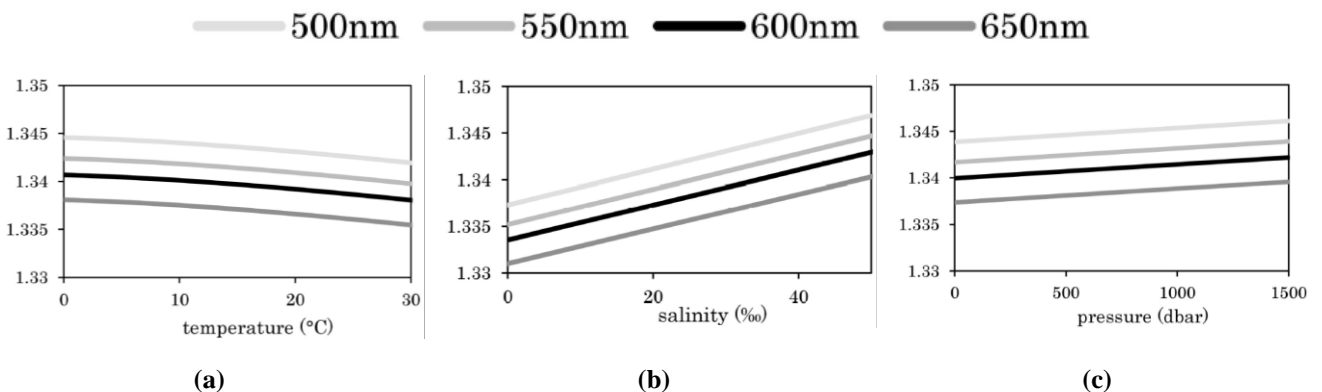


Figure 2-63 The refractive index as a function of: (a) temperature, (b) salinity and (c) pressure, for different transmission wavelengths in seawater [107].

### 2.3.10 Background noise

Another important factor for UOWC is the background noise, which is highly dependent upon operating wavelength as well as water body situation. Usually, harbor areas are noisier than deep oceans because of human activities. The main sources of background noise are: widespread diffusion, the Sun and space, as well as scattered light collected by the receiver and other received scattered light. In the euphotic zone of the ocean solar interference is the main component of background noise, while at deeper waters it is the biological luminance, centered on the blue-green region [57].

In order to reduce background noise, a narrow band spectral filter is used, as for example in submarines LASER communications [110]. There are other sources of noise such as the photodetector itself, back-scattered light radiated by the medium, preamplifier noise, shot noise or thermal noise.

For optimization of the UOWC system, the amount of background light could be minimized by reducing the overall *Field Of View* (FOV) and maximizing the amount of desired signal energy captured with an adaptive optics system. Given ' $\Omega_s$ ' is the solid angle FOV of the source and ' $\Omega_{FOV}$ ' the one of the receiver. Figure 2-64 shows the geometry of point ( $\Omega_s < \Omega_{FOV}$ ) and extended sources ( $\Omega_s > \Omega_{FOV}$ ) relative to the receiver [57].

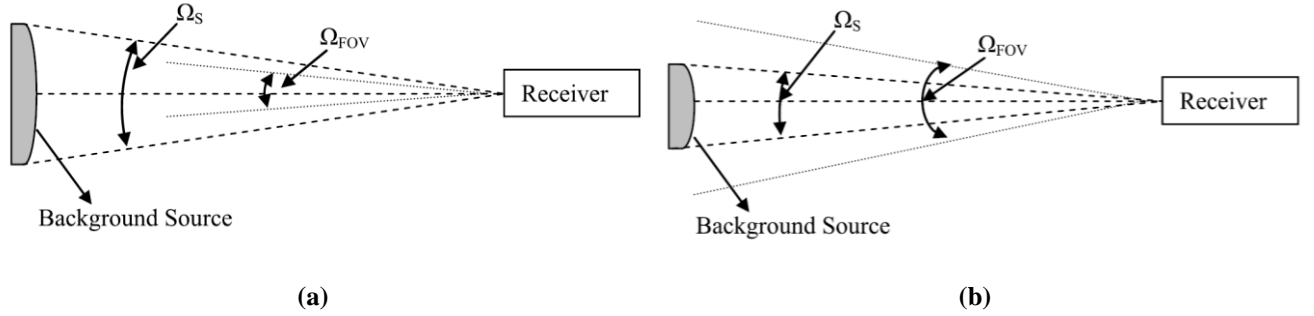


**Figure 2-64 Geometry of (a) extended and (b) point source relative to the receiver [57].**

### 2.3.11 Radiance

Radiance " $L(\lambda)$ " is the radiant flux<sup>9</sup> emitted, reflected, transmitted or received by a given surface, per unit solid angle, per unit projected and per unit area (Watts/m<sup>2</sup>/sr). It is a relevant radiometric variable in UOWC given it models the UOWC channel because of relating IOPs with AOPs through the Radiative Transfer Equation.

Figure 2-65(a) shows how radiance distribution can be obtained with the RTE once boundary conditions and water body properties are known. Nevertheless, in some cases, water body properties are not known, whereas radiance can be measured. This is what the inverse radiative transfer problem consists of: calculating IOPs with a simple mathematic model once radiance distribution has been measured and boundary conditions are known Figure 2-65(b). When IOPs are calculated, water body properties such as chlorophyll concentrations or phytoplankton physiology, and functional groups can be determined [58].

<sup>9</sup> Flux " $\Phi(\lambda)$ ": For a given wavelength, it is the integral of the light power that reaches the detector during the integration time. The light power is called spectral flux (Watts/μm) [111].

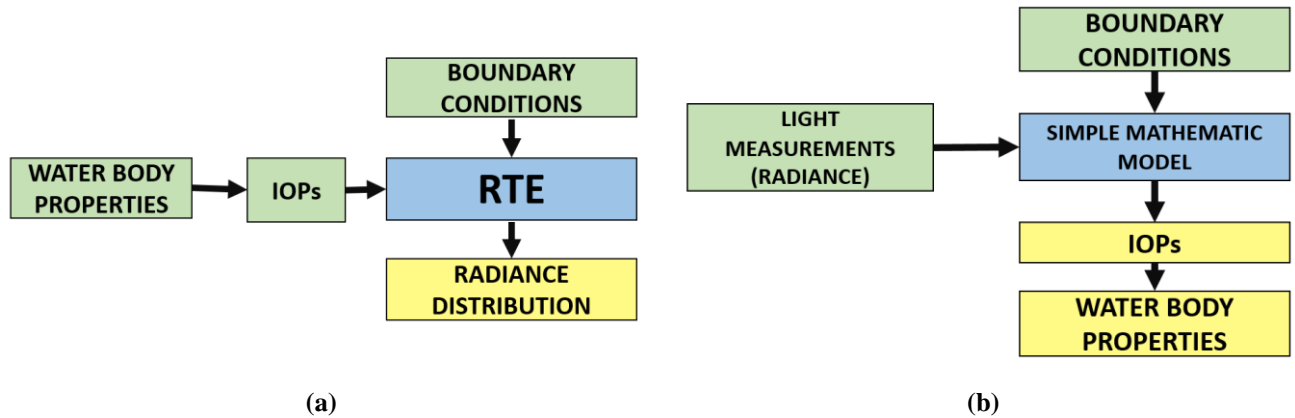


Figure 2-65 The conceptual process involved in solving (a) the forward radiative transfer problem and (b) remote-sensing inverse radiative transfer problem.

The inverse radiative transfer process is used in ocean color remote sensing, which obtains information from aircraft or satellite instruments data to determine the constituents of natural waters, its IOPs, or the bottom type and depth [58]. One of the properties measured in remote sensing is total the upwelling radiance “ $L_u$ ”, which is the altered radiance from direct sunlight. The contributions to total upwelling radiance are shown in Figure 2-66, where:

- $L_u$ : Altered sunlight radiance that has not absorbed by materials within the water column, the reason why it depends on the types and concentrations of the various components within the water column. The total upwelling radiance “ $L_u$ ” is the sum of “ $L_w$ ”, “ $L_r$ ” and “ $L_a$ ”.
- $L_w$ : Leaving radiance is a portion of  $L_u$  that is scattered back out and carries information about the water column.
- $L_r$ : Radiance reflected by the sea surface that contains information about the wave state of the sea surface.
- $L_a$ : Radiance generated in the atmosphere by scattering.

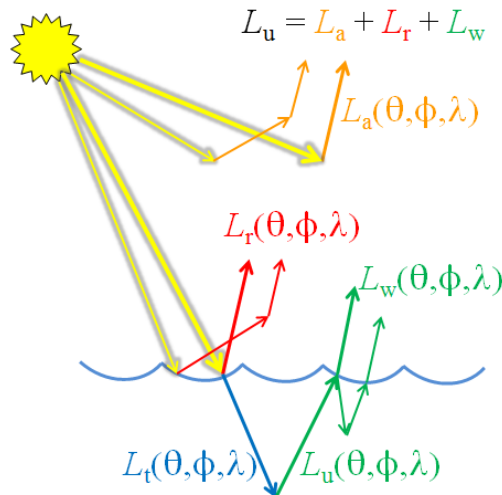


Figure 2-66 Contributions to the total upwelling radiance above the sea surface [58].

There are other radiometric values used in ocean optics, such as irradiance. Irradiance “ $E(\lambda)$ ” (Watts/m<sup>2</sup>) refers to the flux reaching the detector per surface unit, so it depends on its FOV [111]. Irradiance reflectance “ $R$ ” is an AOP defined as the ratio of the irradiance reflected out to the solar irradiance ( $R = E_u/E_d$ ), so its spectra depends on many different combinations of the water column IOPs. Remote sensing reflectance is when a sensor passively records reflectance [58]. The “ocean color signature” is recorded by remote sensing, as well as the water column reflectance spectra, which corresponds to a very large number of various combinations of water column IOPs [112].

## 2.4 Water classification according to its different optical properties.

A theoretical model capable of describing long distance UOWC in a practical underwater environment is not available yet due to its strong dependence on turbulence and specific characteristics of the dissolved matter.

In ocean water, turbulence is the main limiting factor to the performance of an UOWC, which is caused by the fluctuations in the index of refraction resulting from temperature and salinity variations. Through weak oceanic turbulence, a complete “model” can be implemented to predict and evaluate light propagation using the Monte Carlo method [20].

Nevertheless, a more exhaustive study of the complex-chemical underwater environment should be conducted in order to have a better understanding of underwater optical propagation. The constantly changing circumstances of the aquatic medium set an additional difficulty to its parametrization. Measurements and models for attenuation of light in various types of the seawaters are reviewed in detail [113], [114] and [115]. However, in general, water is classified into four different types: pure, clear and coastal ocean water and turbid harbor [57]. Table 2-10 shows the typical values of chlorophyll concentration “C”, absorption “ $a(\lambda)$ ”, total scattering “ $b(\lambda)$ ” and spectral beam attenuation “ $c(\lambda)$ ” for each water type. Parameters “ $a(\lambda)$ ”, “ $b(\lambda)$ ”, “ $c(\lambda)$ ” have been obtained in a spectral band with “ $\lambda$ ” centered at 532 nm (green color) [20].

Water types	C (mg/m <sup>3</sup> )	$a(\lambda)$ ( m <sup>-1</sup> )	$b(\lambda)$ ( m <sup>-1</sup> )	$c(\lambda)$ ( m <sup>-1</sup> )
Pure sea water	0,005	0,053	0,003	0,056
Clear ocean water	0,31	0,069	0,08	0,151
Coastal ocean water	0,83	0,088	0,216	0,305
Turbid harbor water	5,9	0,295	1,875	2,170

**Table 2-10 General classification of water and the typical values of chlorophyll concentration “C”, absorption “ $a(\lambda)$ ”, total scattering “ $b(\lambda)$ ” and spectral beam attenuation “ $c(\lambda)$ ” for each type.**

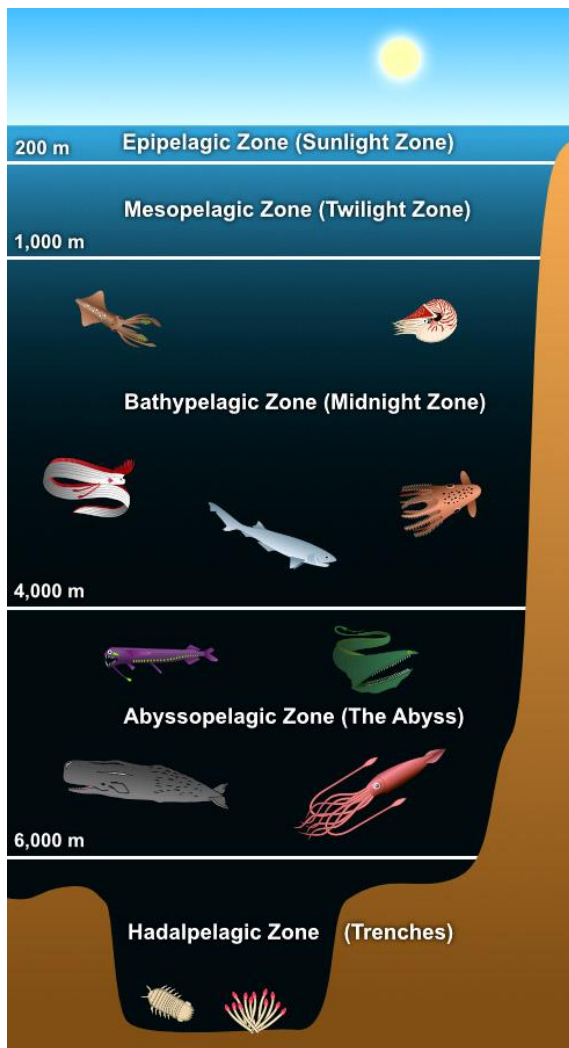
It can be inferred from Table 2-10 that:

- In ***pure sea waters***, absorption is the most limiting factor, primarily due to water molecules and some relatively small concentrations of salts, and, hence, it is very similar to that of pure water [31].
- In ***clear ocean waters*** scattering affects more than absorption. Because of the relatively large concentrations of types of salts that can be roughly classified into different groups according to light transmittance [116].
- In ***coastal ocean waters***, there is much higher concentration of planktonic matters, detritus, and mineral components, increasing absorption and scattering at a variety of wavelengths. Acids produced by dead and decaying organic matter increase absorption in the blue region. Hence, coastal waters typical colors may exhibit green-yellow schemes [58].
- In ***turbid harbor waters***, there is the highest concentration of dissolved and in-suspension matters. This is because not only are there high concentration of inorganic salts, phytoplankton and zooplankton, but also of inorganic particles, which leads to extremely high absorption and multiple scattering, limiting light transmission just to a few meters [33] [58].

Apart from the previous seawater zone classification depending on its optical properties, deep ocean waters are commonly divided into five main layers, also known as zones, which do also have distinguished optical parameters [117]. These are the Epipelagic, Mesopelagic, Bthypelagic, Abyssopelagic and Hadalpelagic Zone, which are shown in Figure 2-67 with their specific properties.



The strongly different properties depending on its depth and its location lead to the challenging underwater propagation of the optical beam.



(a)

- **Epipelagic/Sunlight Zone**  
It is the zone where most of the visible light exists. Heat comes with the light, which is responsible for the wide range of temperatures that occur in this zone changing in both latitude and season.
- **Mesopelagic/Twilight Zone**  
It is also known as midwater zone as sunlight this deep is very faint. It has the greatest temperature changes. Bioluminescence begins to appear on life within this zone due to absence of light.
- **Bathypelagic/Midnight Zone**  
From this depth on, the only light comes from the bioluminescence of the animals themselves. The temperature in this zone is constant.
- **Abyssopelagic Zone/Abyss**  
It is the pitch-black bottom layer of the ocean in which lie three-quarters of the area of the deep-ocean floor lies. Only a few creatures can be found at these crushing depths, where the water temperature is constantly near freezing.
- **Hadalpelagic Zone/Trenches**  
In this very bottom zone, temperature is constant at just above freezing, but still life exists.

(b)

Figure 2-67 (a) Diagram of the five layers of the ocean [118] and (b) their characteristics [117].

As it can be inferred from Figure 2-67, ocean environment changes according to the vertical depth, resulting in changes of optical characteristics in underwater. Taking into account phytoplankton concentrations, three main zones can be identified: the euphotic, the dysphotic and the aphotic zone (Figure 2-68) [28]. The euphotic zone reaches a depth of 200 meters in clear ocean waters and receives enough sunlight to promote phytoplankton growth, resulting in an important light absorption. Chlorophyll attenuation coefficient is shown in Figure 2-68, which is related to its concentration and following a Gaussian profile [119]. The dysphotic zone is the middle layer, which reaches up to a few kilometers depth, resulting in insufficient sunlight for photosynthetic growth. Finally, the aphotic zone is bottom layer, which is not reached by sunlight [57]. Besides, the salinity distribution varies with depth, with lower concentrations at deeper zones, changing the refractivity index (Figure 2-68) [28].

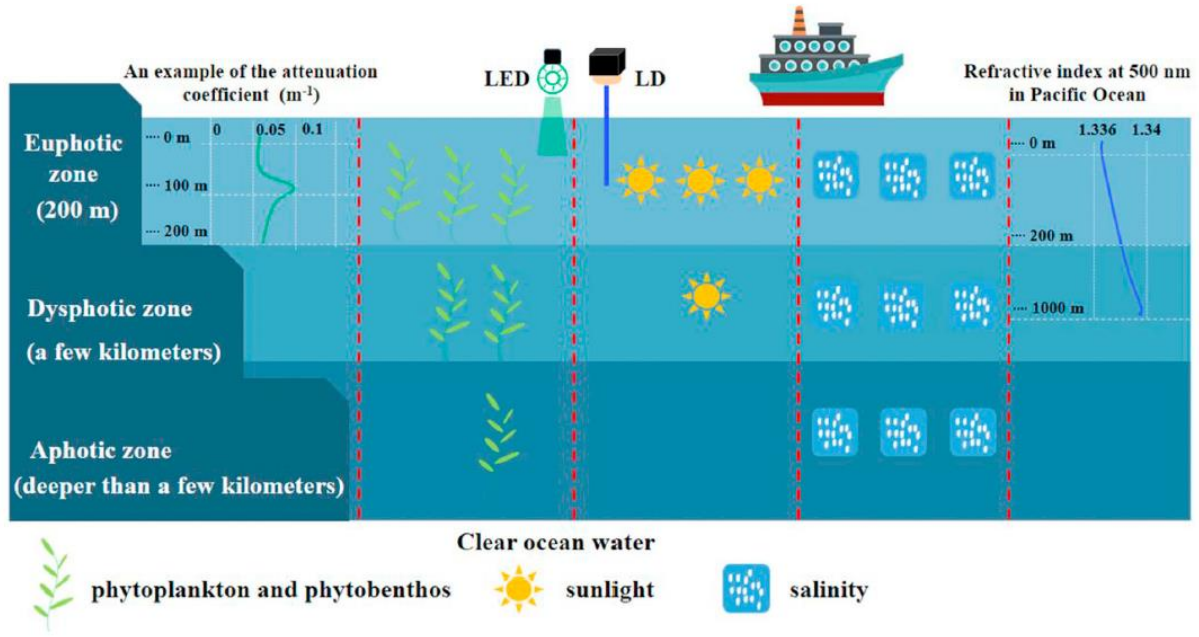


Figure 2-68 Schematic diagram of a vertical layered environment in the ocean [28].

Continuing with optical properties through depth, the variations of temperature and light penetration at surface depths are shown Figure 2-69. These variations change the refractivity index and the background noise respectively, affecting UOWC as well. It can be deduced that bringing light deep into the ocean is a challenge, but at the same time, it carries the opportunity to make many discoveries in the vast unexplored and perpetually dark regions of the ocean.

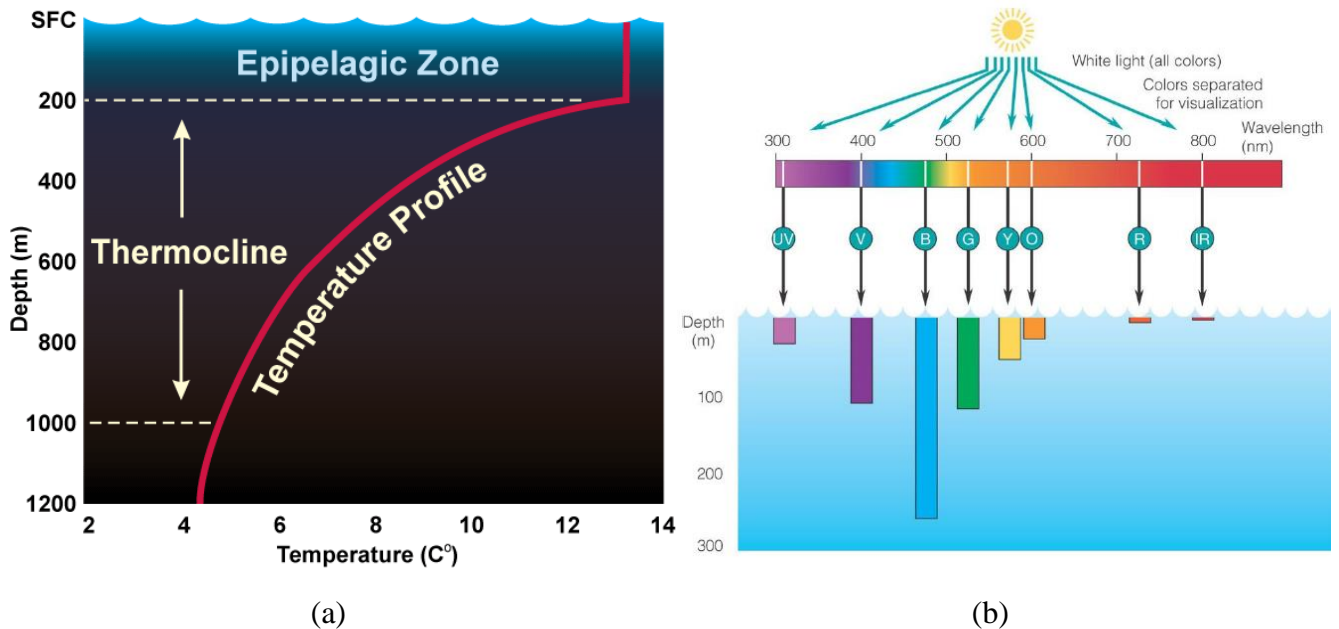


Figure 2-69 (a) Typical seawater temperature profile with increasing depth [117] and (b) light penetration across different depths [120].

All in all, it can be concluded that each zone has its specific physical characteristics, which require a corresponding UOWC link design. Indeed, the underwater environment has a diverse number of distinguishing features that make it unique and rather different from any other propagation environments where traditional communication systems are deployed.





### 3 BENCHMARKS AND RESULTS

In this section, all the experiments conducted in this final degree project will be explained in detail. The aim of designing a UOWC prototype is to test the theoretical research carried on this field, by using the scientific method<sup>10</sup>. First, a simple UOWC link will be established under specific laboratory conditions. Once it is established, different hypothesis will be constructed and tested, such as:

- LEDs provide easier alignment than LASER beams.
- In clear water, green and blue light suffer less attenuation than red light.
- The effects of different colored waters depend on the color of the optical source.
- Turbid water increases light attenuation.
- Turbulent water increases scattering, as well as BER and ISI.
- Constant temperature does not have a remarkable effect on underwater light propagation.
- CDOM increases light attenuation depending on the transmitter wavelength.

#### 3.1 Simple UOWC prototype

Initially, a simple prototype was designed, consisting of: two microcontroller Arduino UNO, a red LASER (transmitter), a solar panel (receiver), a water tank and a computer, which was used as the power supply and for the microcontrollers' configuration (baud rate and data sent).

The simplified block diagram of this initial prototype is shown in Figure 3-1.

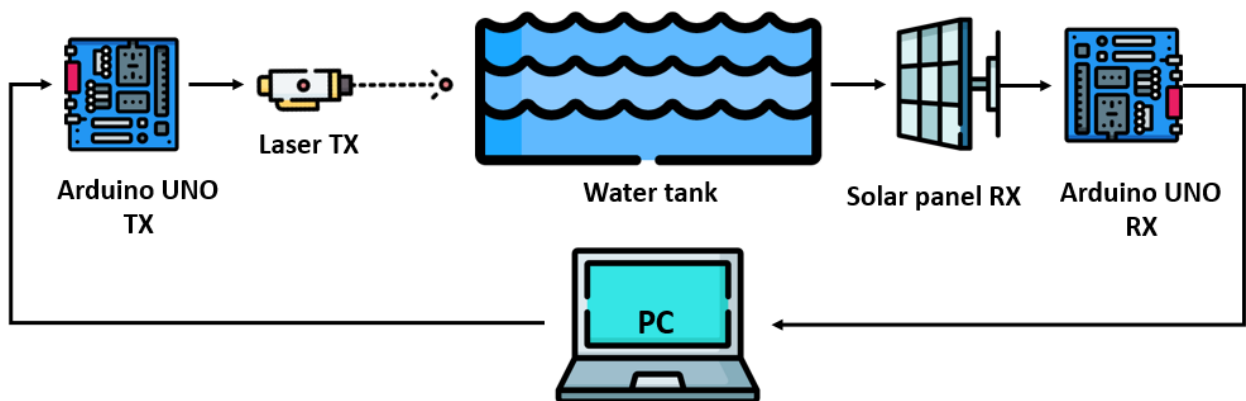


**Figure 3-1 Simplified block diagram of the initial prototype.**

---

<sup>10</sup> The main steps of scientific method are: asking a question, doing background research, constructing a hypothesis, testing it by doing an experiment, analyzing the data, draw a conclusion and communicate the results.

This prototype had a simple performance procedure:

- First, a data transmission program was created and loaded into the transmitter microcontroller (Arduino UNO TX). This program was configured to transmit the uploaded message time after time. In the experiment, the uploaded message was: “*Hola mundo*”.
- Secondly, a data reception program was created and loaded into the receiver microcontroller (Arduino UNO RX). This program was configured to print the received information on its serial monitor.
- Afterwards, the physical connections between the components of the transmitter, as well as between the ones of the receiver, were made carefully.

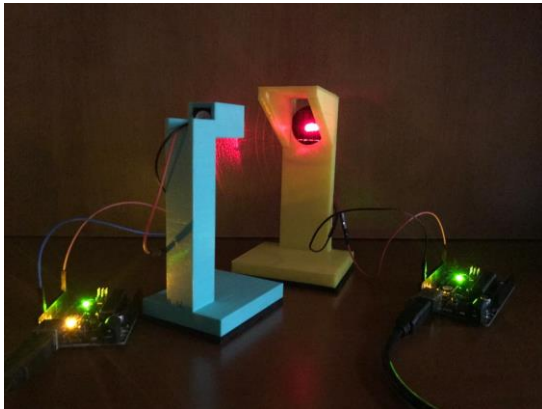
The system was previously tested on free space, as shown in Figure 3-2 (a), where it could be appreciated the low levels of voltage provided by the solar panel even at very short distances (Figure 3-2 (b) and (c)).

Therefore, the design and inclusion of an amplifier in-between the panel and the receiver was needed. The design of the OA is shown in Figure 3-3, which could be powered by Arduino UNO using the 5V pin.

The voltage gain chosen for the amplifier is related to Eq.(18), where with  $R1=1k\Omega$  and  $R2=10 k\Omega$ , obtaining a voltage gain of 11.

$$V2 = \left(1 + \frac{R2}{R1}\right) * V1 \quad (18)$$

All set, the prototype was tested as a FSOC system, transmitting and receiving properly the data frame “*Hola mundo*”.



(a)



(b)



(c)

Figure 3-2 Solar panel output current measurement. (a) shows the position of the oscilloscope cables, and (b) the oscilloscope display. The measurement of the output current was 100 mV.

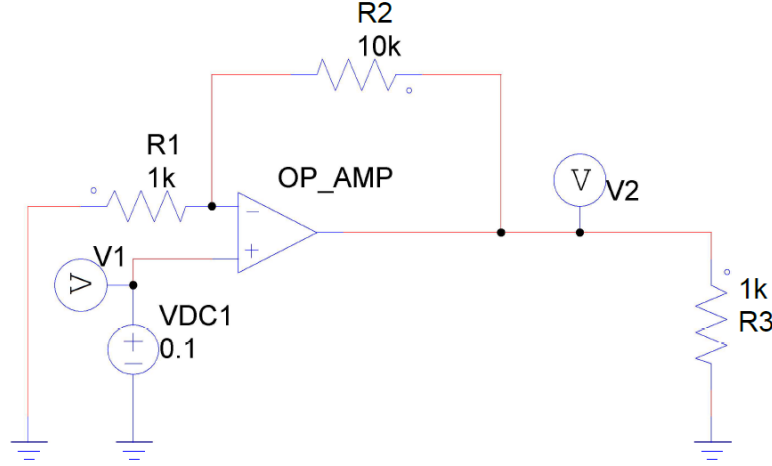


**Figure 3-3 Operational Amplifier designed with PSIM.**

### 3.1.1 Light sources under test

As a result of all the research done on the UOWC field, its optical components are already very developed, and their selection depends on the properties of the water zone they are going to be used. The most widely used light sources are in the blue-green region because it corresponds to the lowest absorption coefficient of pure water. Usually, LASER Diodes (LDs) and LEDs are the typical transmitter devices employed in UWOC systems. Other light sources that are commonly used as transmitters are the Super Luminescent Diode (SLD), vertical-cavity surface-emitting LASER (VCSEL) and the micro-LED ( $\mu$ LED) [28].

On the one hand, a LD works with stimulated emission of radiation and produces coherent radiation by injection current. On the other hand, a LED works with spontaneous emission of radiation and the emitted beam is incoherent and diffused [121]. While LDs have a narrow divergence angle (about a few mrad) and concentrate the transmitted energy because of its coherent and directional photons, LEDs have wider divergence angles, so light diffuses to a larger area [72]. Consequently, LEDs reach shorter distances but provide easier alignment than LDs, which need a precise alignment.

In addition, LDs have a higher cost and power consumption because of their larger current density and output power. Thus, although LEDs are more cost-efficient, several are required to obtain high drive currents and power for long-distance communication [122]. Table 3-1 shows a comparison and summary of all the above-mentioned parameters of LEDs and LDs.

At the same time, VCSEL, SLD and  $\mu$ LED are also employed in the UWOC system due to their excellent features such as their high modulation bandwidth. In order to improve the system performance, various distinguished technologies can be used like light injection locking, optoelectronic feedback techniques or equalization technology. Optical beam reducer/expander and array fabrication of devices are both effective solutions for expanding the system coverage area and making alignment easier [28].

Light sources chosen for the laboratory tests are a red LD and four LEDs, whose wavelengths are displayed in Table 3-2. The specifications of the LASER module are listed in Table 3-3. During the laboratory test, the different properties of LEDs and LD listed above were demonstrated. Interestingly, diffuse light resulted more effective for this specific prototype, as it strongly simplified the alignment procedure and enabled establishing the link at the designated water tank distance.

Parameter	LD	LED
Emission	Stimulated	Spontaneous
Radiation	Coherent	Incoherent
Optical Power	10-1000 mW	~1W
Optical bandwidth	1-2 nm	20-50 nm
Electrical bandwidth	0,6-1GHz	10-15 MHz
Beam emission angle	20°	120°
Thermal management	Strongly needed	Mildly needed
Cost	High	Low
Advantages	Long-distance. High speed. High modulation bandwidth. High directivity.	Wide divergence angle. Low power consumption. Easier alignment.
Disadvantages	Difficult alignment. High power consumption.	Short-distance. Lower directivity. Low modulation bandwidth.

Table 3-1 Comparison between optical sources for UOWC.

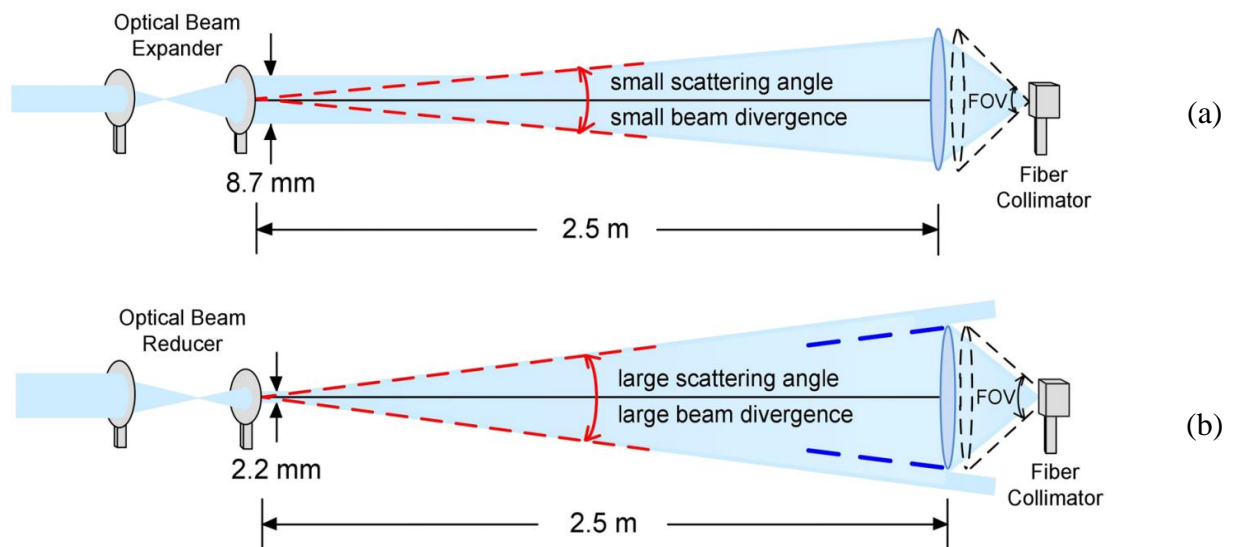


Figure 3-4 Optical beam (a) expander and (b) reducer result in different scattering angles result in different beam divergences [42].

Optical Source	Wavelength ( $\lambda$ )
Red LASER/LD	645-655 nm
Red LED	660 nm
Green LED (high luminosity)	565 nm
Blue LED	460 nm
White LED (high luminosity)	450 nm

**Table 3-2 Wavelengths of the light sources used for the prototype.**

INPUT VOLTAGE	3.5 - 4.5	v dc
OPERATING CURRENT	< 25	mA
WAVELENGTH	645-655	nm
OPTICAL POWER	< 5	mW
TTL BLANKING	NO	kHz
BEAM DIAM.	0.75 +/- 0.05	mm
DIVERGENCE	>0.5	mRad
WARM UP TIME	<1.0	sec
Operating Temperature	-10 - +50	deg C
POLARITY	RED +ve	BLACK -ve

**Table 3-3 Specifications of HLM1230 5mW red LASER module [123].**

Source is going to transmit a digital signal, which has been previously uploaded on the microcontroller as a 'char' variable. This signal is modulated with *On-Off-Keying* (OOK), which is a particular case of amplitude shift modulation *Amplitude-Shift Keying* (ASK). In OOK, the modulator circuit behaves like a switch, representing digital data as presence or absence of a carrier signal (light, in this case) [12]. As it is shown in Figure, a logic level "1" generates a wave with a determined frequency and on the opposite case; it does not oscillate, corresponding to level "0".

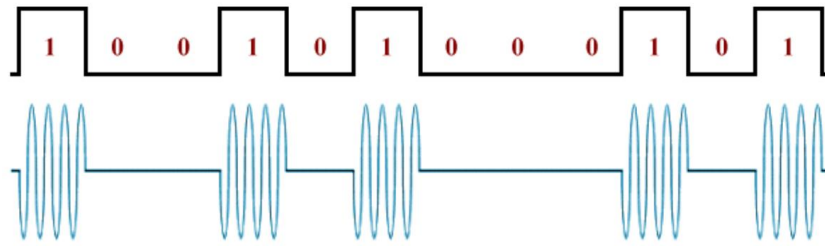


**Figure 3-5 OOK modulation. Logic levels are shown on the top chart, and the transmitted signal is shown on the bottom chart [124].**

### 3.1.2 Light sensor under test

An electro-optical sensor converts the received light into an electronic signal. In this experiment, the electronic signal will be a digital signal, in which the presence of the signal is translated to the logic value “1”, and its absence to “0”. The signal will be received and processed in the microcontroller, and besides, it can be shown on the serial monitor.

The electro-optical sensor could have been an array of photodetectors, like in [125], however, despite being a common technology, it has poorer resolution and greater assembly complexity than a solar cell. A solar cell is made up of two types of semiconductors (the p-type and the n-type), disposed in filaments, with opposite charges. When light strikes a solar cell, electrons are ejected from one layer to its opposite, creating a flow of electricity, see Figure 3-6 [126]. This helpful insight about the possibility of using a solar cell is acknowledged in [12].

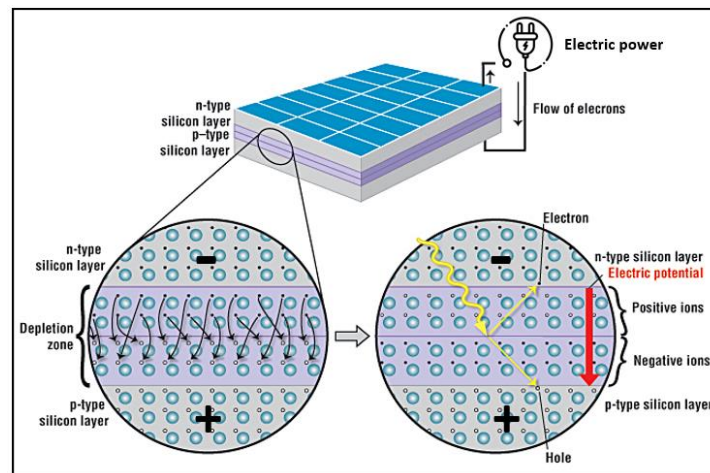
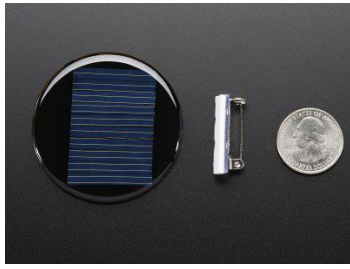


**Figure 3-6 Schematic representation of a solar cell. The n-type and p-type layers –the filaments- are shown, with a close-up view of the depletion zone, as well as the electron flow, once they are excited by incident light.**

In [12], it was carried a study of the feasibility of the three different solar cells that were available at the laboratory (see Figure 3-7). The aim of the study was to decide the best option taking into account their different sizes, spacing between layers and sensibility.

The results in [12] showed that the big solar cell (Figure 3-7 (c)) was not a viable option, given the LASER beam was so narrow compared to the spacing between filaments, that neither did it eject the electrons nor gave a signal. The plate of the small square solar cell (Figure 3-7 (b)) had a higher density of filaments, but its sensitivity resulted higher than the power provided by the LASER, so a signal could not be stimulated there. Consequently, the only feasible option was the small round solar cell (Figure 3-7 (a)), whose technical characteristics are shown in Table 3-4. Therefore, this solar cell will be the one used in this prototype, as well as it was in [12].





(a)



(b)



(c)

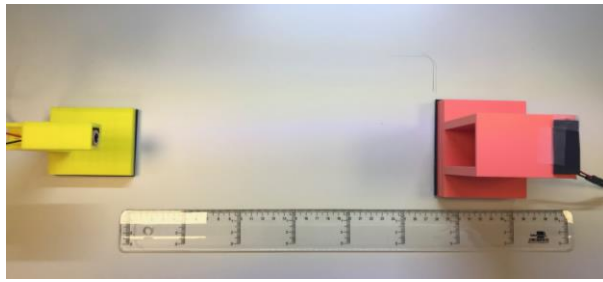
**Figure 3-7** Different solar cells available at the laboratory. (a) and (b) are small solar cells, while (c) is a bigger one [12].

Model No.:	SBED67
Cell Type:	Polycrystalline
Cell Efficiency:	16%
Product Structure:	Epoxy Resin + Cell + PCB
Power Tolerance:	+/-3%
Max Output Power (Wmp):	0.25W
Max Power Voltage (Vmp):	2V
Max Power Current (Imp):	125mA
Open Circuit Voltage (Voc):	2.4V
Short Circuit Current (Isc):	135mA
Size:	dia 67mm
Size Tolerance:	-0.3mm
Life Span:	1-2 years
Warranty:	6 months
Testing Conditions (STC):	Irradiance 1000W/m <sup>2</sup> , Temperature 25°C, AM 1.5

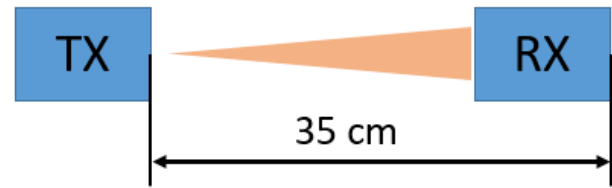
**Table 3-4** Specifications of the chosen solar panel.

### 3.2 Experimental setup

Many experiments were done, whose setup, results and conclusions are detailed along this section. The experiments took place in the laboratory, using the solar panel and the already detailed light sources (3.1.1). In all different measurements, there was a distance of 35 cm between the transmitter and the receiver (Figure 3-8). The transmission rate chosen was 1200 bauds for all cases and light source and water tank properties for each case are shown in Table 3-5. The transmitter and receiver mounts were designed and printed with a 3D printer, whose design and views can be seen in Appendix I.



(a)



(b)

Figure 3-8 Setup for case 1 that shows the distance between the LASER and the solar panel.

CASE #	LIGHT SOURCE	WATER TANK	V <sub>rx</sub> (V)	Received message
1	Red LASER	Free Space Measurement	4,8V	Yes
2	Green LED	Free Space Measurement	4,8V	Yes
3	Green LED	Tap water (14°C)	4,8V	Yes
4	Green LED	Tap water (56°C)	4,8V	Yes
5	Green LED	Blue tap water (2 drops of blue ink)	4,8V	Yes
6	Green LED	Blue tap water (8 drops of blue ink)	1,57V	No
7	Green LED	Green tap water (2 and 12 drops of green ink)	4,8V	Yes
8	Blue LED	Green tap water (12 drops of green ink)	4,8V	Yes
9	Red LED	Green tap water (12 drops of green ink)	1V	No
10	Red LASER	Green tap water (12 drops of green ink)	2,62V	Yes
11	Red LASER	Green tap water (15 drops of green ink)	2,28V	No
12	Green LED	Green tap water (19, 40 and 50 drops of green ink)	3-4,1V	Yes
13	Blue LED	Blue tap water (2-16 drops of blue ink)	2,7-4,3V	Yes
14	Red LASER	Water with brown CDOM	1,7V	No
15	Red LED	Water with brown CDOM	1,5V	No
16	White LED	Tap water	4,8V	Yes
17	White LED	Water with white suspension particles	1,95V	No
18	Green LED	Water with white suspension particles	2,85V	Yes
19	Red LASER	Water with white suspension particles	2,6V	Yes
20	Red LED	Water with white suspension particles	2,8V	Yes
21	Green LED	Harbor water	-	Yes

Table 3-5 Summary of all different cases and their corresponding light source and water tank.



### 3.2.1 Red LASER without water tank-Free Space Measurement

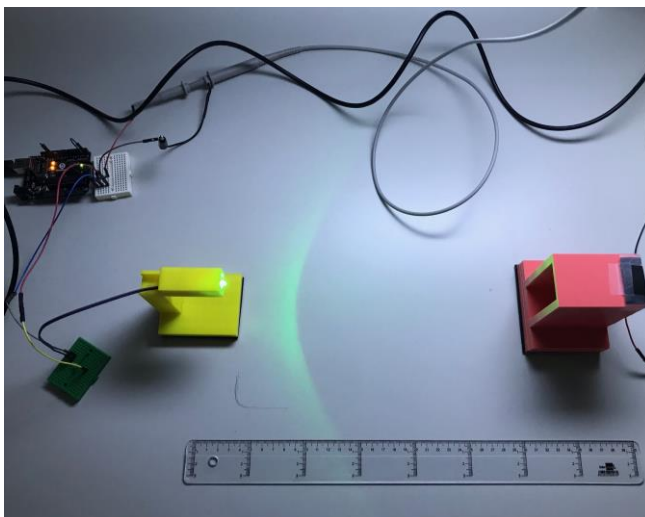
In this first case, the prototype was tested without the water tank. The transmitted and received signal are displayed in the oscilloscope in Figure 3-9, where the transmitted signal is the yellow and the received one is green. It can be observed how there are also falling peaks at the beginning of each pulse, due to the solar panel parasitic capacitance. Regarding the received signal, taking into account that it receives a “1” when the signal is above 2,5 V, it can be notice that there is a little pulse lengthening that if elongated a little more could result in the loss of the message. In order not to oversaturate the receiver, the LASER could only illuminate a little side of the solar panel, resulting in a challenging alignment. This is the reason why it was decided to try a LED afterwards.



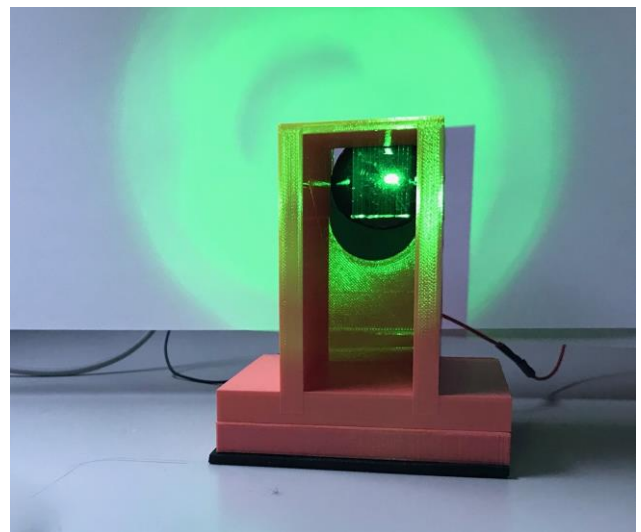
Figure 3-9 Case 1 oscilloscope display. The yellow signal is measured at the transmitter signal and the green one at the receiver.

### 3.2.2 Green LED without water tank - Free Space Measurement

A green LED was tested in this case (Figure 3-10) and it showed a better performance than the LASER. It could be observed that diffuse light enhances light alignment, improving the link reliability considerably. The LED FOV is greater than the one for the LASER, and so it is the range in which the receiver is able to receive the signal, which makes the lining up much easier.



(a)



(b)

Figure 3-10 Case 2 (a) setup and (b) illumination of the solar panel by the diffuse light of the green LED.

Figure 3-11 shows the received signal has a little delay in the arrival of each pulse, which could have been caused by diffusivity and decrease in emitted power. There is a pulse spreading as well, very similar to the one observed when using the LASER on the previous case, because it depends on the solar panel and not on the light source used.

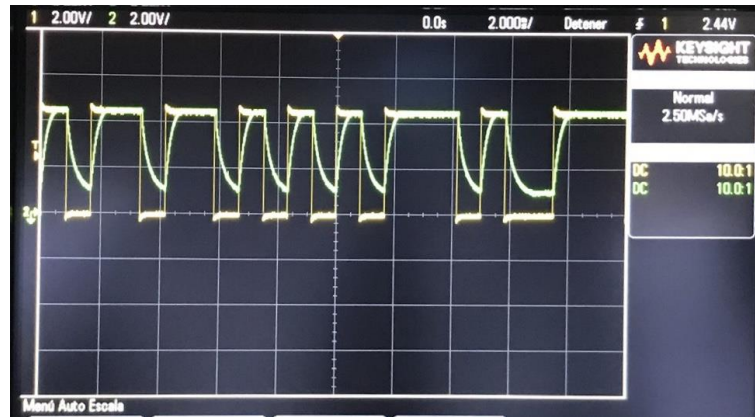
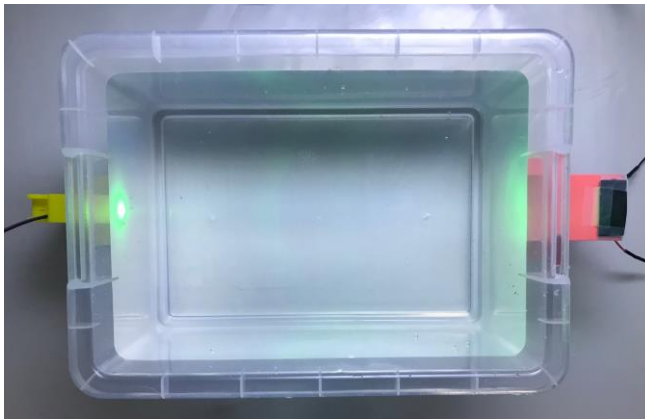


Figure 3-11 Case 2 oscilloscope display.

### 3.2.3 Green LED with water tank (14°C)

After having established a Free Space (FS) link with the LED, the water tank was introduced between the transmitter and the receiver to test the prototype as a UOWC system. Even though it is true that using a LED the received power is reduced, the design met communication expectations of the prototype, since the data was properly received at the designated baud rate. Therefore, all at once, the LED showed greater advantages than the LASER for this specific system, as it is a short-range link.

Then, the relation between underwater light propagation and temperature was tested. Literature states that constant water temperature does not have a remarkable effect on light behavior, whereas a temperature gradient does. In fact, a temperature gradient results in a change on the refractivity index, which indeed affects light propagation direction. In order to prove this assumption, the temperature of the water tank was measured (illustrated in Figure 3-12(b)), obtaining a value of 14°C.



(a)



(b)

Figure 3-12 (a) Setup for Case 3 and (b) temperature measurement with thermal camera (FLIR).

The oscilloscope display is similar to the previous case without the water tank, as it is shown in Figure 3-13. Nevertheless, there is a slight difference on the delay at the beginning of each pulse, which is shorter. It could be because some of the emitted photons reflect on the water tank walls, so more of them are received and the signal reaches the solar panel sensitivity is reached earlier, in a similar way to the LASER, which had even less delay.



Figure 3-13 Case 3 oscilloscope display.

### 3.2.4 Green LED with hot water tank (56°C)

This case is similar to the previous one, but with hotter water (56°C), measured as shown in Figure 3-14. The signals measured with the oscilloscope were very similar to the ones with colder water at 14°C (Figure 3-13). As a result, it was confirmed that with clear water there are no remarkable changes on light propagation because of temperature variations. Therefore, it has been verified that constant temperature does not have a significant effect on underwater light propagation. Although literature states that temperature does not affect light propagation, temperature gradient does, but it is hard to analyze in small water columns. Nevertheless, for short UOWC links, the temperature gradient is usually little, and thus, temperature could be negligible for short links applications in areas where the temperature is usually constant, for example, in diver's communications.

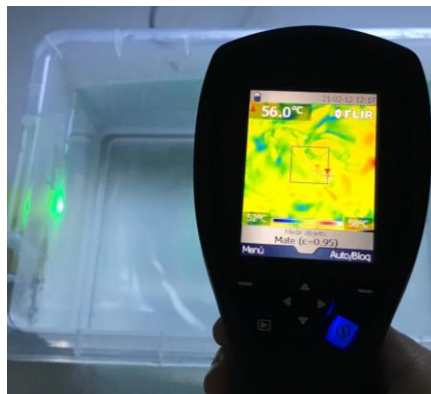


Figure 3-14 Measurement of water temperature in case 5.

### 3.2.5 Green LED with blue colored water (2 drops of blue ink)

From this case onwards, water temperature is going to be stable in-between 10-14°C in all cases, which is close to real ocean temperature.

The relationship between different species of phytoplankton and the wavelength (color) of the light source is analyzed from this case to number 13. Literature states that light absorption depends on both the concentration and specie phytoplankton, and the source light wavelength. In order to do so, blue ink was added to the tank considering its behavior pattern similar to phytoplankton.

The setup and blue colored water aspect for this case is shown in Figure 3-15. While was being stirred in order to get a homogeneous mixture, turbulences were originated, and interestingly, they resulted in a rocking of the received signal. This rocking refers to the received voltage, which was steadily shifting from high to low values because of the water movement (turbulence shown in Figure 3-16).



The transmitted and received signals were measured in the oscilloscope, turning out to be very similar to the ones in case 3 (Figure 3-13), without any noticeable change in their values. This fact shows that a little amount of blue ink does not have a notorious effect on green LED light underwater propagation.

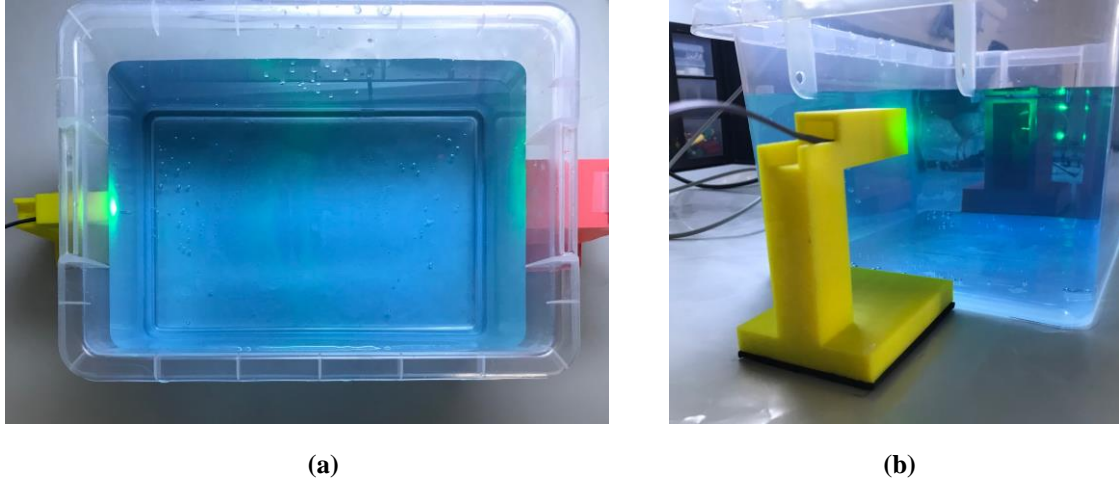


**Figure 3-15** Different perspectives of Case 5: (a) plant view and (b) side view.



**Figure 3-16** Water tank with turbulence affects UOWC.

### 3.2.6 Green LED with blue colored water (8 drops of blue ink)

Afterwards, six blue ink drops were added to the water tank (see Figure 3-17). The received signal was attenuated, but still well received. With these new properties of the water body, the absorption increased up to a level that the received signal was below the threshold of the Arduino, so the “*Hola mundo*” message could not be received.

The oscilloscope display is shown in Figure 3-18. It can be noticed that the received signal (1,57 V) is below 2,5 V, therefore the message cannot be received. In addition, it has a little delay. Nevertheless, as the signal is still received, with a more complex amplifier (adding a preamplifier, filtering and several power amplification stages) the message could be obtained.

After this experiment, more drops of blue ink were added, so the water was darkened up to a point where the signal was not received any more, it was completely attenuated, as shown in Figure 3-17 (b) and Figure 3-18.

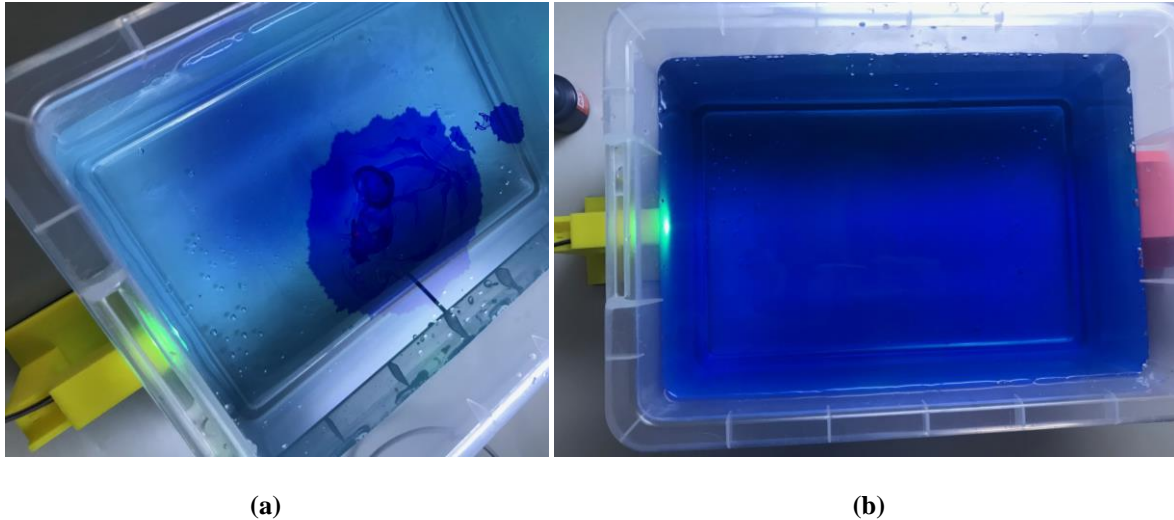


Figure 3-17 (a) blue ink drops being added and (b) final aspect of the water tank.



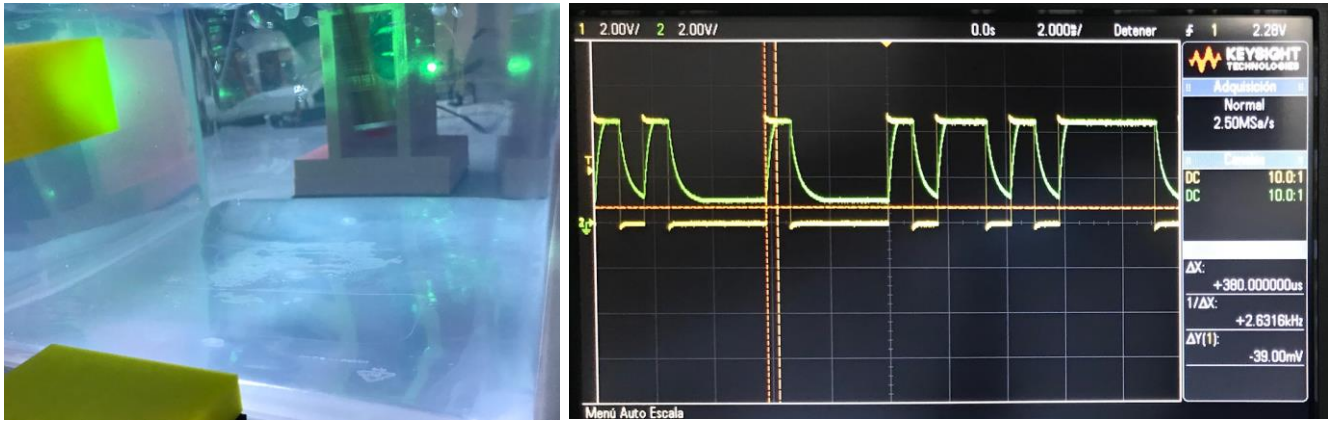
Figure 3-18 Case 6 oscilloscope display.

### 3.2.7 Green LED with green colored water

To emulate the effect of the different plankton species, blue ink was replaced by green ink. Therefore, 2 drops of green ink were added, getting the water aspect showed in Figure 3-19 (a) and Figure 3-20 (a). The received signal is displayed on the oscilloscope in Figure 3-19(b).

It is very similar to the case with blue colored light, even with the little pulse spreading (3.2.5). For that reason, it was concluded that low plankton concentrations result in low levels of light absorption. Moreover, if the absorption is so small that it is barely noticeable, the effect of the different types of plankton will not be perceived either.

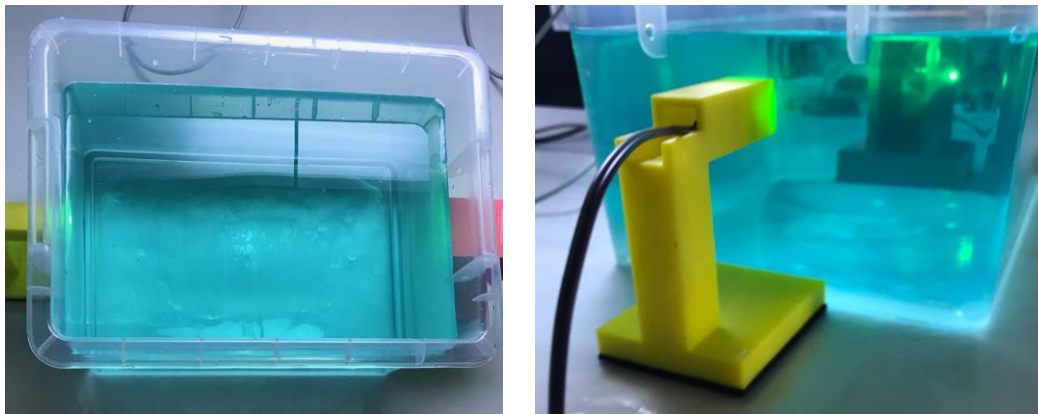
In order to see the effect of increasing plankton concentration, 12 green ink drops were totally added. The water aspect is shown in Figure 2-22, which is lighter than in the previous case with only 8 drops of blue ink (3.2.6). While in the previous case the light was completely attenuated, in this one the message was fully received, even though it had little pulse delays as it can be observed in Figure 3-21.



(a)

(b)

Figure 3-19 (a) Case 7.1 consists of a green LED with green colored water (2 drops of ink) and (b) its oscilloscope display.



(a)

(b)

Figure 3-20 Different perspectives of 7.2: (a) plant view and (b) side view.



Figure 3-21 Case 7.2 oscilloscope display.



### 3.2.8 Blue LED with green colored water

After having tested the propagation of green light in green water, other color LEDs were tested, such as the blue LED in this case (see Figure 3-22 (a)). The measured signals are displayed in Figure 3-22(b), where it can be observed that the light absorption in these conditions is similar to the previous case with the green LED.

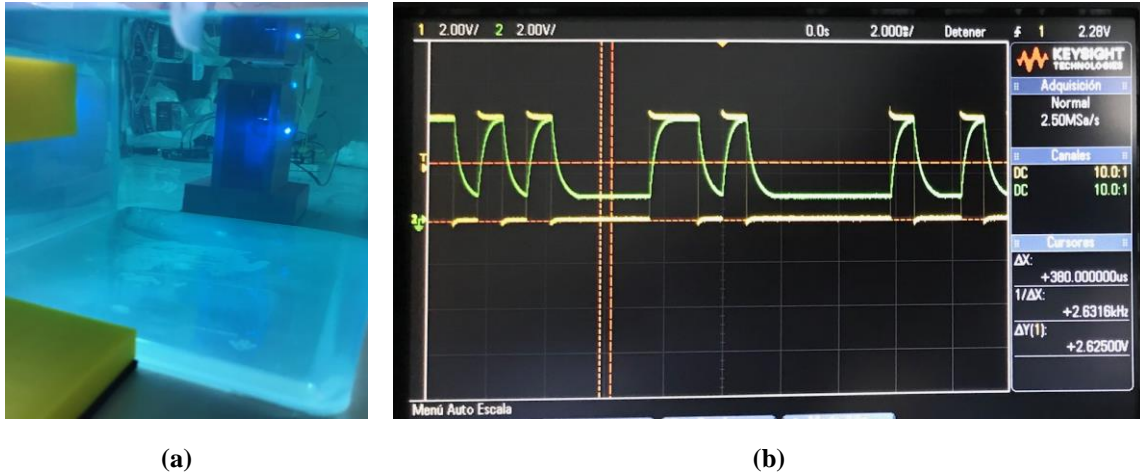


Figure 3-22 (a) Setup and (b) oscilloscope display for case 8.

### 3.2.9 Red LED with green colored water

Then, the prototype was tested with the previous water body, but with a red LED (Figure 3-23 (b)). However, in this case, no signal was received and all red light was attenuated, as it is displayed in the oscilloscope in Figure 3-23(b).

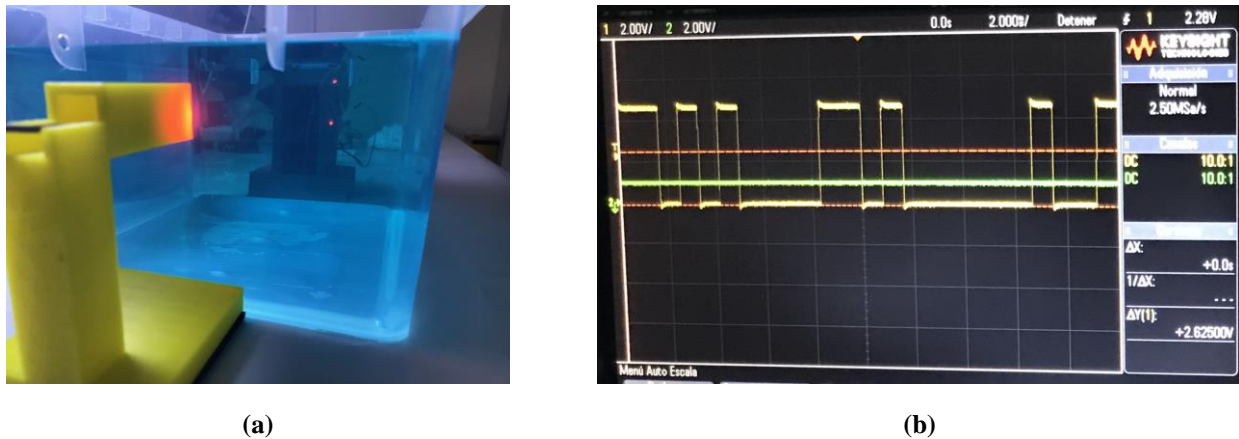


Figure 3-23 (a) Red LED with a green colored water tank and (b) the oscilloscope display for case 9, which shows that it is not received the LED signal.

### 3.2.10 Red LASER with green colored water

Afterwards, it was tested with the red LASER (Figure 3-24(a)). Although in this case, the signal was received, it was highly attenuated as it is shown in Figure 3-24(b). The message could barely be received, given the signal was 2,64 V, only 0,14 V larger than the threshold. This test demonstrates the LASER is more powerful than the LED and therefore it can reach greater distances than a LED of the same wavelength.

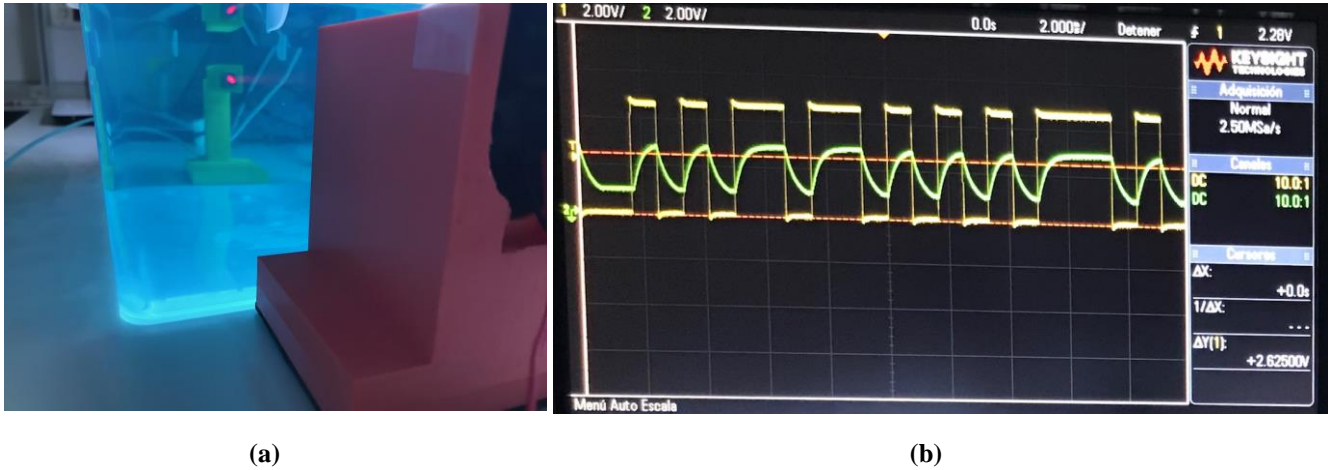


Figure 3-24 (a) Red LASER with a green colored water tank and (b) the oscilloscope display for case 10.

### 3.2.11 Red LASER with green colored water

In order to see when the message stopped being received, more green ink was added to the water tank, up to 15 drops of green ink. Then, although the signal was received, the message was not, as it is illustrated in Figure 3-25. Therefore, with a better signal conditioning the message could be understood. With 34 drops of blue ink, the signal was not even received. The oscilloscope displays a constant received signal of 1 V, which comes from ambient light, similarly to Figure 3-23(b) in case 9 (3.2.11).



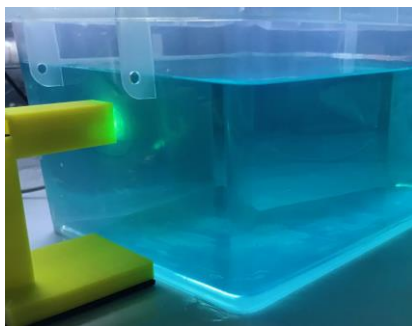
Figure 3-25 Oscilloscope signal display for case 12.



### 3.2.12 Green LED with green colored water

Under this water tank conditions, the green LED was tested again varying the plankton concentration. First, it was tested with 19, 40 and 50 drops of green ink, shown in Figure 3-26 (a)(b); (c)(d) and (e)(f) respectively. The light started to be gradually attenuated with 19 drops, and the test ended with 50 drops, where the message was still perfectly received. As a result, it was demonstrated that light wavelength is determinant in the achievement of an UOWC link and that different types of CDOM have a different effect on light propagation.

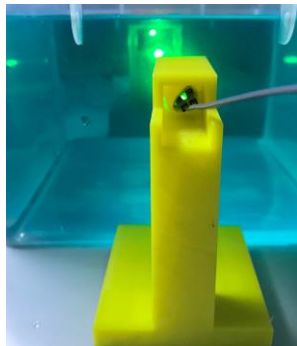
Looking back to the case in which the green LED was used with blue colored water, the message could not be received with just eight ink drops, whereas with this same quantity of green ink, the signal was not notoriously attenuated. The concentration level has a lower impact in this case, as many more drops had to be added in order to notice a mayor change on the attenuation level. Nevertheless, it can also be notice that a drop of blue ink darkens water aspect more than one of green ink. The relationship between plankton concentrations and the amplitude of the received signal is plotted in Figure 3-27.



(a)



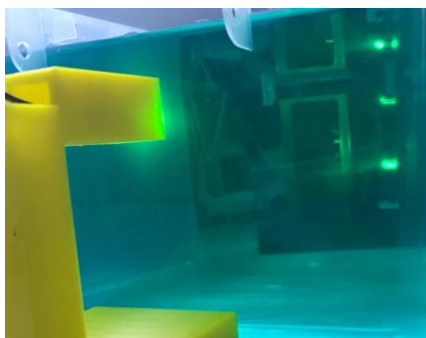
(b)



(c)



(d)



(e)



(f)

**Figure 3-26** Green LED tested in green colored water tank dyed with (a) 19, (c) 40, (e) 50 drops of green ink and their respective oscilloscope displays (b),(d) and (f).

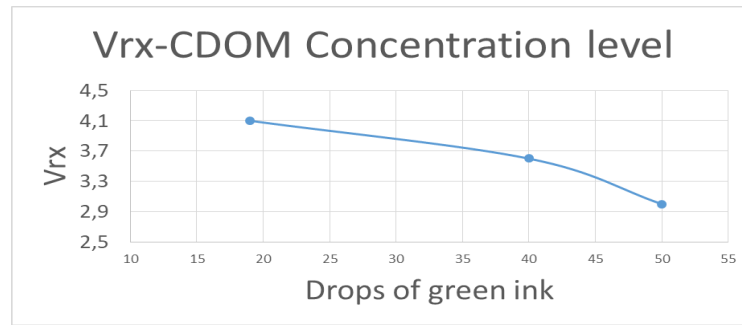


**Figure 3-27 Relationship between the amplitude of the received signal and the increase of ink drops in the green colored water (simulating CDOM).**

### 3.2.13 Blue LED with blue colored water

In this case, the prototype was tested with blue light and blue colored water. The drops of blue ink were gradually added resulting in the signal being progressively attenuated, as it is displayed in Figure 3-28. In all these cases, the message was correctly received, but with two more water drops even though the signal was received, the message was not. Pictures of the colored water body and the oscilloscope display for different drop quantities are shown in Figure 3-29.

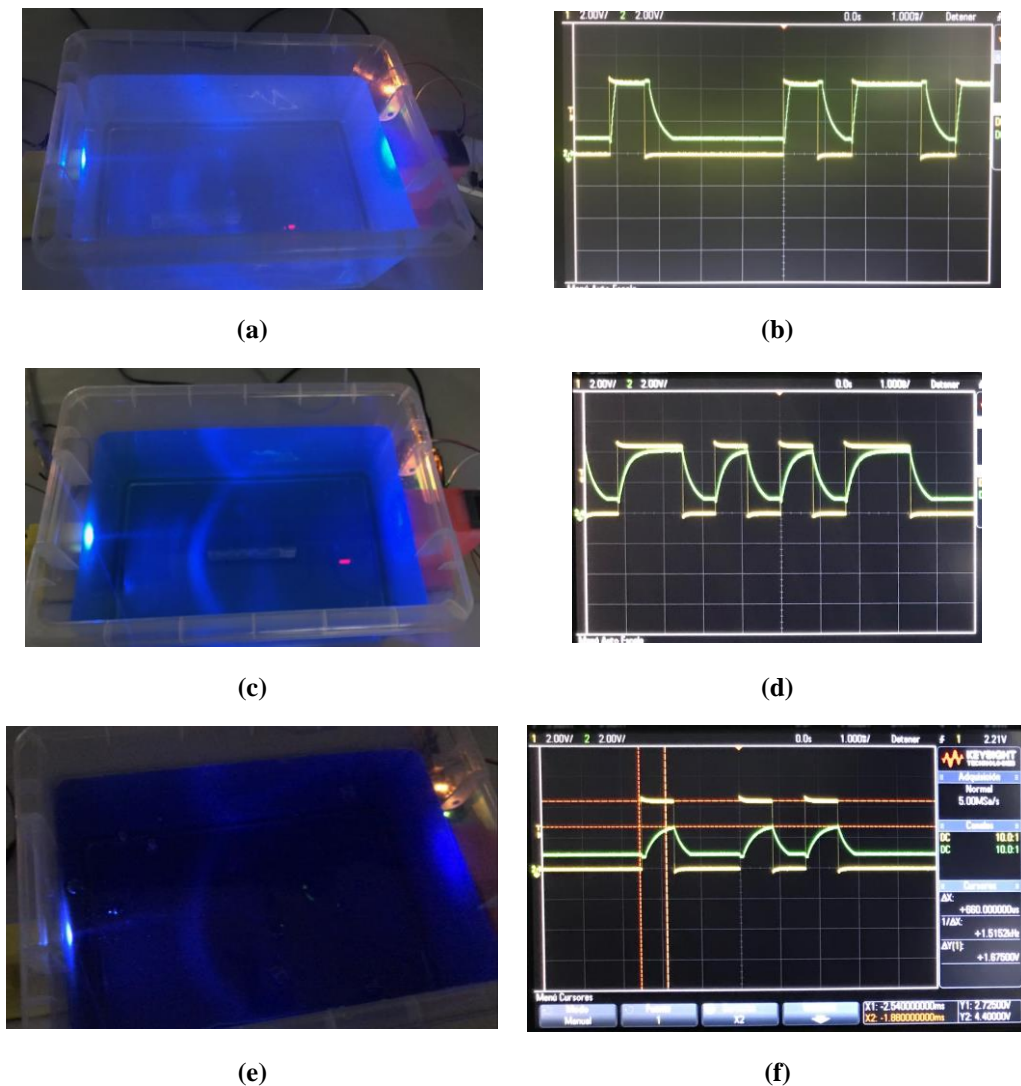
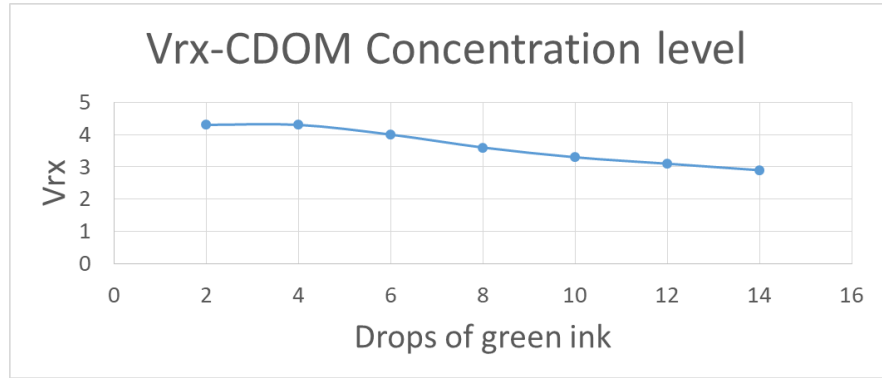


**Figure 3-28 Picture of the colored water body for different tests and their corresponding oscilloscope display for (a)(b) 2 drops of blue water, (c)(d) 6 drops of blue water and (e)(f) 16 drops of blue ink.**

CASE Nº	16
Drops of blue ink	Vrx
2	4,3 V
4	4,3 V
6	4 V
8	3,6 V
10	3,3 V
12	3,1 V
14	2,9 V
16	2,7 V

(a)



(b)

**Figure 3-29 Relationship between the amplitude of the received signal and the increase of ink drops in the blue colored water (simulating plankton).**

While stirring the water in order to a homogeneous fluid, some little air bubbles were originated (in Figure 3-28(e)). It could be observed how they increased light attenuation, due to an absorption rise. In addition, the originated turbulence resulted in fluctuations and instability, which increased the BER. Figure 2-31 displays the oscilloscope measure for this case in which the message was received with some errors. This fact demonstrates the increase in BER and ISI because of turbulence, which has been previously discussed in the literature.



**Figure 3-30 Capture of an oscilloscope display video in which the water in the tank was turbulent. It can be seen how the received signal is fluctuating and unstable.**

Through this laboratory tests, it has been proven how different color particles and concentrations affect very differently depending on the color of the light. All in all, it has been demonstrated that blue and green light suffers less attenuation than red. Moreover, LEDs have proved to be low power light effective sources in a short UOWC system, while LASERS provide greater coverage at the expense of a more complex alignment.

### 3.2.14 Red LASER with water with brown CDOM

To begin with, the tests of brown CDOM, a tablespoon of cocoa was diluted in the water tank. All light sources were tested in such conditions, but none of their light signal did even reach the receiver. The aspect of the water body can be seen in Figure 3-31, as well as the high scattering of the light. There, the different light beams of LEDs and LASERs can be clearly noticed, as well as how all the light is absorbed and scattered before approaching the receiver.

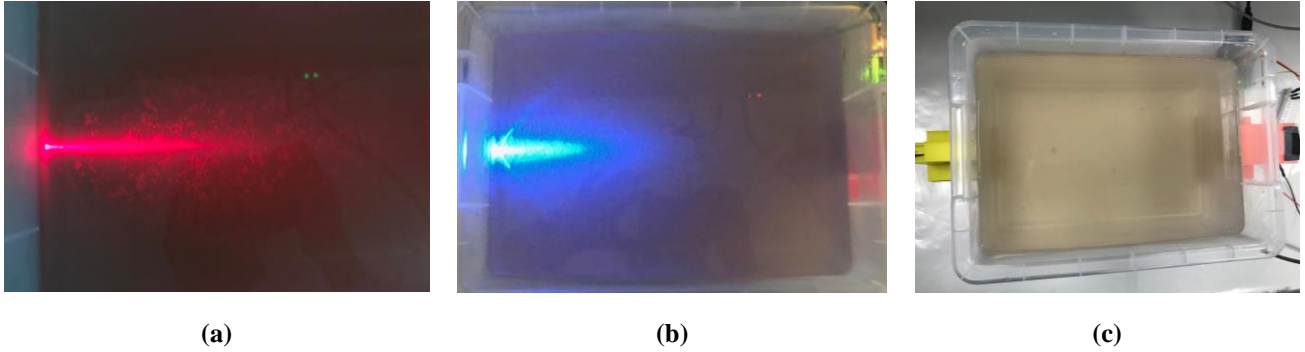


**Figure 3-31** Water with Brown CDOM and (a) the red LASER and (b) the blue LED. (c) Water body with brown CDOM once in was diluted more.

To continue, the brown CDOM was diluted with more tap water and the prototype was tested with the red LASER (Figure 3-32). In this case, the signal could be appreciated at the receiver, but as it was lower than the threshold, the message was not received. As it was said before, in such cases the message could be interpreted by implementing a more sophisticated signal conditioner.

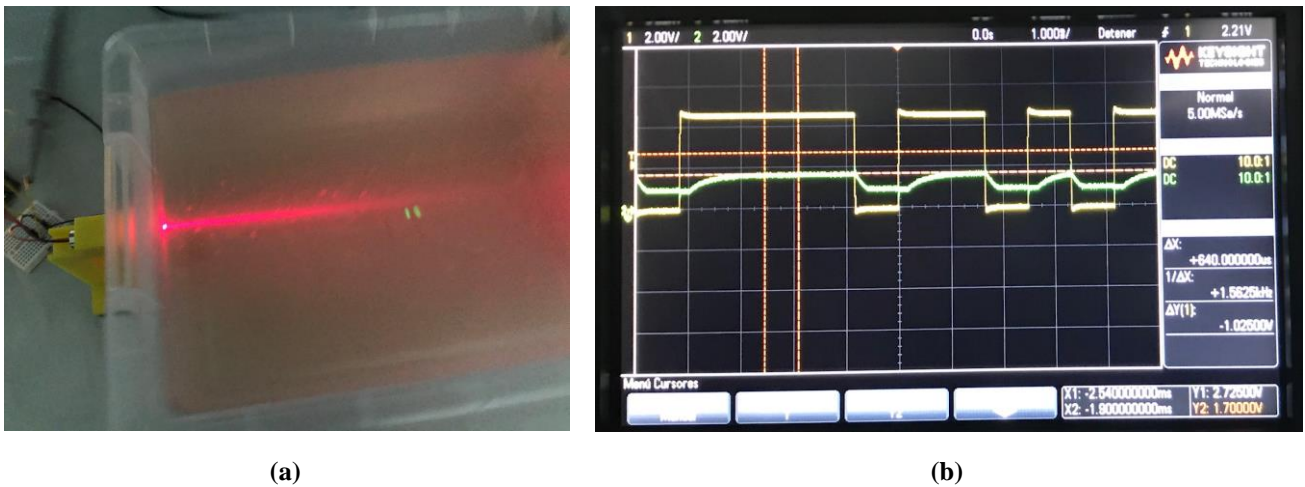


**Figure 3-32** (a) Red LASER tested with a brown colored water tank and (b) its oscilloscope display.

### 3.2.15 Red LED with water with brown CDOM

Subsequently, the red LASER was replaced by a red LED, which had a slightly different behavior: only a 0,2 V difference in the received signal. The greater beam divergence of LEDs, already studied in the literature can be observed in Figure 3-33, next to the oscilloscope display for this case.



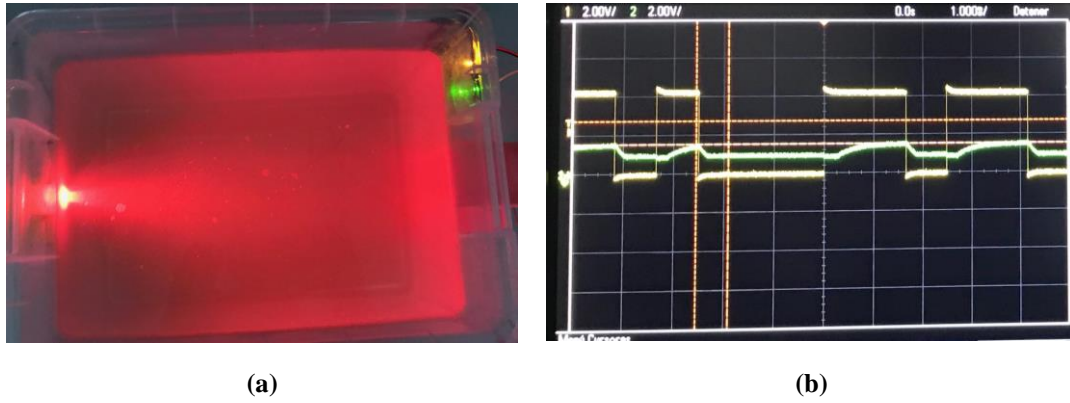


Figure 3-33 (a) Red LED tested with a brown colored water tank and (b) its oscilloscope display.

### 3.2.16 White LED with tap water

Up to this point, the white LED had not been tried, so to begin with, it was tested with tap water. This case is shown in Figure 3-34, where it is noticed that although the signal suffers little attenuation, the pulse delay (slow rate) is greater than with other sources such as the green LED (3.2.3). The chosen white LED emits blue light and a phosphor material around the source converts the light from blue to *similar-to-white* light.

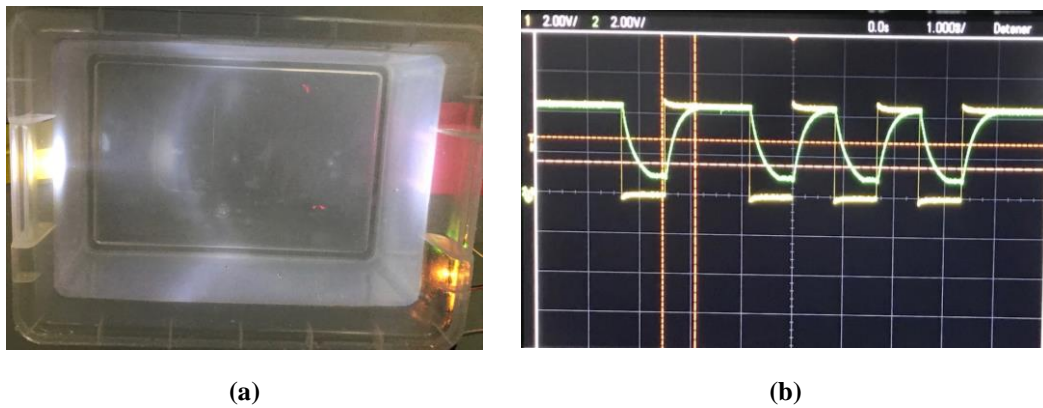


Figure 3-34 (a) White LED tested with tap water and (b) its oscilloscope display.

### 3.2.17 White LED and water with NAP

Afterwards, little white suspension particles (flour) were added to the water tank, to study NAP concentration effect on light wavelength. The attenuation of the signal increased, as a result of the rise in absorption and scattering and, consequently, the message was not received (Figure 3-35).

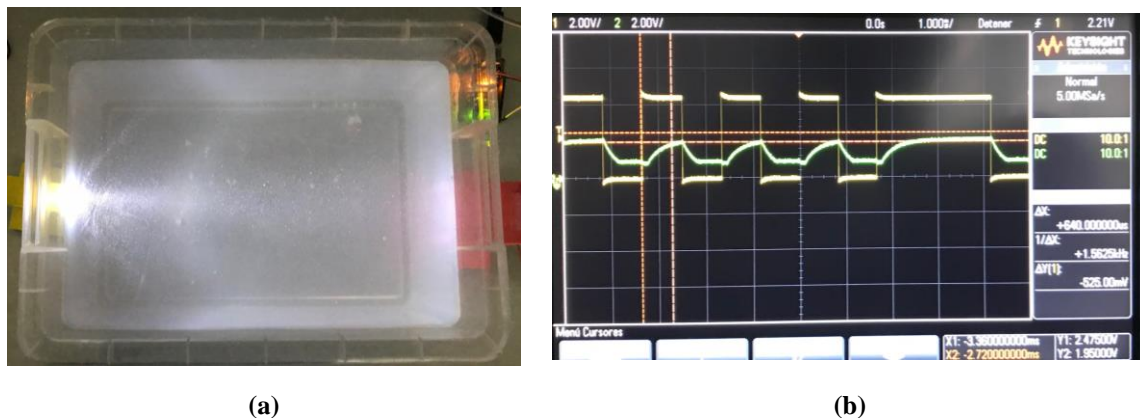


Figure 3-35 (a) White LED tested in water with white suspension particles and (b) its oscilloscope display.

### 3.2.18 Green LED and water with NAP

Next, the white LED was replaced with the green LED, in which case the message was received despite the signal attenuation (Figure 3-36). It can be distinguished that water is not as homogeneous with suspension particles as it used to be with CDOM. Consequently, more light is reflected outside, a fact that could explain the overall greener aspect of the water tank.

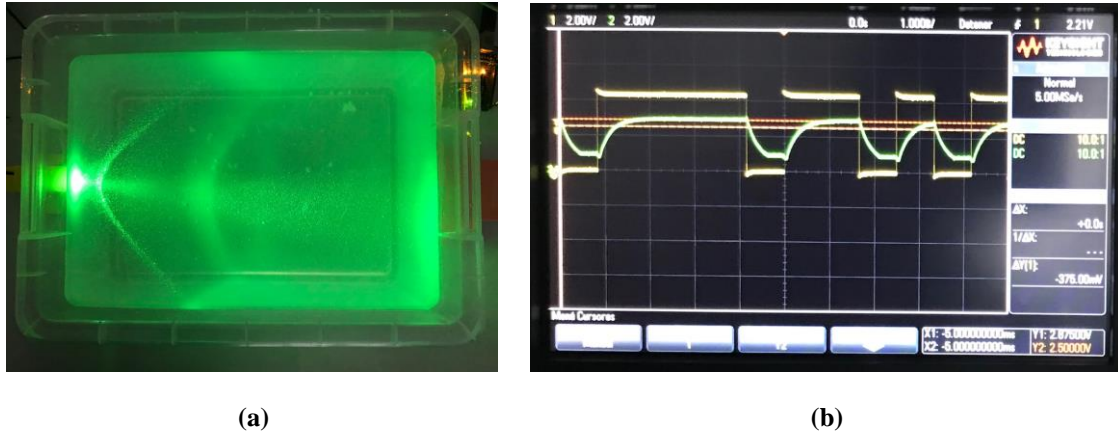


Figure 3-36 (a) Green LED tested in water with white suspension particles and (b) its oscilloscope display.

### 3.2.19 Red LASER and water with NAP

In this case, the red LASER was tried under the same circumstances than the previous analysis with the green LED. Surprisingly, the light was not attenuated as it can be notice in Figure 3-37. Notwithstanding, the pulse lengthens significantly and has a delayed ascent.

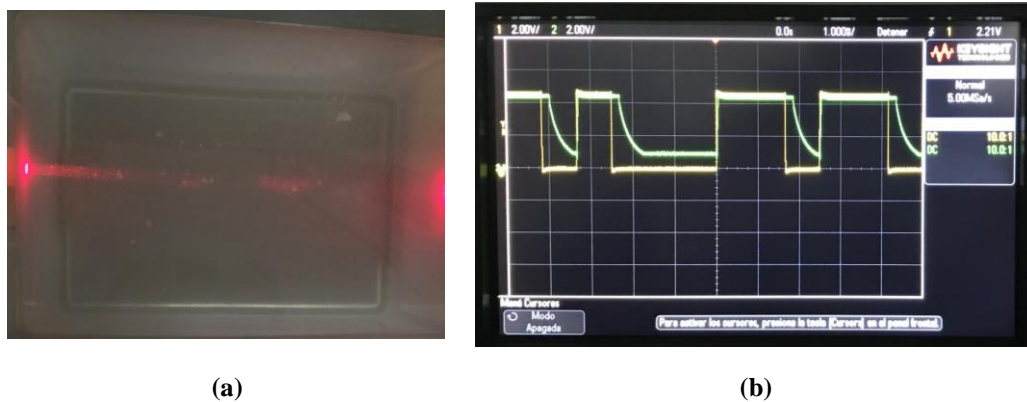
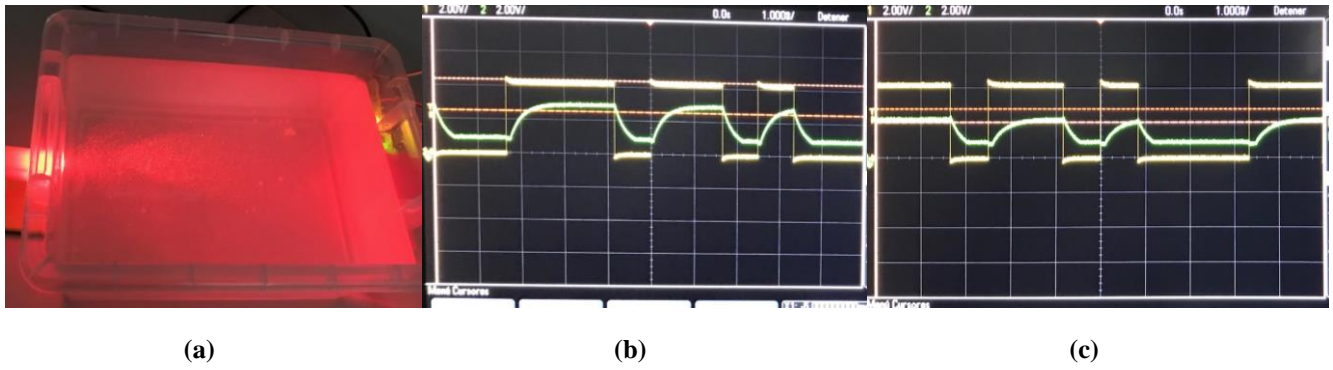


Figure 3-37 (a) Red LASER tested in water with white suspension particles and (b) its oscilloscope display.

### 3.2.20 Red LED and water with NAP

Following, a LED was tried with the white suspension particles, and the results showed an attenuation growth. Although the attenuation enabled the UOWC link, it was higher than in all previous cases that involved water with suspension particles. As a result, from the past two cases, it can be interpreted that powerful directed light beams as LASERs have a better behavior and are less attenuated in water with suspension particles than divergent light beams such as LEDs.

Figure 2-38 shows this case's process. First, it was tried without touching the water tank (Figure 2-38(a)), but it was noticed that some suspended particles were laying at the bottom of the water tank. Therefore, the water tank was stirred obtaining the results shown in Figure 2-38(c). This validates that the higher the concentration of suspension particles, the higher the absorption.



**Figure 3-38 (a) Red LED tested in water with white suspension particles and its oscilloscope display (b) at first and (c) after having been stirred.**

### 3.2.21 Green LED in harbor waters

Finally, the last analysis was performed in the harbor. One of the current applications of UOWC is communication with divers. A survey was made to military divers [127], and they coincide in that one of the common missions is checking the hull and ship propellers, which is done in harbor waters. Consequently, this simple prototype was tried there to analyze its performance. To begin with, the maximum range the prototype could operate in free space was measured, which turned out to be ~70 cm with negligible background noise (Figure 3-39).

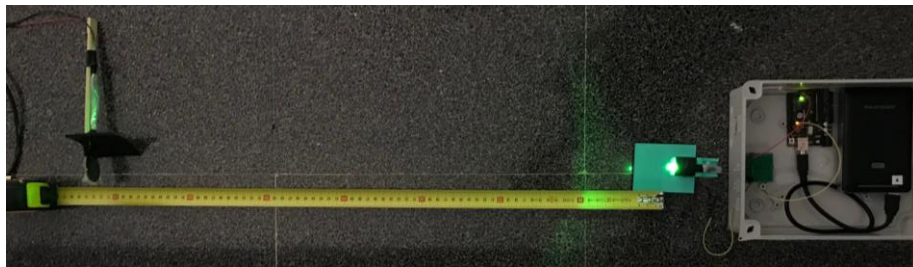


**Figure 3-39 Measurement of the maximum range of the prototype tested as a free space system.**

Afterwards, the prototype transmitter and receiver were waterproofed in order to be tested in the harbor water. Firstly, the prototype was tested during the day, but the communication link was not effective, because of the background noise caused by sunlight. This could be improved by adding a sensitivity regulator on the receiver, but with such basic tester-prototype, reception was not feasible.

Since the design of a more sophisticated transceiver is beyond the scope of this work, the prototype was tested during the night (Figure 3-1). Even though the communication link was established, the alignment was difficult and the message was received with a remarkable BER. Nevertheless, it is not surprising, as it was proved in the surface water with high turbulences. On the one hand, as soon as the prototype deepens gradually, the turbulence decreases. On the other hand, once it gets closer to the bottom, water becomes more turbid, worsening UOWC.



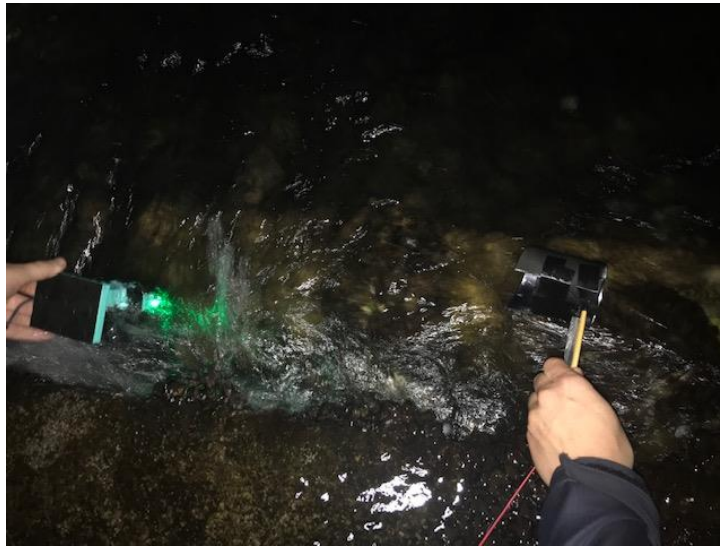


**Figure 3-1 The prototype being tested in harbor water during the night.**

As a whole, it can be concluded that in most cases, the best wavelength source is a green light source.

In terms of the decision on whether to use a LED or a LASER, it will depend on the range of communication that wants to be achieved and if its alignment is going to be an obstacle or not.

In addition, it is not only the light source what matters, but also the receiver, as its sensibility and SNR determine whether the communication is going to be successful or not. A complex sophisticated signal processor can make the difference between establishing the communication link or not.

Lastly, as excepted, turbulence, turbidity and particles types and concentrations do also have a substantial effect on UOWC.

## 4 MILITARY APPLICATIONS

After having demonstrated that UOWC is a technology field with a wide range of capabilities, current and potential applications will be discussed through this chapter. Several UOWC systems have been designed for many different areas such as ocean biology, environmental research, surveillance, seismic monitoring, ship hull monitoring, communicating with submarines and diver communications among others. In all of them, UOWC gives a remarkable advantage over other communication technologies regarding bit rate, speed and bandwidth. Consequently, it does also make the difference if applied into the military.

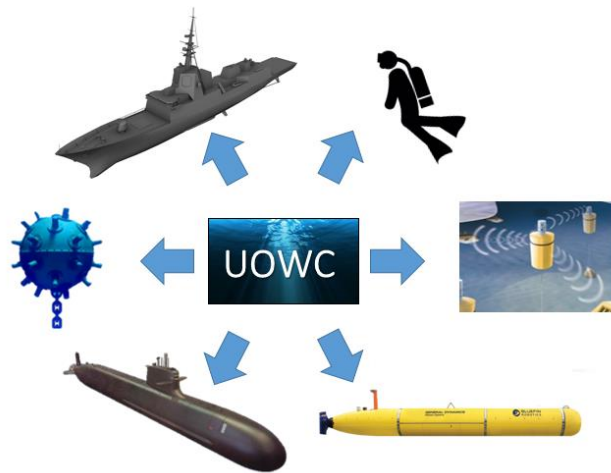


**Figure 4-1 Different applications of UOWC in the military field.**

In the military, UOWC systems could improve mine detection and communications with divers, UUVs and submarines. In addition, an underwater sensor network could give a considerable advantage in *Anti-Submarine Warfare* (ASW).

In this section, developed UOWC systems will be detailed, explaining how they could be applied in the military. However, all disclosed information comes from unclassified sources, and thus there might be much more sophisticated systems, but since they are classified, no information is freely available. Moreover, the different applications of UOWC in the military field will be explained, focusing in the Navy since they are the ones in charge of the surveillance, security, efficient use and freedom maintenance of the seas, which also includes underwater environment [128].

To begin with, the distinguished features of UOWC allow it to accomplish the characteristics of naval communications: confidence, safety and speed [129]. One of the biggest benefits of this communication technique is the safety they provide given the alignment requirement; and even if the

signal were intercepted, the information would have to be decrypted. Regarding speed, UOWC meets any requirement above expectations, provided its high velocity, bandwidth and bit-rate. Nevertheless, in order to achieve confidence, UOWC must be employed through modeled channels with a relatively low risk of turbulence or variation in their properties. For this reason, UOWC is better designed for short distance links or, in case long distances need to be covered, relay nodes should be used to ensure confidence.

Therefore, weapon applications will not be discussed because UOWCs depend on the underwater environment and do not cover long distances. The applications that have been considered feasible and interesting for the implementation of UOWC systems are divers, UUVs, underwater sensor network, anti-submarine warfare and mine warfare.

#### 4.1.1 Divers

The implementation of UOWC as a communication system among divers is thought to be very attractive. Therefore, a survey was conducted to identify requirements, necessities, current shortcomings, major challenges and future perspectives of their communications.

Thirty-four Spanish Navy divers were surveyed, each of them with different studies on the field as well as different operations carried out (Figure 4-2) where six of them are from the Spanish Special Naval Warfare, specialized in combat operations such as sabotage and infiltration. It can be observed that the most typical operations are SAR, hull inspections, underwater searches, mine warfare and explosive operations. From this data, it can be inferred that most of their operations take place in unknown areas or turbid waters such as harbors. Nevertheless, to confront this assumption, they were asked in which type of water they usually dive into, obtaining the results shown in Figure 4-5.

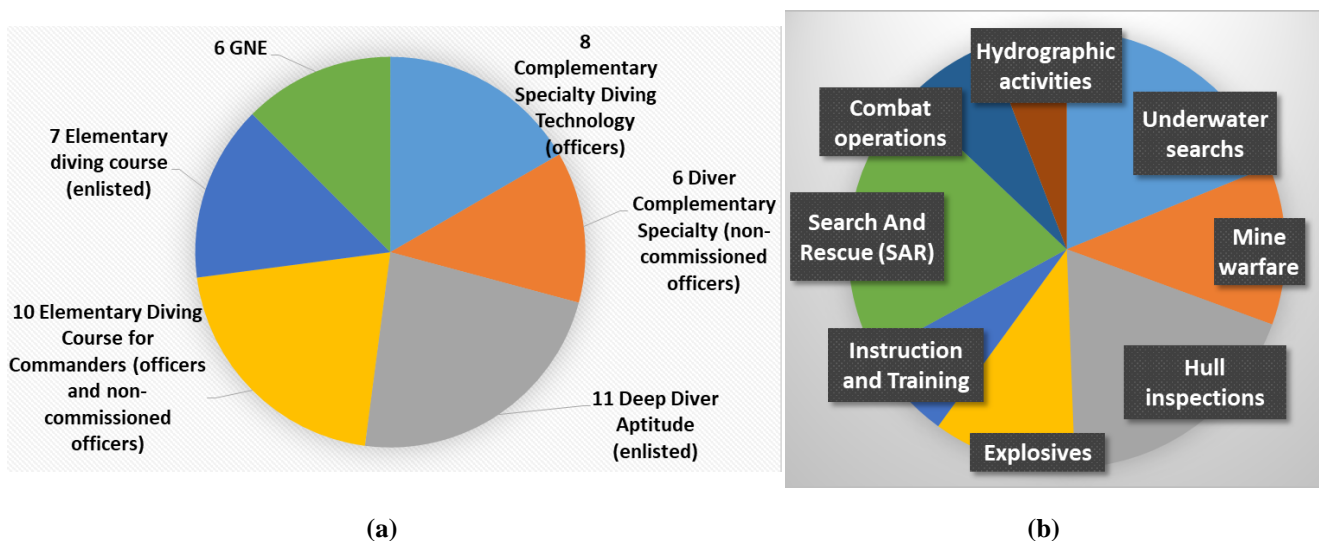


**Figure 4-2 (a) Diving formation of questioned divers and the (b) types of operations they have carried out.**

In order to understand the need for an additional communication system, divers were asked if they had a miscommunication during their dive. The results show that 85% of them (29 divers) have ever needed an extra communication system at depth, compared to 15% (5 divers) who had not. In most of the cases this failure was because one of the most frequent way of communicating is optically, through sign language, so if the water is either too dark or too turbid, they cannot be seen. In addition, some of the divers mentioned that there was no adequate signal to express what they needed to say. The means of communication which are currently available in the Spanish Navy should be taken into account, as well as which of them are the most widely used (Figure 4-3).

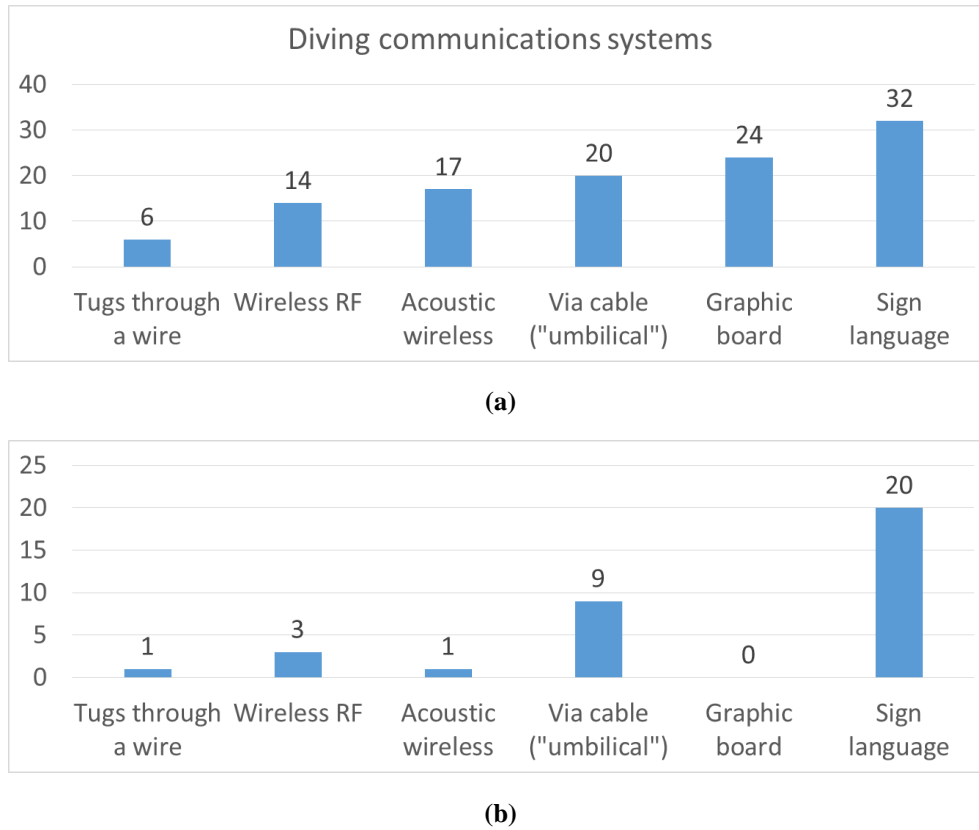


**Figure 4-3 (a) Diving communications systems used at least once by the 34 surveyed divers and (b) the most used one for each of the divers.**

According to the survey, sign language is still the most used communication system among divers. The main advantage of this method is its ease of use, but it is very limited to specific preset messages and turbidity, even more than UOWC, as they depend on independent external light sources. Some of these signals are shown in Figure 4-4(a).

Figure 4-4(b) shows what divers call “umbilical”, which is widely used as well. Interestingly, the wire is not only used to transmit data, but also for sending *tugging* signals.

Most divers have also tried (at least once) a graphic board to communicate, but none of them uses it as the principal communication system. Regarding non-optical wireless methods, even though there are some RF and acoustic wireless systems available, their use is not as common as sign language. RF provides short distances coverage, while acoustic covers much wider zones.

Moreover, there are brand new sophisticated systems such as PowerCom 5000D which has 8 different channels and a nominal range of up to 3000 meters (Figure 4-4(c)) [9].

Figure 4-3(d) shows an example of an UOWC real prototype: the LUMA X and LUMA 500ER modems from Hydromea, a Swiss company. LUMA X is the flagship optical communication modem of Hydromea, with their highest speed (10 Mbit/s), longest range (50 m), HD-quality video, 4K image transfer in real-time, opening up new possibilities for subsea communication and possibility of being up to 6000 meters deep.



(a)



(b)



(c)



(d)

**Figure 4-4** Examples of some communication systems among divers: (a) diving optical manual signals, (b) diver's communication via cable ("umbilical") and example of Acoustic Wireless System, (c) PowerCom 5000D, a Wireless RF system [9] and (d) LUMA X and LUMA 500ER modems from Hydromea, an UOWC system [130].

The type of water in which divers usually operate was asked as well, obtaining the results showed in Figure 4-5. From this data, it can be inferred that most of their operations take place in harbor and coastal waters, where water is turbid and UOWC have shorter range. However, when performing a hull inspection, the needed link range is limited. Under these circumstances, UOWC happens to be an advantageous alternative to other wireless communications systems as well as sign language.

In addition, a few divers said they usually dive during the night, which makes UOWC much more efficient thanks to the reduced background noise. At the same time, these night dives are usually in order to avoid being detected, so in those cases, the use of a LASER instead of a LED will be appealing despite the more difficult alignment, resulting in a reduced beam widespread that would hardly be detected.



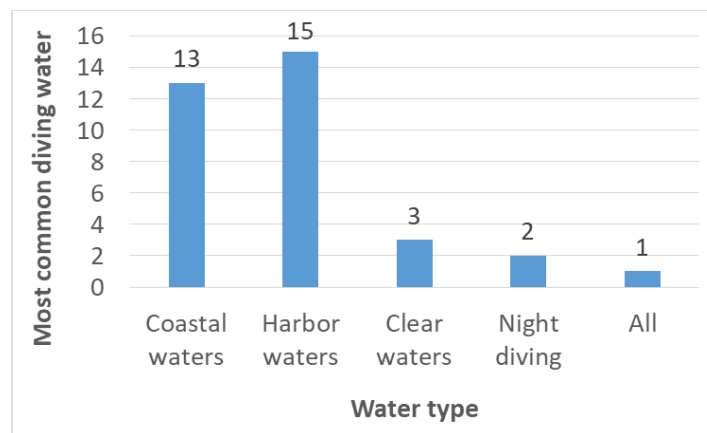


Figure 4-5 Most common diving waters of surveyed divers.

Divers were also asked to rank from one to five the importance of four communication parameters: discretion, bandwidth, speed and maximum range (see Figure 4-6). Results revealed that the factor that is considered most important is speed, followed by maximum range, bandwidth and discretion. The responses were grouped together because slight differences between different performed operations could be observed. The groupings made were one hull inspection (12 divers); SAR (8 divers), GNE (6 divers), instructors (4 divers) and a diver specialized in countermining. Undoubtedly, for GNE, discretion is vital. The larger the group, the better the general opinion will be.

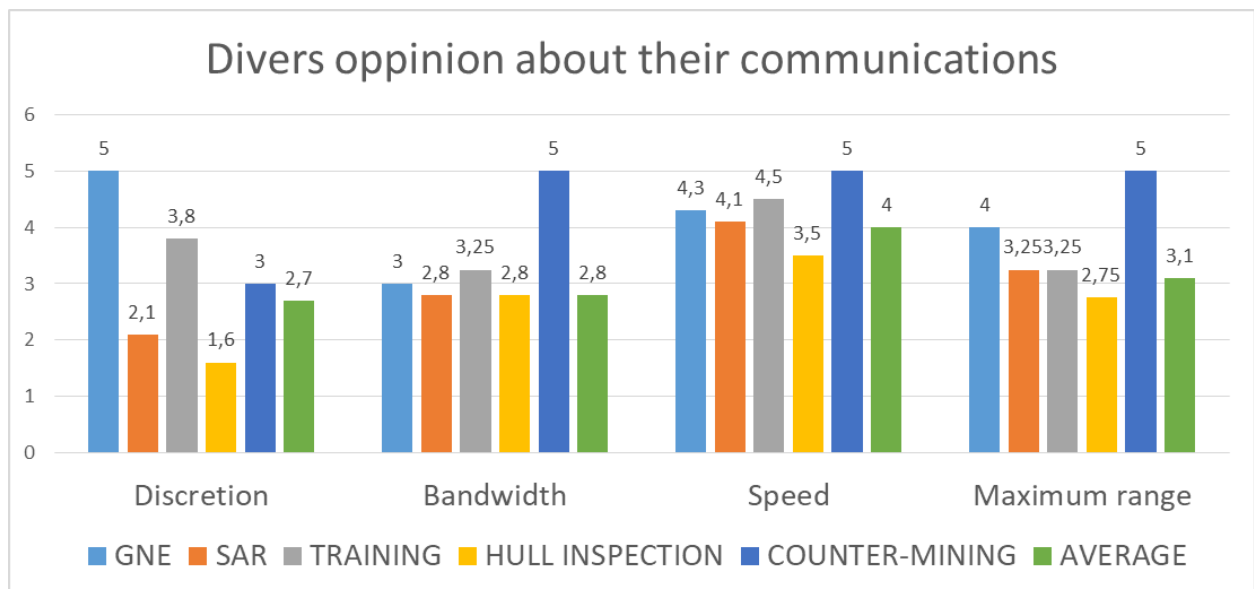
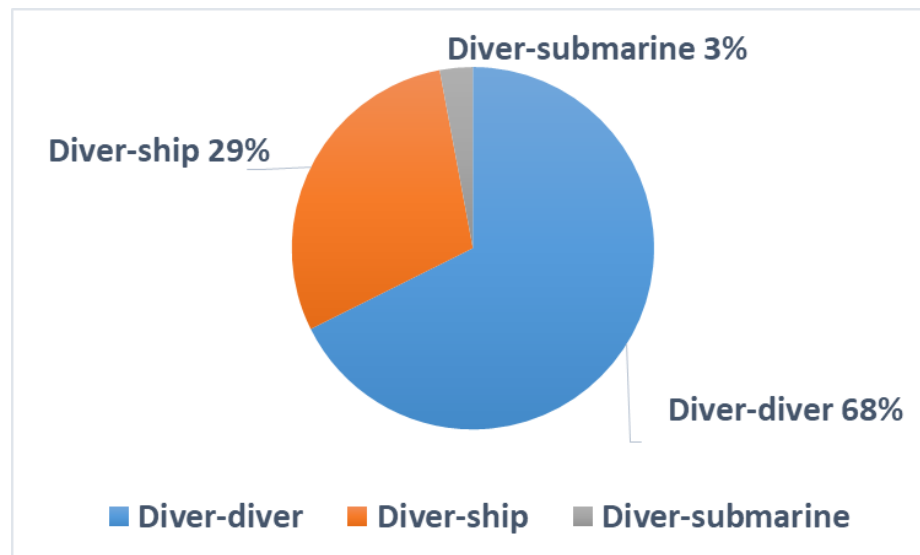


Figure 4-6 Divers opinion on their most important communication requirements based on different operations.

In order to determine the feasibility of a UOWC system, divers were also asked whether they usually communicate with other divers, submarines or ships besides their corresponding communication distances. Responses are shown in Figure 4-7. The average distance required are: 2-3 meters for diver-diver; 20 meters for diver-ship and in the case of the diver-submarine, which was just one diver's most common communication link, the diver responded that he usually dove to a depth of 6 meters depth and the maximum depth he had ever dove was 96 meters.



**Figure 4-7 Most common communication links among surveyed divers.**

To conclude the survey, it was asked how valuable would it be the implementation of a feasible UOWC system in the Navy, in which diving field would they implement it. The average result was “4,6” out of “5”, and the fields in which they believe it would be more useful are GNE infiltrations and hull inspections (Figure 4-8). It should be noted that of the 34 surveyed divers, only eleven had heard about UOWC systems before, and of those eleven, only two had ever tried a prototype before. Interestingly, these two divers valued the implementation with a “5” out of “5”, and believed these systems would be useful at every kind of diving operations, especially GNE infiltrations.

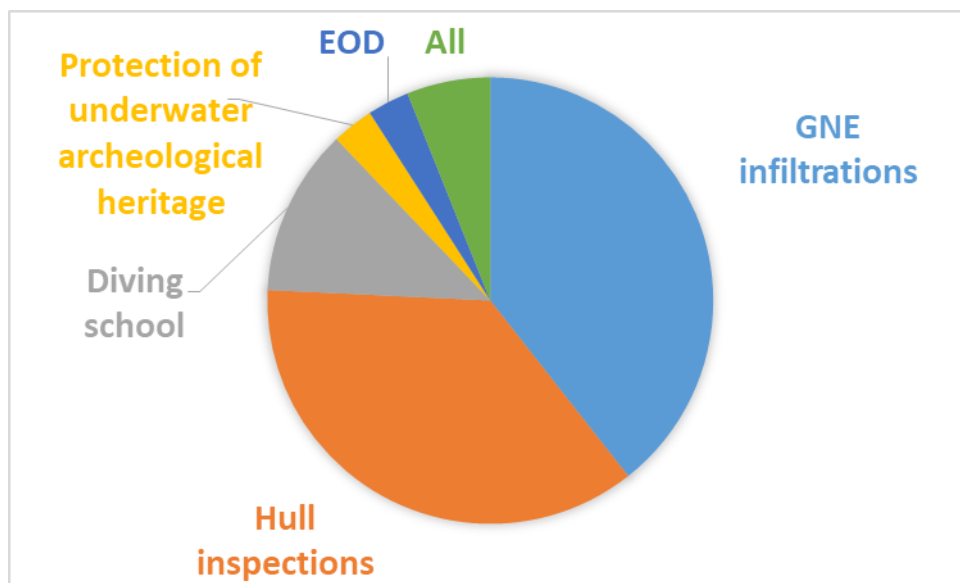


**Figure 4-8 Diving fields in which UOWC would be more useful according to surveyed divers.**

A portable UOWC device for divers is not a futuristic dream, as there are already some commercial devices. For example, Aqua-Fi (May 2020), which is a LASER Wifi system, one of the latest advances in UOWC. It consists of low power and compact underwater optical wireless system, which was deployed by Researches from King Abdullah University of Science and Technology, bringing Internet to the water to support today’s applications. Aqua-Fi provides bidirectional wide-range communication services with different requirements, using a LASER or LED, while having low cost and simple implementation [127].



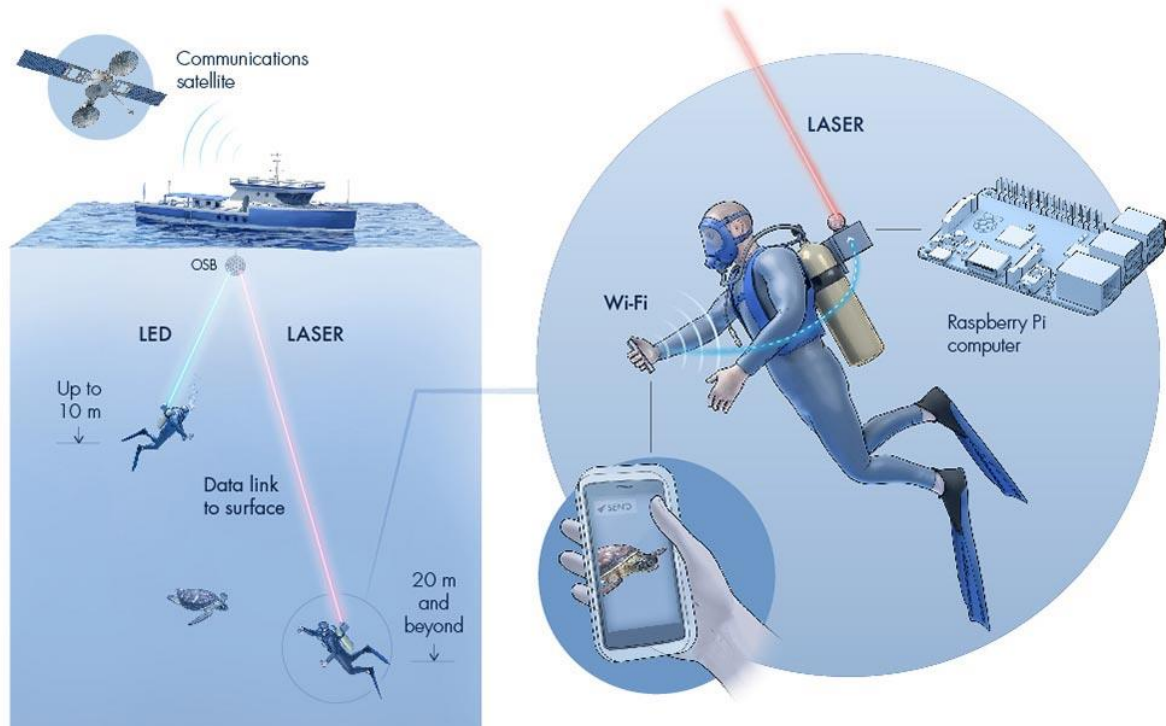


**Figure 4-9**Aqua-Fi would use radio waves to send data from diver’s smart phone to a “gateway” device attached to their gear, which would send the data via light beam to a computer at the surface that is connected to the Internet via satellite [127].

Maybe, in the Navy, there is not a need of being connected to the Internet (it could even be inconvenient), but as it has been explained, communications among divers can be improved in order to develop a greater strategic operability. Command and Control (C2) and decision-making are necessary characteristic of military forces, which are enhanced and improved by effective communication means and procedures.

After analyzing all of them, the most feasible and useful applications happened to be GNE operations, hull inspection, instruction, and training. Further investigation on UOWC system improvement can be done to reduce the background noise, facilitate the alignment and reducing the attenuation to reach larger distances. For example, in GNE operations, the UOWC system could be implemented with LASERs, so that the light beam does not diverge much and nothing is seen from proximities. On the other side, in hull inspections the discretion is not that important, but new researches should be focused on reducing attenuation, alignment requirement and communication through NLOS path.

Regarding instruction and training, the future seems bright as well.

In SAR and Hydrography operations, the most useful communication would be between the ship and the diver, so greater distances shod be overcome. Nevertheless, the design of a feasible UOWC system for such operations would enable live streaming which could be of great help. Still, countermining and EOD might not be the ideal application operations for UOWC systems, due to new-sophisticated activation systems of mines.

Table 4-1 summarizes the advantages and disadvantages of each of them.

Applications	Advantages	Challenges
GNE operations	<p>High discretion level.</p> <p>High effectivity against electronic countermeasures.</p> <p>Very short distances between divers.</p> <p>Low background noise during the night.</p> <p>Continuous communication among divers during the insertion.</p>	No light should be seen around.
Instruction and training	<p>Continuous communication between instructor and student, enhancing the learning.</p> <p>Short distances among divers.</p>	When diving in a harbor, turbulence and turbidity.
SAR and hydrography	<p>Continuous communication with the ship during the search.</p> <p>High bandwidth than could enable live streaming, enhancing C2 and decision-making.</p>	The distance from the diver to the ship, which could be very large in specific areas.
Hull inspection	Continuous communication with the ship during the inspection, enhancing C2 and decision-making.	<p>High background noise during the day.</p> <p>Depending on the weather and the type of seabed, turbulence may be high if close to the surface, as well as turbidity if close to the bottom.</p>
Counter-mining / EOD	Continuous communication with the ship during the operation, enhancing C2 and decision-making.	<p>A sophisticated mine could be activated with light.</p> <p>The distance from the ship is very large.</p> <p>The larger the distance, the more difficult the alignment and the less discretion level.</p>

Table 4-1 Advantages and disadvantages of the implementation of UOWC systems.

#### 4.1.2 Underwater Wireless Sensor Network (UWSN)

In the military, preparation and early warning are vital to face the enemy. Nevertheless, underwater environment presents serious challenges for surveillance, monitoring, data collection and tracking. This fact was acknowledged a long time ago, since during WWI and WWII German U-boats were an essential component of Germans war strategy [131]. Therefore, allied forces started developing underwater sensors to address the high address submarine threat. Several advances in underwater acoustics were made during this war period, although much of the work done was not published until many years later [132].

Afterwards, during the Cold War, technology continued developing and the U.S. Navy laid fixed networks of underwater hydrophones on the ocean floor called the “Sound Surveillance System” (SOSUS) to detect Soviet submarines [133].

Nowadays, when defense spending is growing despite global crisis [134], some countries do already have an UWSN and the many of the ones who does not have it, have its development as a future goal. For example, China does already have some UWSN in the South China Sea [135] as well as the US [136], which already had underwater sensing devices since last century [133].

In Spain, however, it is not a reality yet, but it is under research for a future development, as it appears on the *Technology and Innovation Strategy 2020*, which establishes the main Research and Development (R&D) objectives in a long term (2021-2027) [137]. Among all the objectives, the objective number 4.1.2 is the investigation and technology development based on sensor networks for the protection of maritime zones of surface and submarine threats. The sensor net will be considered multi-sensor distributed, autonomous, cooperative and remote, with the possibility of being supported by maritime UAVs.

Most of the already developed UWSN are acoustic, which significantly limits their bandwidth. For this reason, alternative ways such as optical links have been investigated as an alternative to acoustic links. Interestingly, the results show that the most efficient UWSN would be hybrid optical-acoustic sensor networks [55].

On the one hand, underwater acoustic sensor networks cover large areas, but with low data rate, high power consumption, high cost as well as damage to marine mammals. On the other hand, underwater optical communications provide high data rate, although their networking is difficult and obtain short communication distance. As a result, it has been proposed an *Optical-Acoustic hybrid Underwater Wireless Sensor Network* (OA-UWSN) which combines the advantages of acoustic and optical communication, enabling high bit-rate and high bandwidth transmissions as well as long range communications [55].

In Figure 4-10 it can be observed how an hybrid link is more efficient than an optical or acoustic, in addition to consuming relatively less energy than the acoustic link, and only a little more than the optical [138].

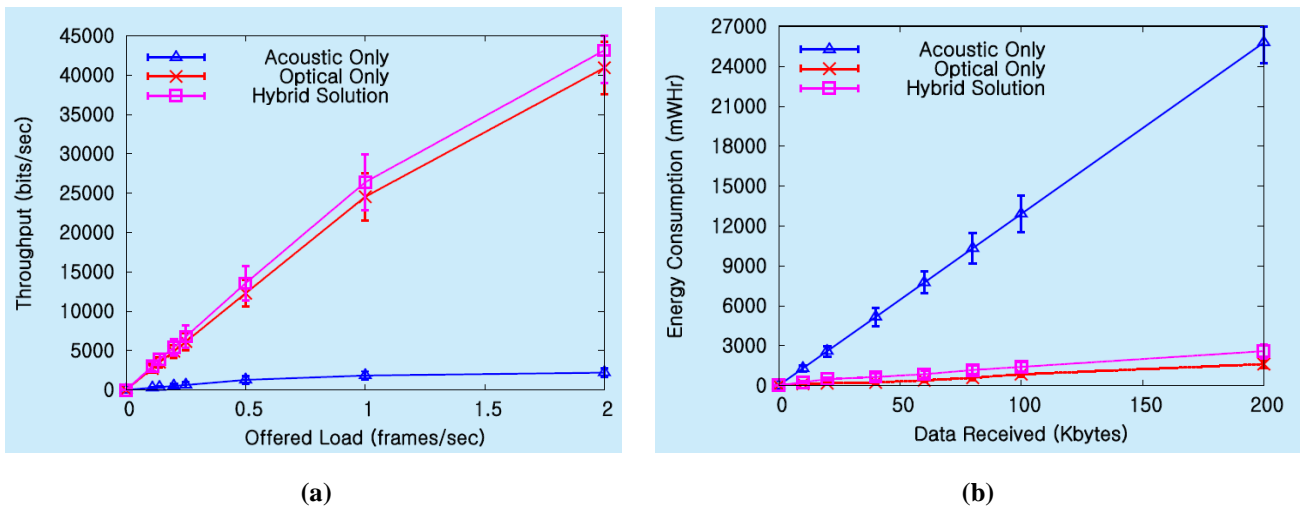


**Figure 4-10 Comparison between Acoustic, optical and hybrid links, regarding their (a) throughput as a function of offered load and (b) energy consumption with varying data size [138].**

An UWSN performs task monitoring in a specific region, thanks to its sensors and vehicles that communicate cooperatively through wireless connections [139]. Figure 4-11 shows an example of an OA-UWSN with aerospace and terrestrial communication. It involves sensors, ROVs, submarines, communication buoys, relay nodes, onshore data center and satellites.

An example of an UWSN distribution consists of the different relay nodes such as underwater sensors, ROVs, or divers, located around an optical access point (OAP) [140]. These nodes send information to the OAP through UOWC, which retransmits it to other nodes similarly, wirelessly to a seabed fiber-optic cable or even to terrestrial and aerospace devices (Figure 4-11).

The implementation of UOWC in UWSN soars their speed, bandwidth and transmission rate. Consequently, it is a promising technology to support the concept of *Internet of Underwater Things*<sup>11</sup> (IoUT). These UWSN are of great interest to the military, as they provide intelligence, command and control in an adverse changing environment. If this sensor network were developed, a myriad of sensors would acquire full situational awareness and control over diverse underwater zones and conflicting areas [140].

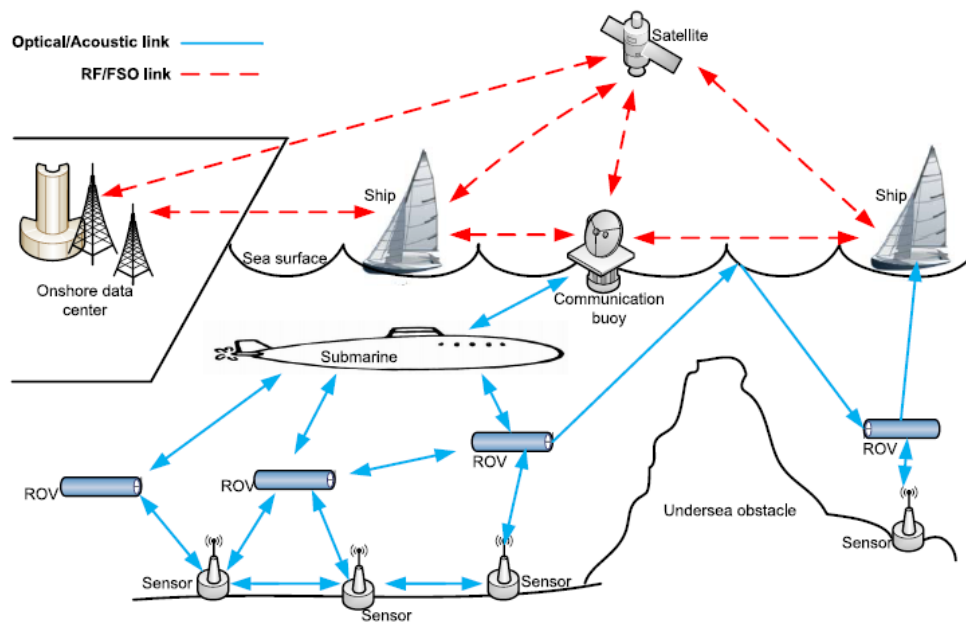


**Figure 4-11** An underwater wireless sensor network with aerospace and terrestrial communication [27].

It can be concluded that in the military field UWSN have multiple applications such as distributed tactical surveillance, early warning, assisted navigation and monitoring of port or harbors. The requirements of UWSNs are longevity, accessibility, complexity, environmental sustainability, security and privacy [139]. Then, the implementation of UOWC in UWSN has a bright future, given their lower power consumption, high security and complexity.

#### 4.1.3 Unmanned Underwater Vehicles (UUVs)

Another military application of UOWC is UUVs, which are thought to be the future of Submarine Warfare [141] [142]. There are two types of UUVs: *Remotely Operated Vehicles* (ROV), which are controlled by a human operator; and *Autonomous Underwater Vehicles* (AUV), which are operated independently of direct human input. The main challenge for UUVs is their communications systems, which has been studied for years [143].

<sup>11</sup> IoUT is defined as the network of smart interconnected underwater devices and objects [140].

As communications with an UUV are complex due to the sea environment and their movement, it is believed that the best solution for establishing communications with them should combine the three subsea wireless communications options into an hybrid system (2.2) [8]. There is little disclosed information about the already developed prototypes and their communication systems but from the analysis of UOWC, it can be said that the implementation of UOWC in such devices will improve their capabilities.

The integration of a UOWC system in UUVs will improve their strategic operability, allowing them to transmit data at very high rates in short distances and being less vulnerable to electronic countermeasures. If UUVs were required to establish long range communications, the best solution for would be an optical-acoustic hybrid system. Figure 4-12 (a) shows an UAV operating close to an OAP of an UWSN, which is an effective way of permanently covering vast underwater zones. An example of recent developed UUV is the Boeing Orca, an extra-large UUV designed by Boeing (Figure 4-12 (b)). It is not disclosed communication system it has, it can be laid discretely from standoff ranges and hundreds of miles from the nearest friendly unit [8].

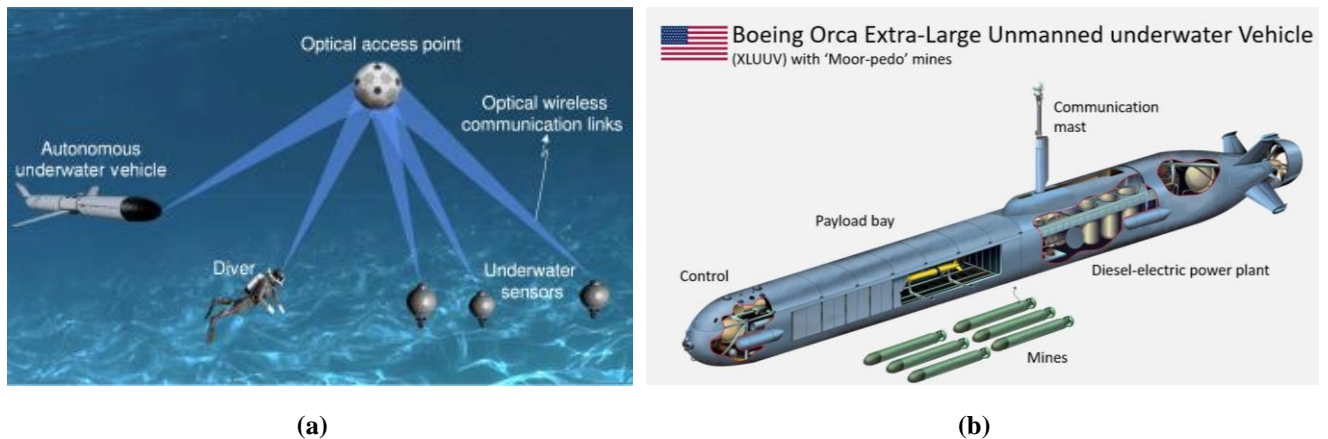


**Figure 4-12 (a) An AUV operating in UOWC network scenario [140] and (b) The U.S. Navy's first extra-large UUV, the Boeing Orca [144].**

In the Spanish Navy, there are currently four different types of UUVs. Two of these are in countermining vessels, and the other two in the underwater SAR vessel “*Neptuno*” as well as in the Navy dive center. Regarding countermining operations, the *Minesniper* is a ROV that goes to the mine and exploits with it, whereas the *Pluto Plus* is a ROV that gathers information about the mine and its zone around. The other two UUVs are designed for underwater SAR operations. These are the *Scorpio-03* and the *Navajo*, which can dive up to 600 meters and 300 meters respectively. There is a debate on whether should the Spanish Navy acquire new UUVs for ASW, but nowadays there is not any UUV for this purpose [145]. Nevertheless, there is an ongoing program called “Barracuda” which is evaluating the available UUVs in the Spanish market, both ROVs and UAVs [146].

Another advance in the application of UOWC to UUVs is an underwater Wifi system, which has been developed by France. This technological breakthrough could lead to a small revolution in the operation of UUVs, both in the civil and military sectors. It allows sharing heavy data, such as videos, without a wire link, thanks to the outstanding features of the optical communication [147].

Table 4-2 analyzes the general advantages and difficulties that come from the implementation of UOWC systems in UUVs, referred to the accomplishment of their missions. The missions of UUVs correspond to the ones of the Spanish Navy UUVs, but also from ASW UUVs such as the Boeing Orca [144]. Specifically, the integration of UWOC systems in to the Spanish UUVs, would be an interesting idea. If integrated in the SAR UUVs, when the search is within reach, live streaming with the SAR vessel could be done, notoriously improving communication. An example of the interoperability and



integration of UOWC in UUV is shown in Figure 4-14, which could be similar to Scorpio or Navajo UUVs once they are implemented an UOWC system. Another possible application would be with the upcoming maritime action and underwater intervention vessel (BAM-IS), which could carry UUVs for underwater intervention [148].

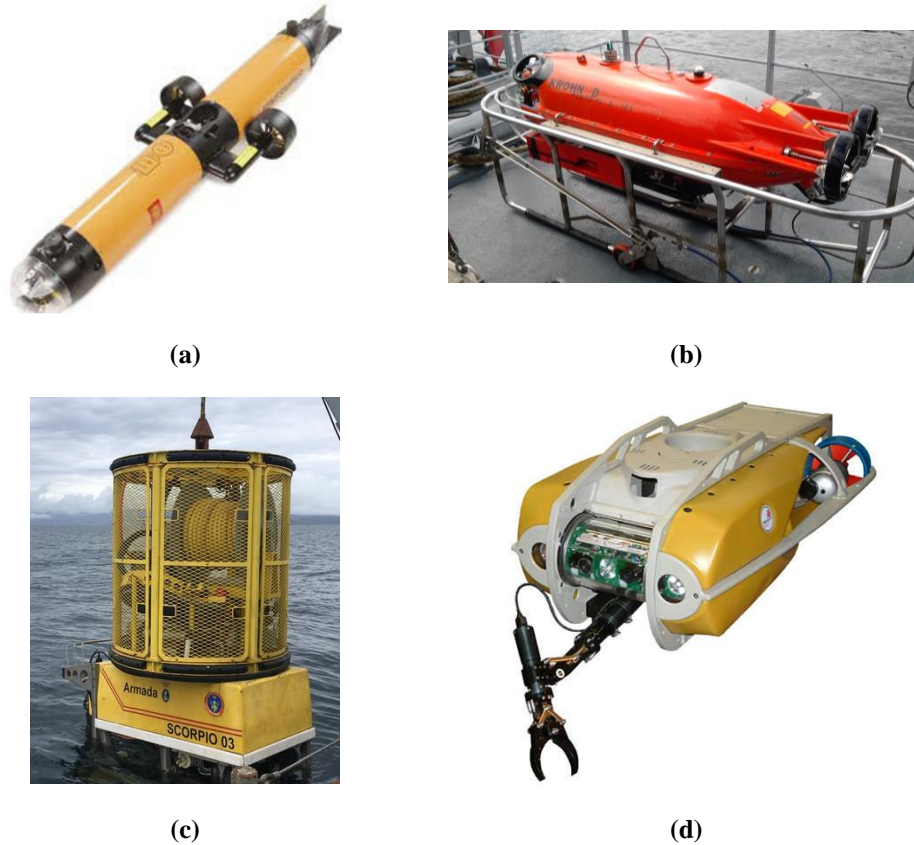


**Figure 4-13 Different UUVs at the Spanish Navy: (a) Minesniper, (b) Pluto PLUS [149], (c) Scorpio [150] and (d) Navajo [151].**

Missions of UUVs	Advantages	Difficulties of its implementation
Counter-mining	Better underwater picture and reconnaissance level.	Short range.
SAR	Higher discreetness.	High dependence on underwater environment.
Underwater surveillance	Enhanced interoperability (UWSN, UAVs, divers, submarines).	The interoperability is much better within an UWSN, which is not always available.
Seabed-to-space network	High bandwidth that could enable live streaming.	
Intelligence	Instant communication.	
Hydrographic Surveys		
Data collecting		

**Table 4-2 Advantages and difficulties of the implementation of an UOWC system in UUVs according to its most common missions.**



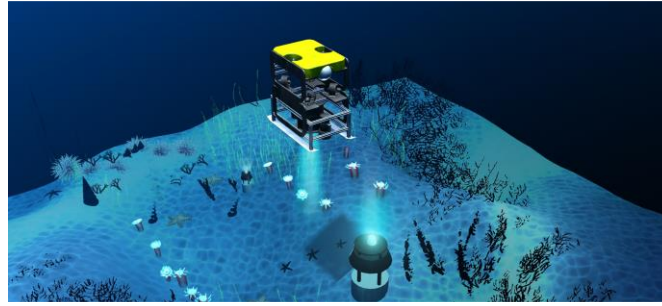


Figure 4-14 UUV serving as a data mule to collecting data from seafloor platforms by UWOC [93].

#### 4.1.4 Submarine Warfare (SW)

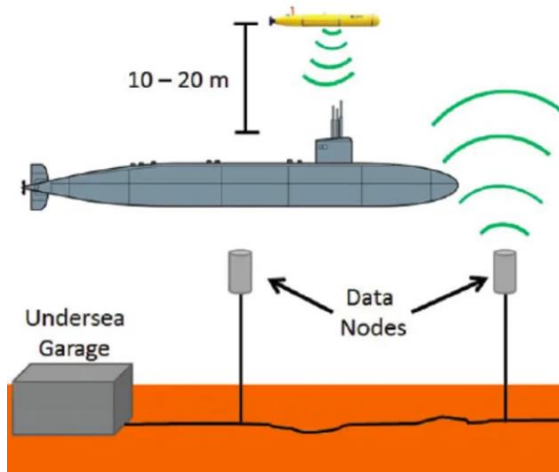
Submarines are warfare units with a high offensive capability, in addition to having the advantage of operating covert during long periods. This characteristics makes them especially useful in the generic mission of *Deterrence and Defense*, and more specifically in the *Operational role of Control of the Sea*, in order to deny its access to the enemy as well as giving freedom to maneuver to merchant traffic and to one's own forces [152]. In order to discuss the feasibility of integrating UOWC systems in submarines, they are going to be divided in two big groups: conventional and nuclear. Whereas the conventional submarines need snorkel<sup>12</sup> to operate, nuclear submarines immersion limit depends on the logistics on board.

Although UOWC with submarines might sound modern, many studies on this field were carried during the last century. The first successful submarine-to-aircraft optical communications is thought to have been achieved by the *USS Dolphin*, which was commissioned in 1968 [153]. More studies about this specific type of communication have been carried [30], but most the found studies date back to last century [154]. This could be because further information cannot be disclosed. The communication of a submarine with a satellite or a plane while it is submerged is a considerable advantage in submarine warfare (SW), as submarines will not have the need to surface and rise the antenna communicate. Hence, why this communication system could make the difference with nuclear subs, as the only need they have to surface is communications and logistics. The main difficulty of stablishing an optical communication link between a submarine and a satellite or plane is the alignment, which might require of the knowledge of the transmitter and receiver exact position.

Nevertheless, submarine could also communicate with a UWSN, which might be easier as the receiver position (node) could be known (Figure 4-15). These would be a very effective way of implementing UOWC into a submarine. In this way, they are similar to UUVs; moreover, some countries such as the United States are designing XLUUV as part of their next generation of submarines. In this specific case, communications would be even more important, and implementing underwater optical technology would have similar advantages and difficulties to the ones mentioned with UUVs. Moreover, the communication between an UUV, diver could be implemented as well, which could be much easier through an UWSN.

---

<sup>12</sup> To rise a short tube to exchange air with the atmosphere, maintaining the rest of the submarine submerged.



(a)



(b)

**Figure 4-15 (a) Interface between submarine, UUV, and data nodes [155] and (b) Echo Voyager and Orca XLUUV [156].**

#### 4.1.5 Mine Warfare (MW)

Mines are explosive device that are placed in the water with the intention of sinking or causing damage to ships, or just to make them desist from navigating a certain area. MW encompasses all mine-related activities, including both mining operations and the parallel use of all available measures to counter mine threats, also known as *Mine Counter Measures* (MCM) [53].

One of the characteristics of mines is their activation method, which is very important because if not known, a mine cannot be disabled. In mine operations, factors such as the wait time until detonation or the type of target must be taken into account in order to decide the activation method. Having said that, UOWC could be used for two main different purposes: (1) for mine search and (2) mine activation and deactivation.

A UOWC system for detection could be very useful. In order to be able to detect and classify mines, the clarity of water column, vertically and horizontally, is vital. In addition, influence mines use the target's signature for the detonation. This influence can be traditional such as variations in the acoustic, pressure and magnetic field; or more sophisticated methods such as variations in IR, submarine electrical potential, seismic effect, an optical contrast is a sophisticated and interesting mean of activating mines. Therefore, it would not be a favorable idea to implement UOWC systems when approaching the mine. Meanwhile, if UOWC systems continue growing, it might be a good a good idea to design a mine that detonates due to a specific light radiation.



**Figure 4-16 Mine Detection with a UOWC system [157].**

To conclude this section, in addition to the potential military applications suggested taking into account the analysis of the state of the art on UOWC and similar systems already developed in other countries, some Spanish defense companies were asked to address such applications. For example, the firm SAES, a company specialized in underwater radiations such as electrical, magnetic and especially acoustic admitted that it would be very interesting to develop an underwater optical system to complement underwater acoustics.

They suggested similar applications, such as mine detection, diver-to-diver communications and sensor networks, as well as communications between surface ships and submarines if the right technology is developed. Other areas where underwater optical technology could be applied include underwater positioning systems, underwater obstacle detection systems and seabed survey systems, but these applications do not fall within the field of communications.



## 5 CONCLUSIONS AND FUTURE DEVELOPMENTS

### 5.1 Conclusions

This section presents the conclusions drawn from each of the stages of this project. Thus, these ideas will be the analysis of the state of the art, IOPs and AOPs, underwater light attenuation, alignment, channel modeling, turbulence, refractive index, background noise, prototype design and military applications. Moreover, a final conclusion is reached, declaring the fulfillment or non-fulfillment of the objectives initially set for this project. In addition, a series of possible future developments will be established, which will continue the line of research opened in this project.

#### 5.1.1 *Analysis of the state of the art*

Since the middle of the last century, profuse research in UOWC has been carried out, leading to significant advances. Its major advantage over other underwater technologies is that it has greater bandwidth, without having a range as low as that of RF. Moreover, many feasible UOWC systems have been designed and developed in the last years and are now beginning to be commercialized. Nevertheless, there are still some unknowns and uncertainties due to their vast, complex and changing environment. Meanwhile, the increasing defense and security concerns of countries lead to complete control of the sea, including the underwater domain. This, in addition to the growth in the number of UUVs and underwater devices that require high bandwidth and capacity, has triggered scientific and military attraction to the UOWC field for high-bandwidth information transfer, soaring its development.

#### 5.1.2 *IOPs and AOPs*

In order to have a better understanding of underwater light propagation, since it depends on the properties of the water mass, these must be studied in depth. There are two well-distinguished groups of underwater optical properties: inherent and apparent. Each of them has its own advantages when studying underwater light propagation. On the one hand, if the exact type and composition of the water body is known the IOPs can be calculated and the optical underwater propagation can be predicted. On the other hand, it is sometimes easier to measure AOPs than the exact composition of the water body. Consequently, AOPs provide a less difficult alternative for determining what the water body is composed of.

#### 5.1.3 *Underwater light attenuation*

One of the main phenomena affecting underwater light propagation is attenuation, which is remarkably superior to underwater acoustic propagation. Light attenuation is the sum of absorption and scattering, which are indirectly related since a photon that is absorbed cannot be scattered. As both properties are IOPs, they depend on the type and concentration of matter in the analyzed water. Generally, this matter is classified into four distinct categories regretting its optical properties: water

molecules, phytoplankton, colored dissolved organic matter and non-algae particles. The type and concentration of these particles determines the level up to which a specific beam is going to be attenuated. Moreover, attenuation does also depend on the wavelength, so the most appropriate light source will depend on the specific environment of each case. As a result, it can be concluded that for deep waters blue and green lights happen to be the most appropriate light source, as it is the least attenuated by water molecules. On the other hand, in coastal, harbor and shallow waters, the concentration of phytoplankton, CDOM and NAP is usually higher, so the most suitable wavelength shifts to the green-yellow zone of spectrum.

#### *5.1.4 Alignment*

In terms of the alignment, it is concluded that it is a critical characteristic when establishing a link through UOWC, as it can be one of the biggest challenges provided either the transmitter or the receiver, or even both, may be moving. Additionally, it has been detailed and demonstrated how different light sources have different levels of alignment complexity. Thus, due to the greater beam divergence of the LED, it provides much easier alignment than the LASER.

#### *5.1.5 Channel modeling*

Once the propagation of light underwater was detailed, the possibility of modeling the channel was studied. Hence, it is concluded that there are two different mathematical models to describe the underwater optical channel, depending on whether it has LOS alignment or not. Beer Lambert's law describes the LOS link channels, while the RTE describes the NLOS, which has a complex solving which is usually reached by the Monte Carlo method.

#### *5.1.6 Turbulence*

Underwater turbulence is caused by currents, winds, underwater life pattern and some other unpredictable factor. It has been studied and demonstrated how it can result in the breakdown or impossibility of a UOWC link, as well as in increased BER and ISI. Therefore, turbulent waters remain a major challenge for the development a wide coverage UOWC system.

#### *5.1.7 Refractive index effect on underwater propagation*

The underwater propagation of light also depends on the refractive index, which causes refraction and reflection when it changes. Nevertheless, changes on the refractive index are caused by fluctuations in salinity, density and temperature, whose gradients are most noticeably in long ranges and coastal zones. It is concluded that although the refractive index affects the underwater propagation of light, it does not noticeably alter its course on average, since current UOWC links are short range.

#### *5.1.8 Background noise*

Like any other communication technology, there is also background noise in UOWC, which is luminic in this case. However, this background noise comes mostly from the sunlight, which does not penetrate the water more than three hundred meters. Therefore, UOWC prototypes designed for deeper zones will only have the background noise of similar systems or bioluminescent living beings, which can be considered negligible. As a conclusion, in deep zones, background noise can usually be neglected, while in shallow water it can greatly worsen the performance of a UOWC system during the day.

#### *5.1.9 Prototype design*

Despite the simplicity of the design and low power of the prototype, it resulted feasible and effective. Consequently, its features and performance can be enormously enhanced with a more sophisticated prototype. Some of the improvements that could be made are the implementation of an ambient light level regulator, a more powerful source, waterproofing the whole system, adding the possibility of sending and receiving audio, a source formed by an array of LEDs of different colors, adding a filter to



the receiver, improving the OA or the modulation technique, among many others. However, these enhancements are beyond the scope of this project, and will be presented as future developments.

#### *5.1.10 Military applications*

Military applications of UOWC are wide and varied, although most of the advances made in this field cannot be disclosed in open sources. Nevertheless, the fact that a LASER link was established between a submerged submarine and a satellite decades ago [30] [31], in addition to knowledge about the development of UWSN by some countries [133] [135] are sufficient reason to consider that UOWC can provide greater operability and strategic capability to the military. The military fields in which UOWC implementation has been considered are diving, UUVs, UWSN, submarine and mine warfare. In conclusion, the most feasible and useful applications are thought to be diver-to-diver and a hybrid UWSN that provides underwater surveillance and intercommunicates divers, UUVs, submarines and satellites.

#### *5.1.11 Final conclusion*

Overall, this final project has more than met its initial objectives. Not only has it analyzed the state of the art of UOWCs and its applications in the military field, but it has also designed and tested the literature with a real prototype. Indeed, it is the culmination of an engineering degree, and reflects the capacity of analysis and prototypes development skills acquired, in this case, within the field of underwater telecommunications.

## **5.2 Future developments**

Finally, the possible applications of this work for the future are discussed, both short and long term.

### *5.2.1 Short term*

In continuity with this project and extending it, it is proposed to improve the prototype to study its feasibility in harbor and coastal waters at different depths. As mentioned before, many components can be added to the system and those already in use can be refined. Some of the possible improvements of the prototype are:

- The receiver. In order to make it less vulnerable to noise, an ambient light sensor that subtracts it could be added, as well as a filter that allows only the characteristic light of the emitter to pass through. In addition, its area could be increased to reduce alignment challenge.
- The transmitter. To achieve greater distances a more powerful source is needed. This source could be an array of LEDs, or a green-blue LASER, which is less attenuated than a red LASER on average. It would be interesting to test communication among divers and analyze how hard it is to align a moving transmitter and receiver.
- The signal processing. The prototype could be improved in order to allow sending and receiving voice messages. If this objective were achieved, the prototype would be of great interest to divers. The modulation technique and the OA could also be improved to make signal processing more efficient.

In order to be able to submerge it at test it at different depths, it goes without saying that all components should be submersible, so it must be waterproof. Once the prototype is perfected, tests similar to those performed throughout this project could be conducted to analyze its feasibility and characteristics.

### 5.2.2 *Long term*

With regard to medium to long-term future developments, this analysis in UOWC opens up a promising future for its development, specifically in the Spanish military field. The Spanish Ministry of Defense has set itself the objective of studying and developing these systems by 2027, establishing it in its Defense Technology and Innovation Strategy 2020 [137]. The military could take advantages of the test and prototype proposed as the short-term development to incorporate this technology to its communications. Thinking in accordance with the line established by the Ministry of Defense and adding the results of this analytical project, among long-term developments, the nearest future for this technology in the military would be:

- Implementation of UOWC to communicate divers, submarines, underwater platforms, networks and infrastructures UUVs, enhancing the current transmission bandwidth in the underwater environment.
- Investigation and development of a hybrid UWSN that includes acoustic technologies to give it reach, and optical technologies to provide it bandwidth.
- Integrate the UOWC in SAR operations, in order to communicate the UUVs with its mothership so the UUV can do live streaming thanks to the high bandwidth it provides, facilitating decision-making.
- A submarine-to-satellite communication system. Once the S-80 submarines have their AIP system implemented, developing this communication system would be useful for missions in which the submarines are not wanted to surface for long periods. Until then, it is less useful to develop such system, as current submarines need to snorkel very frequently, so they can then communicate with the satellite. However, if the system is to be implemented, the sooner the research begins, the better, given its complexity.

## 6 REFERENCES

- [1] U. o. Deusto, "The Engineering Faculty of the University of Deusto," 26th March 2015. [Online]. Available: <http://www.ingenieria.deusto.es>. [Accessed 17th January 2021].
- [2] V. C. Coffey, "The Challenges of Facing Submarine Optical Communications," *Optics and Photonics News*, vol. March, pp. 27-33, 2014.
- [3] Chao Wang, Hong-Yi Yu, Yi-Jun Zhu,, "A Long Distance Underwater Visible Light Communication System With Single Photon Avalanche Diode," *IEEE Photonics Journal*, vol. 8, no. 5, pp. 1-11, 2016.
- [4] D. J. O'Donohue, "Joint Electromagnetic Spectrum Operations," *Joint Publication 3-85*, pp. I-1, 2020.
- [5] H. Wilson, "Today's battle for the electromagnetic spectrum," *Military and Aerospace Electronics*, vol. August, pp. 10-17, 2016.
- [6] T. E. L. Calderón, «Apoyo Logístico 4.0,» *Revista General de Marina*, vol. August, pp. 211-213, 2018.
- [7] N. G. Pandavenes, "Infodefensa," Infodefensa, 28th January 2021. [Online]. Available: <https://www.infodefensa.com/es/2021/01/28/noticia-nuevo-jemad-marca-objetivo-apoyarse-cuarta-revolucion-industrial-transformar.html>. [Accessed 1st March 2021].
- [8] GMC, "Unlocking subsea communications," *Global Military Communications Magazine*, November 2016.
- [9] D. D. Marketing, "Ocean Technology Systems," OTS, 2021. [Online]. Available: <https://www.oceantechnologysystems.com/store/military/wireless-military/powercom-5000d/>. [Accessed 1st March 2021].
- [10] Gee-Kung Chang, Yu-Ting Hsueh, Shu-Hao Fan, "Advances in 1–100GHz Microwave Photonics: All-Band Optical Wireless Access Networks Using Radio Over Fiber Technologies," *In Optics and Photonics, Optical Fiber Telecommunications*, no. Sixth Edition, pp. 873-889, 2013.

- [11] "Cyberphysics," Cyberphysics, [Online]. Available: <https://www.cyberphysics.co.uk/topics/radioact/Radio/EMSpectrumcolor.jpg>. [Accessed 17th January 2021].
- [12] E. A. M. González, *Diseño y desarrollo de un sistema de comunicaciones ópticas inalámbricas para transmisión de voz*, Universidad de Vigo: Centro Universitario de la Defensa en la Escuela Naval Militar, 2020.
- [13] Mary B. James, David J. Griffiths, "Why the speed of light is reduced in a transparent medium," *American Journal of Physics*, vol. 60, no. 4, pp. 309-313, 1992.
- [14] Dale Janssen, Cory Janssen, "Techopedia," [Online]. Available: <https://www.techopedia.com/definition/24942/optical-communication>. [Accessed 17th January 2021].
- [15] Mohammad D. Al-Amri, Mohamed M. El-Gomati, M. Suhail Zubairy, *Optics in Our Time*, Cham, Switzerland: Springer Company, 2016.
- [16] Tom Garlington, MAJ Joel Babbitt, George Long, "Analysis of Free Space Optics as a Transmission," *U.S. Army Information Systems Engineering Command*, no. AMSEL-IE-TS-05001, 2005.
- [17] H. Technologies, "Submarine Cable Map," HMN Technologies, [Online]. Available: <https://www.submarinecablemap.com/>. [Accessed 2021].
- [18] Lydia K. Gkoura, George D. Roumelas, Hector E. Nistazakis, Harilaos G. Sandalidis, Alexander Vavoulas, Andreas D. Tsigopoulos, George S. Tombras, "Underwater Optical Wireless Communication Systems: A Concise Review," *IntechOpen*, Vols. Turbulence Modelling Approaches - Current State, Development Prospects, Applications,, no. 9, pp. 219-236, 2017.
- [19] Chrysovalantou Christopoulou, Harilaos G. Sandalidis, Nicholas Vaiopoulos, "Performance of an Underwater Optical Wireless Link With a Randomly Placed or Moving Receiver," *IEEE Journal of Oceanic Engineering*, 2020.
- [20] Giuseppe Schirripa Spagnolo, Lorenzo Cozzella, Fabio Leccese,, "Underwater Optical Wireless Communications: Overview," *Sensors*, MDPI, 2020.
- [21] "Kass Kochi Arts & Science Space," KASS, [Online]. Available: [https://kartsci.org/science\\_computers/history-telegraph-telephone/](https://kartsci.org/science_computers/history-telegraph-telephone/). [Accessed 2021].
- [22] G. B. Díaz-Montenegro, *Diseño e implementación de un sistema de seguimiento para sistemas de comunicaciones basados en LASER en plataformas navales*, Universidad de Vigo: Centro Universitario de la Defensa en la Escuela Naval Militar, 2019.
- [23] S. Navy, Artist, [Art]. Naval Museum of Madrid, 2021.
- [24] H. T. S. o. T. E. a. UPV, "Museo de la Telecomunicación Vivente Miralles Segarra," Polytechnic University of Valencia, [Online]. Available: <https://museotelecomvlc.webs.upv.es/heliografo-de-campana/>. [Accessed 2021].
- [25] D. Hutt, K. Snell, P. Bélanger, "Alexander Graham Bell's Photophone," *Opt. Photon. News*, vol. 4, no. 6, pp. 20-25, 1993.
- [26] Guillemin, Amédée, "El mundo físico : gravedad, gravitación, luz, calor, electricidad, magnetismo," *Barcelona Montaner y Simón*, 1882.

- [27] Zhaoquan Zeng, Shu Fu, Huihui Zhang, Yuhan Dong, Julian Cheng, "A Survey of Underwater Optical Wireless Communications," *IEEE Communications Surveys & Tutorials*, vol. 19, no. 1, 2017.
- [28] Shijie Zhu, Xinwei Chen, Xiaoyan Liu, Guoqi Zhang, Pengfei Tian, "Recent progress in and perspectives of underwater wireless optical communication," *Progress in Quantum Electronics*, vol. 73, p. 100274, 2020.
- [29] G. D. Gilbert, T. R. Stoner, J. L. Jernigan, "Underwater Experiments On The Polarization, Coherence, And Scattering Properties Of A Pulsed Blue-Green Laser," *Underwater Photo Optics*, vol. I, 1966.
- [30] S. KARP, "Optical Communications Between Underwater and Above Surface (Satellite) Terminals," *IEEE Transactions on Communication*, Vols. COM-24, no. 1, pp. 66-81, 1976.
- [31] M. B. Callaham, "Submarine Communications," *IEEE Communications Magazine*, vol. 19, no. 6, pp. 16-25, 1977.
- [32] Thomas F. Wiener, Sherman Karp, "The role of blue/green laser systems in strategic submarine communication," *IEEE Transactions on Communications*, Vols. COM-28, no. 9, pp. 1602-1607, September 1980.
- [33] G. Cossu, "Recent achievements on underwater optical wireless communication," *Chinese Optics Letters*, vol. 17, no. 10, pp. 1000091-1000097, October 2019.
- [34] Stephen Fasham, Shaun Dunn, "Developments in subsea wireless communications," *IEEE Underwater Technologies*, pp. 1-5, 2015.
- [35] Chao Shen, Yujian Guo, Hassan M. Oubei, Tien Khee Ng, Guangyu Liu, Ki-Hong Park, Kang-Ting Ho, Mohamed-Slim Alouini, Boon S. Ooi, "20-meter underwater wireless optical communication link with 1.5 Gbps data rate," *Optical Express*, vol. 24, no. 22, p. 25502, 2016.
- [36] Pengfei Tian, Xiaoyan Liu, Suyu Yi, Yuxin Huang, Shuailong Zhang, Xiaolin Zhou, Laigui Hu, Lirong Zheng, Ran Liu, "High-speed underwater optical wireless communication using a blue GaN-based micro-LED," *Optics Express*, vol. 25, no. 2, pp. 1193-1201, 2017.
- [37] A. S. Fletcher, C. E. Devoe, I. D. Gaschits, F. Hakimi, N. D. Hardy, J. G. Ingwersen, R. D. Kaminsky, H. G. Rao, M. S. Scheinbart, T. M. Yarnall, S. A. Hamilton, "Undersea Laser Communications Field Test at the Naval Undersea Warfare Center (NUWC)," *Proceedings of Oceans 2016*, p. 1, 2016.
- [38] Zhuoyuan Song, Eric Schwartz, Kamran Mohseni, "A Low-Power Optical Communication Modem for Compact Autonomous Underwater Vehicles," *Proceedings of 2017 IEEE*, 2017.
- [39] Xiaoyan Liu, Suyu Yi, Xiaolin Zhou, Zhilai Fang, Zhi-Jun Qui, Laigui Hu, Chunxiao Cong, Lirong Zheng, Ran Liu, Pengfei Tian, "34.5 m underwater optical wireless communication with 2.70 Gbps data rate based on a green laser diode with NRZ-OOK modulation," *Opt. Express*, vol. 25, no. 22, p. 27937, 2017.
- [40] G. Cossu, A. Sturniolo, A. Messa, S. Grechi, D. Costa, A. Bartolini, D. Scaradozzi, A. Caiti, and E. Ciaramella, J. Light., "Full-Fledged 10Base-T Ethernet Underwater Optical Wireless Communication System," *IEEE Journal on selected areas in communications*, vol. 36, no. 1, pp. 5371-5380, 2018.

- [41] X. Liu, S. Yi, X. Zhou, S. Zhang, Z. Fang, Z.-J. Qiu, L. Hu, C. Cong, L. Zheng, R. Liu, P. Tian, "Laser-based white-light source for high-speed underwater wireless optical communication and high-efficiency underwater solid-state lighting," *Opt. Express*, vol. 26, no. 15, p. 19275, 2018.
- [42] Wen-Shing Tsai, Hai-Han Lu, Hsiao-Wen Wu, Chung-Wei Su, Yong-Cheng Huang, "A 30 Gb/s PAM4 underwater wireless laser transmission system with optical beam reducer/ expander," *Scientific Reports*, vol. 9, no. 8605, 2019.
- [43] "3.075 Gb/s underwater visible light communication utilizing hardware pre-equalizer with multiple feature points," *Optical Engineering*, vol. 58, no. 5, p. 056117, 2019.
- [44] Jeimei Wang, Chunhui Lu, Shangbin Li, Zhengyuan Xu, "100 m/500 Mbps underwater optical wireless communication using an NRZ-OOK modulated 520 nm laser diode," *Opt. Express*, vol. 27, no. 9, pp. 12171-12182, 2019.
- [45] Y. Han, Y. Zheng, K. Shi, T. Wang, X. Xie, J. Meng, W. Wang, T. Duan, B. Han, R. Wan, K. Sun, "Research on underwater high-speed blue-green optical communication technology based on blue LD array," *Proc. SPIE 11068*, Vols. Second Symposium on Novel Technology of X-Ray Imaging, no. 110680U, 2019.
- [46] Jingjing Wang, Changfeng Tian, Xinghai Yang, Wei Shi, Qiuna Niu, T Aaron Gulliver, "Underwater wireless optical communication system using a 16-QAM modulated 450-nm laser diode based on an FPGA," *Applied Optics*, vol. 58, no. 16, p. 4553, 2019.
- [47] Fangchen Hu, Guoqiang Li, Peng Zou, Jian Hu, Shouqing Chen, Qingquan Liu, Jianli Zhang, Fengyi Jiang, Shaowei Wang, Nan Chi, "20.09-Gbit/s Underwater WDM-VLC Transmission based on a single Si/GaAs-substrate Multichromatic LED array chip," *Optical Fiber Communication Conference (OFC)*, vol. M3I.4, 2020.
- [48] Honglan Chen; Xinwei Chen; Jie Lu; Xiaoyan Liu; Jiarong Shi; Lirong Zheng; Ran Liu; Xiaolin Zhou; Penfei Tian, "Toward Long-Distance Underwater Wireless Optical Communication Based on A High-Sensitivity Single Photon Avalanche Diode," *IEEE Photonics Journal*, vol. 12, no. 3, pp. 1-10, June 2020.
- [49] Dario Pompili, Ian F. Akyildiz, "Overview of Networking Protocols for Underwater Wireless Communications," *Underwater Wireless Communications*, vol. 47, no. 1, pp. 97-102, 2009.
- [50] Camila M. G. Gussen, Paulo S. R. Diniz, Marcello L. R. Campos, Wallace A. Martins, Felipe M. Costa, and Jonathan N. Gois, "A Survey of Underwater Wireless Communication Technologies," *Journal of Communication and Information Systems*, vol. 31, no. 1, pp. 241-255, 2016.
- [51] M. Lanzagorta, Underwater Communications, CA, USA: Morgan & Claypool, 2013.
- [52] Xianhui Che, Ian Wells, Gordon Dickers, Paul Kear, and Xiaochun Gong, "Re-Evaluation of RF Electromagnetic Communication in Underwater Sensor Networks," *Topics in Ad Hoc and Sensor Networks*, pp. 143-151, 2010.
- [53] Spanish Naval Academy, *Tiro Naval II*, Marín, Pontevedra: Juan José Rivas Calvar, 2020.
- [54] U. Navy, "Naval Postgraduate School," Department of Oceanography, [Online]. Available: <https://www.oc.nps.edu/~bird/oc2930/acoustics/summary.html>. [Accessed enero 2021].
- [55] Jingjing Wang, Wei Shi, Lingwei Xu, Liya Zhou, Qiuna Niu, Ju liu, "Design of optical-acoustic hybrid underwater wireless sensor network," *Journal of Network and Computer Applications*, no. 92, pp. 59-67, 2017.



- [56] B. G. Ferguson, "Defense Applications of Acoustic Signal Processing," *Defence Science and Technology (DST)*, pp. 10-18, 2019.
- [57] Hemani Kaushal, Georges Kaddoum, "Underwater Optical Wireless Communication," *IEEE Access*, vol. 4, pp. 1518-1547, 2016.
- [58] Curtis Mobley, Emmanuel Boss, Collin Roesler, "Ocean Optics Book," 2021. [Online]. Available: <https://www.oceanopticsbook.info/view/overview-optical-oceanography/introduction>. [Accessed 26th February 2021].
- [59] S. Sathyendranath, "Inherent Optical Properties of Natural Seawater," *Defense Science*, vol. 34, no. 1, pp. 1-18, 1984.
- [60] M. Stomp, *Colourful Coexistence: A New Solution to the Plankton Paradox*, The Netherlands: ResearchGate, 2008, pp. 1-137.
- [61] Rebecca Lindsey and Michon Scott, "NASA Earth Observatory," NASA, 13th July 2010. [Online]. Available: <https://earthobservatory.nasa.gov/features/Phytoplankton>. [Accessed 29th January 2021].
- [62] Juan Luis Cifuentes Lemus, Pilar Torres-García, Marcela Frías M., "EL océano y sus recursos V: Plancton," Biblioteca Digital, [Online]. Available: [http://bibliotecadigital.ilce.edu.mx/sites/ciencia/volumen1/ciencia2/35/htm/sec\\_6.html](http://bibliotecadigital.ilce.edu.mx/sites/ciencia/volumen1/ciencia2/35/htm/sec_6.html). [Accessed 31st January 2021].
- [63] E. Zurich, "Mapping the global distribution of phytoplankton," 22 May 2019. [Online]. Available: [www.sciencedaily.com/releases/2019/05/190522120509.htm](http://www.sciencedaily.com/releases/2019/05/190522120509.htm). [Accessed 31st January 2021].
- [64] K. Olli, "The diversity of aquatic photosynthetic pigments," *Botaanika Osakond*.
- [65] D. A. Siegel, S. Maritorena, N. B. Nelson, D. A. Hansell, M. Lorenzi-Kayser, "Global distribution and dynamics of colored dissolved and detrital organic materials," *Journal of Geophysical Research*, vol. 107, no. C12, 3228, pp. 21.1-21.13, 2001.
- [66] Nazanin Chaichitehrani, Eurico J. D'Sa, Dong S. Ko, Nan D. Walker, Christopher L. Osburn, and Robert F. Chen, "Colored Dissolved Organic Matter Dynamics in the Northern Gulf of Mexico from Ocean Color and Numerical Model Results," *Journal of Coastal*, vol. 30, no. 4, pp. 800-814, 2014.
- [67] Ciren Nima, Øyvind Frette, Børge Hamre, Jakob J. Stamnes, Yi-Chun Chen, Kai Sørensen, Marit Norli, Daren Lu, Qianguo Xing, Dennis Muyimbwa, Taddeo Ssenyonga, Knut H. Stamnes, Svein Rune Erga, "CDOM Absorption Properties of Natural Water Bodies along Extreme Environmental Gradients," *MDPI*, 2019.
- [68] Y. Ahy, *Proprietes optiques des particules biologiques et minerales presentes dans l'ocean. Application : inversion de la reflectance.*, Paris, France: Ph.D. Thesis, Univ. Pierre and Marie Curie, 1999.
- [69] Qinghua Fu, Shixin Wang, Yi Zhou, Fuli Yan, Yani Liua, "Modeling the spectral shape of absorption by water constituents in Taihu Lake," *Institute of Remote Sensing Applications, Chinese Academy of Sciences*, no. IV, pp. 954-957, 2008.
- [70] Liangliang Shi, Zhihua Mao, Jiaping Wu, Mingliang Liu, Yiwei Zhang, Zheng Wang, "Variations in Spectral Absorption Properties of Phytoplankton, Non-Algal Particles and

- Chromophoric Dissolved Organic Matter in Lake Qiandaohu," *MDPI*, vol. 9, no. 352, pp. 1-20, 2017.
- [71] Mackenzie, Fred T. , Byrne, Robert Howard and Duxbury, Alyn C., "Seawater, Density, Composition, Salinity, Distribution, & Facts," *Encyclopedia Britannica*, Nov 2020.
- [72] Nasir Saeed, , Abdulkadir Celik, Tareq Y. Al-Naffouri, Mohamed-Slim Alouini, "Underwater Optical Wireless Communications, Networking, and Localization: A Survey," *IEEE*, 28 Feb 2018.
- [73] N. G. Education, "National Geographic," 23rd July 2015. [Online]. Available: <https://www.nationalgeographic.org/encyclopedia/ocean-vent/>. [Accessed 7th February 2021].
- [74] Xiaodong Zhang, Lianbo Hu, Ming-Xia He, "Scattering by pure seawater: Effect of salinity," *Optics Express*, vol. 17, no. 7, pp. 5698-5710, March 2009.
- [75] A. Morel, "Optical properties of pure water and pure sea water," *Optical Aspects of Oceanography*, pp. 1-24, 1974.
- [76] LV Pei ,HE Junhua , Zhou Renkui, Liu Haiying, "The application of underwater optics and its development," *Information Optics and Photonics Technologies II*, vol. 837.
- [77] H. Volten, J. F. de Haan, J. W. Hovenier, R. Schreurs, W. Vassen, A. G. Dekker, H. J. Hoogenboom, F. Charlton, R. Wouts, "Laboratory measurements of angular distributions of light scattered by phytoplankton and silt," *Limnology and Oceanography*, vol. 43, no. 6, pp. 1180-1197, 1998.
- [78] J.K. Lotsberg, E. Marken, J.J. Starnes, S.R. Erga, K. Aursland, C. Olseng, "Laboratory measurements of light scattering from marine particles," *Limnology and Oceanography: Methods*, vol. 5, pp. 34-40, 2007.
- [79] Annick Bricaud, Andre' Morel, Louis Prieur, "Optical efficiency factors of some phytoplankters," *Limnology and Oceanography*, vol. 28, no. 5, pp. 816-832, 1983.
- [80] R. Acharya, Satellite Signal Propagation, Impairments and Mitigation, Ahmedabad, India: Academic Press, 2017.
- [81] William M. Balch, Katherine A. Kilpatrick, Patrick Holligan, Derek Harbour, Emilio Fernandez, "The 199 1 coccolithophore bloom in the central North Atlantic," *Limnology and Oceanography*, vol. 41, no. 8, pp. 1684-1696, 1996.
- [82] Deyong Sun • Yunmei Li • Qiao Wang, Heng Lv, Chengfeng Le, Changchun Huang, Shaoqi Gong, "Partitioning particulate scattering and absorption into contributions of phytoplankton and non-algal particles in winter in Lake Taihu (China)," *Hydrobiologia*, vol. 644, pp. 337-349, 2009.
- [83] Howard R. Gordon, Marlon R. Lewis, Scott D. McLean, Michael S. Twardowski, Scott A. Freeman, Kenneth J. Voss, G. Chris Boynton, "Spectra of particulate backscattering in natural waters.," *Optics Express*, vol. 17, no. 18, pp. 16192-16208, August 2009.
- [84] T. J. Petzold, "Volume Scattering Functions for selected Ocean Waters," University of California, San Diego, October 1972.
- [85] Annick Bricaud, Andre Morel, "Light attenuation and scattering by phytoplanktonic cells: a theoretical modeling," *Applied Optics*, vol. 25, no. 4, pp. 571-580, 1986.

- [86] Konrad Witkowski, Tadeusz K&l, Andrzej Zieliriski, Edward Kuteri, "A light-scattering matrix for unicellular marine phytoplankton," *Limnology and Oceanography*, vol. 43, no. 5, pp. 859-869, 1998.
- [87] G. Dall'Olmo, T. K. Westberry, M. J. Behrenfeld, E. Boss, W.H. Slade, "Significant contribution of large particles to optical backscattering in the open ocean," *Biogeosciences*, vol. 6, pp. 947-967, 2009.
- [88] Dariusz Stramski, Marcel Babin, Sławomir B. Woz'niak, "Variations in the optical properties of terrigenous mineral-rich particulate matter suspended in seawater," *Limnology and Oceanography*, vol. 52, no. 6, pp. 2418-2433, 2007.
- [89] Marcel Babin, André Morel, Vincent Fournier-Sicre, Frank Fell, Dariusz Stramski, "Light Scattering Properties of Marine Particles in Coastal and Open Ocean Waters as Related to the Particle Mass Concentration," *Limnology and Oceanography* , vol. 48, pp. 843-859, March 2003.
- [90] Woźniak SB, Stramski D., "Modeling the optical properties of mineral particles suspended in seawater and their influence on ocean reflectance and chlorophyll estimation from remote sensing algorithms.," *Applied Optics*, vol. 43, no. 17, pp. 3489-3503, Jun 2004.
- [91] S. '. Vishnoi, "Accurate way to measure angular spread of a laser beam," Physics, 18 11 2014. [Online]. Available: <https://physics.stackexchange.com/users/52364/sudhanshu-sid-vishnoi>. [Accessed 2021 2 16].
- [92] Satish Kumar Rajasekharan; Chaitanya Raorane; Jintae Lee, "LED based real-time survival bioassays for nematode research," *Nature Research*, vol. 8, no. 11531, 2018.
- [93] Yang Weng, Yujian Guo, Omar Alkhazragi, Tien Khee Ng, Jen-Hwa Guo, Boon S. Ooi, "Impact of Turbulent-Flow-Induced Scintillation on Deep-Ocean Wireless Optical Communication," *Journal of Lightwave Technology*, vol. 37, no. 19, pp. 5083-5090, 2019.
- [94] Xiaodong Zhang, Marlon Lewis, Michael Lee, Bruce Johnson, Gennady Korotaev, "The volume scattering function of natural bubble populations," *Limnology and Oceanography*, vol. 47, no. 5, pp. 1273-1282, 2002.
- [95] Chadi Gabriel, Mohammad-Ali Khalighi, Salah Bourennane, Pierre L'éon, Vincent Rigaud, "Misalignment Considerations in Point-to-Point Underwater Wireless Optical Link," *MTS/IEEE Oceans - Bergen, Bergen, Norway*, pp. 1-5, 2013.
- [96] Jeneel Pravin Kachhadiya; Abhinav Kashyap, "Air-Water Optical Communication using an Airborne Radio controlled," *Proceedings of the Second International Conference on Intelligent Computing and Control Systems (ICICCS)*, pp. 631-635, 2018.
- [97] "Underwater Optical Wireless Communications," *School of Engineering University of Warwick*, pp. 1-69, 2017.
- [98] Curtis D. Mobley, Bernard Gentili, Howard R. Gordon, Zhonghai Jin, George W. Kattawar, André Morel, Phillip Reinersman, Knut Stamnes, Robert H. Stavn, "Comparison of numerical models for computing underwater light fields," *Applied Optics*, vol. 32, no. 36, pp. 7484-7504, 1993.
- [99] Shlomi Arnon, Debbie Kedar, "Non-line-of-sight underwater optical wireless communication network," *Journal of the Optical Society of America*, vol. 26, no. 3, pp. 530-539, 2009.

- [100] Shijian Tang, Yuhan Dong, Xuedan Zhang, "On Path Loss of NLOS Underwater Wireless Optical Communication Links," *Oceans 2013 MTS/IEEE Bergen: The Challenges of the Northern Dimension*, June 2013.
- [101] Xiaobin Sun a, Meiwei Kong, Omar Alkhazragi, Chao Shen, Ee-Ning Ooi, Xinyu ZhangUlrich Buttner, Tien Khee Ng, Boon S. Ooi, "Non-line-of-sight methodology for high-speed wireless optical communication in highly turbid water," *Optics Communications*, vol. 461, no. 125264, 2020.
- [102] S. Jaruwatanadilok, "Underwater Wireless Optical Communication Channel Modeling and Performance Evaluation using Vector Radiative Transfer Theory," *IEEE Journal on Selected Areas in Communications*, vol. 26, no. 9, December 2008.
- [103] Frank Hanson, Stojan Radic, "High bandwidth underwater optical communication," *Optical Society of America*, vol. 47, no. 2, pp. 277-283, 2008.
- [104] Chadi Gabriel, Mohammad-Ali Khalighi, Salah Bourennane, Pierre Léon, Vincent Rigaud, "Monte-Carlo-Based Channel Characterization for Underwater Optical Communication Systems," *Journal of Optical Communications and Networking*, vol. 5, no. 1, pp. 1-12, 2013.
- [105] Zahir Ahmad, Roger Green, "Link Design for Multi-hop Underwater Optical Wireless Sensor Network (ICSNC)," *The Seventh International Conference on Systems and Networks Communications*, pp. 65-70, 2012.
- [106] Linda Mullen, Brandon Cochenour, William Rabinovich, Rita Mahon, John Muth, "Backscatter suppression for underwater modulating retroreflector links using polarization discrimination," *Applied Optics*, vol. 48, no. 2, pp. 328-337, January 2009.
- [107] Laura J. Johnson, Roger J. Green, Mark S. Leeson, "Underwater optical wireless communications: depth-dependent beam refraction," *Applied Optics*, vol. 53, no. 31, pp. 7273-7277, 2014.
- [108] H.-N. Kostis, "NASA Scientific Visualization Studio," NASA, [Online]. Available: <https://svs.gsfc.nasa.gov/3652>. [Accessed 31st January 2021].
- [109] Laura Johnson, Roger Green, Mark Leeson, "A Survey of Channel Models for Underwater Optical Wireless Communication," *2nd International Workshop on Optical Wireless Communications (IWOW)*, 2013.
- [110] Roger Stokes, Mark Bernal, Chris Griffith, Randall Blair, EJ Marttila, Greg Mooradian, "An Adaptive Data Rate Controller (ADRC) for the Through Cloud, Undersea Laser Communications Channel," *U.S. Government work not protected by U.S. copyright*, 107-108.
- [111] O. Hagolle, "Radiometric quantities : irradiance, radiance, reflectance," multitemp Sentinel-2, 13th November 2016. [Online]. Available: <https://labo.obs-mip.fr/multitemp/radiometric-quantities-irradiance-radiance-reflectance/>. [Accessed 23th February 2021].
- [112] Jacek Piskozub, Tomasz Neumann, Ludomir Woźniak, "Ocean color remote sensing: Choosing the correct depth weighting function," *Optics Express*, vol. 16, no. 19, pp. 14683-8, October 2008.
- [113] R.C. Smith, K. Baker, "The bio-optical state of ocean waters and remote sensing," *Limnology and Oceanography*, vol. 23, no. 2, p. 247, 1978.
- [114] Raymond C. Smith und Karen S. Baker, "Optical classification of natural waters," *Limnology and Oceanography*, vol. 23, no. 2, pp. 260-267, 1978.

- [115] Wozniak, Bogdian, Dera, Jerzy, Light Absorption in Sea Water, Springer, 2007.
- [116] N. Jerlov, Optical Oceanography, Volume 5, Pages III-VII, 1-194, Elsevier B.V., 1968.
- [117] N. O. a. A. A. (NOAA), "National Weather Service," NOAA, 2014. [Online]. Available: [https://www.weather.gov/jetstream/layers\\_ocean](https://www.weather.gov/jetstream/layers_ocean). [Accessed 24th February 2021].
- [118] "Sea and Sky," 2016. [Online]. Available: <http://www.seasky.org/deep-sea/assets/images/ocean-layers-s00.jpg>. [Accessed 2021 January 31].
- [119] R. a. i. u. o. w. communications, "Johnson, Laura J; Jasman, Faezah; Green, Roger J; Leeson, Mark S," *Society for Underwater Technology*, vol. 32, no. 3, pp. 167-175, 2014.
- [120] K. S. University, 2015. [Online]. Available: <http://ksuweb.kennesaw.edu/~jdirnber/oceanography/LecutresOceanogr/LecOceanStructure/0620B.jpg>. [Accessed 2021 February 24th].
- [121] Fahad Zafar; Masuduzzaman Bakaul; Rajendran Parthiban, "Laser-Diode-Based Visible Light Communication: Toward Gigabit Class Communication," *IEEE Communications Magazine*, vol. 55, no. 2, pp. 144-151, 2017.
- [122] Ruonan Ji, Shaowei Wang, Qingquan Liu, Wei Lu , "High-Speed Visible Light Communications: Enabling Technologies and State of the Art," *Applied Sciences*, vol. 8, no. 4, p. 589, 2018.
- [123] H. Batchen, "SeesStudio," 2010. [Online]. Available: <https://www.seeedstudio.com/document/HLM1230.pdf>. [Accessed 24th January 2021].
- [124] C. J. Wells, "Analogue and Digital Signals," 2020. [Online]. Available: <http://www.technologyuk.net/telecommunications/telecom-principles/analogue-and-digital-signals.shtml>. [Accessed 25th January 2021].
- [125] F. G. d. T. Landín, "Estudio y desarrollo de un sistema de comunicaciones punto a punto basado en láser para buques de la Armada," Centro Universitario de la Defensa en la Escuela Naval Militar, Grado en Ingeniería Mecánica, 2019.
- [126] A. Fernandez, "American Chemistry Society," American Chemistry Society, [Online]. Available: <https://www.acs.org/content/acs/en/education/resources/highschool/chemmatters/past-issues/archive-2013-2014/how-a-solar-cell-works.html>. [Accessed 25th January 2021].
- [127] Basem Shihada, Osama Amin, Christopher Bainbridge, Seifallah Jardak, Omar Alkhazragi, Tien Khee Ng, Boon Ooi, Michael Berumen, Mohamed-Slim Alouini, "Aqua-Fi: Delivering Internet Underwater Using Wireless Optical Networks," *IEEE Communications Magazine*, pp. 84-89, May 2020.
- [128] C. J. M. P. M. y. C. D. R. y. R. d. Cortaza, La Armada Española, Departamento Específico Armada: Escuela Superior de las Fuerzas Armadas, IEEE, Noviembre 2012.
- [129] E. M. d. l. A. Ministerio de Defensa, *Organización de las comunicaciones navales, ACP-176 SP NAVY SUPP-I*, Septiembre, 2008.
- [130] "Hydromea," Underwater Wireless Communications, [Online]. Available: <https://www.hydromea.com/underwater-wireless-communication/>.

- [131] C. J. McMahon, "A Strategy for the Twenty-First Century?," *Naval War College Review, Maritime Trade Warfare*, pp. 1-25.
- [132] T. U. o. R. I. a. I. S. Center, "Discovery of sound in the sea; World War II: 1941-1945," *Dosits.org*, [Online]. Available: <https://dosits.org/people-and-sound/history-of-underwater-acoustics/world-war-ii-1941-1945/>. [Accessed 11th February 2021].
- [133] Mohsin Murad, Adil A. Sheikh, Adil A. Sheikh, Muhammad Asif Manzoor, Muhammad Asif Manzoor, Saad Qaisar, "A Survey on Current Underwater Acoustic Sensor Network Applications," *International Journal of Computer Theory and Engineering*, vol. 7, no. 1, pp. 51-56, 2014.
- [134] F. McGerty, "Global defence-spending on the up, despite economic crunch," *International Institute for Strategic Studies (IISS)*, 25th February 2021.
- [135] J. M. Dahm, "Exploring China's Unmanned Ocean Network," *The Asia Maritime Transparency Initiative and The Center for Strategic and International Studies*, June 2020.
- [136] J. Rice, "Seaweb Acoustic Communication and Navigation Networks," *Calhoun: The NPS Institutional Archive*, 2005.
- [137] M. d. Defensa, "Estrategia de Tecnología e Innovación para la Defensa (ETID)," *Dirección General de Armada, Subdirección General de Planificación, Tecnología e Innovación*, 2020.
- [138] Seongwon Han<sup>1</sup>, Youngtae Noh, Richard Liang, Roy Chen, Yung-Ju Cheng, Mario Gerla, "Evaluation of Underwater Optical-Acoustic Hybrid Network," *China Communications, Integration of Optical and Wireless Networks*, pp. 49-59, May 2014.
- [139] Salmah Fattah, Abdullah Gani, Ismail Ahmady, Mohd Yamani Idna Idris, Ibrahim Abaker Targio Hashem, "A Survey on Underwater Wireless Sensor Networks: Requirements, Taxonomy, Recent Advances, and Open Research Challenges," *Sensors*, vol. 20, no. 18, p. 5393, 2020.
- [140] Chuyen T. Nguyen, Mat T. Nguyen, Vuong V. Mai, "Underwater Optical Wireless Communication-based IoUT Networks: MAC Performance Analysis and Improvement," *Optical Switching and Networking*, vol. 37, p. 100570, May 2020.
- [141] J. Bolton, "Unmanned Underwater Vehicles (UUV) Market Size 2021, Global Industry Analysis By Product Type, Application And Future Technology 2027," *Express Keeper*, March 2021.
- [142] F. S. Bergés, "Drones militares submarinos," *Trufault Historia Militar*, February 2021.
- [143] R. Farley, "The Submarines of the Future Will Be Robotic," *War is Boring*, 26th February 2018.
- [144] H. I. Sutton, "The U.S. Navy's New Orca Drone Submarine Could Get Offensive Role," *Forbes*, 17th December 2019.
- [145] A. C. d. I. Ríos, "Por qué la Armada necesita un UUV antisubmarino," *Revista General de Marina*, pp. 1045-1061, 2020.
- [146] M. d. Defensa, "Portal de Tecnología e Innovación del Ministerio de Defensa," *Gobierno de España*, [Online]. Available: <https://www.tecnologiaeinnovacion.defensa.gob.es/es-es/Contenido/Paginas/detalleevento.aspx?eventoID=535>. [Accessed 2nd February 2021].
- [147] M. e. Marine, "Drones : Un consortium français parvient à développer un Wifi sous-marin," *Subsea Tech*, 29th November 2013.



- [148] J. M. Navarro, "Así será el BAM-IS que Navantia construirá tras la luz verde del Ministerio de Hacienda," *Defensa*, 30 julio 2020.
- [149] T. O. Bermudez, "InfoDefensa," [Online]. Available: <https://www.infodefensa.com/es/2019/09/17/noticia-defensa-explora-mercado-espanol-submarinos-tripulados.html>. [Accessed 2nd March 2021].
- [150] M. d. Defensa, "Armada Española," [Online]. Available: [https://armada.defensa.gob.es/ArmadaPortal/page/Portal/ArmadaEspañola/conocenosnoticias/prefLang-es/00noticias--2016--09--NT-174-NEPTUNO-es?\\_selectedNodeID=2757085&\\_pageAction=selectItem&\\_pageNum=72&paramNo=000000](https://armada.defensa.gob.es/ArmadaPortal/page/Portal/ArmadaEspañola/conocenosnoticias/prefLang-es/00noticias--2016--09--NT-174-NEPTUNO-es?_selectedNodeID=2757085&_pageAction=selectItem&_pageNum=72&paramNo=000000).
- [151] N. Technology. [Online]. Available: Regarding countermining operations, there is the Minesniper, a ROV which goes to the mine and explodes, whereas and the Pluto Plus, a ROV which gathers information about the zone around the mine. The other two UUVs have been designed for underwater SAR op. [Accessed 2021 March 2nd].
- [152] J. M.-D. D. d. Río, "Concepto de Operaciones Navales," *Armada Española*, 2015.
- [153] R. Shermann, "Federation of American Scientists (FAS)," [Online]. Available: <https://fas.org/man/dod-101/sys/ship/agss-555.htm>. [Accessed 2021 March 3rd].
- [154] J. D. Feichtner, "Satellite to Submarine LASER Communications (SLC)-Advanced filter technology," pp. LMSC-P000187R, January 1992.
- [155] F. B. McLaughlin, "Undersea Communications Between Submarines and UnmannedUndersea Vehicles in a Command and Control Denied Environment," *Naval Postgraduate School, Monterey, California*, May, 2016.
- [156] "Naval news," [Online]. Available: <https://www.navalnews.com/wp-content/uploads/2019/01/Boeing-Orca-XLUUV-Team-Submitted-Proposal-for-Phase-II-of-U.S.-Navy-Competition-3.jpg>. [Accessed 2nd March 2021].
- [157] Peter C. Chu, "Effects of Salinity and Chlorophyll on Underwater Optical Communication and Detection," *Naval Postgraduate School, Department of Oceanography*, 2017.



## APPENDIX I: 3D MODELS

Two different supporters can be observed through the figures of this final project (Figure A1-1). The initial idea was to use the supporters that had been previously designed and printed in [12], but they were higher than the water tank. Therefore, it was decided to print new ones. The one on the back comes from [12], and the ones at the front were printed through the prototype design. The new mounts made the alignment easier, as the previous ones were taller than the water tank.

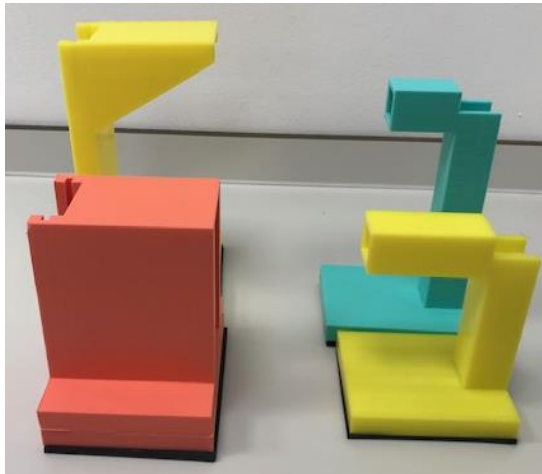
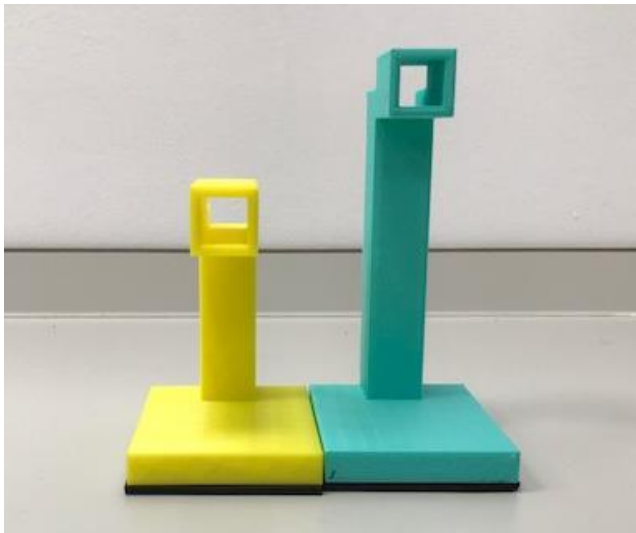


**Figure A1-1** Two different supporters, those on the front side were printed throughout this Final Project, while the ones at the back are from [12].



(a)



(b)

**Figure A1-2** (a) Both transmitter mounts and (b) both receivers mounts. The new one is the shortest in both cases.

The 3D mounts were designed with Thinkercad, an easy design software from Autodesk. Different views of the transmitter holder can be seen in Figure A1-3, and in Figure A1-4 those corresponding to the receiver.

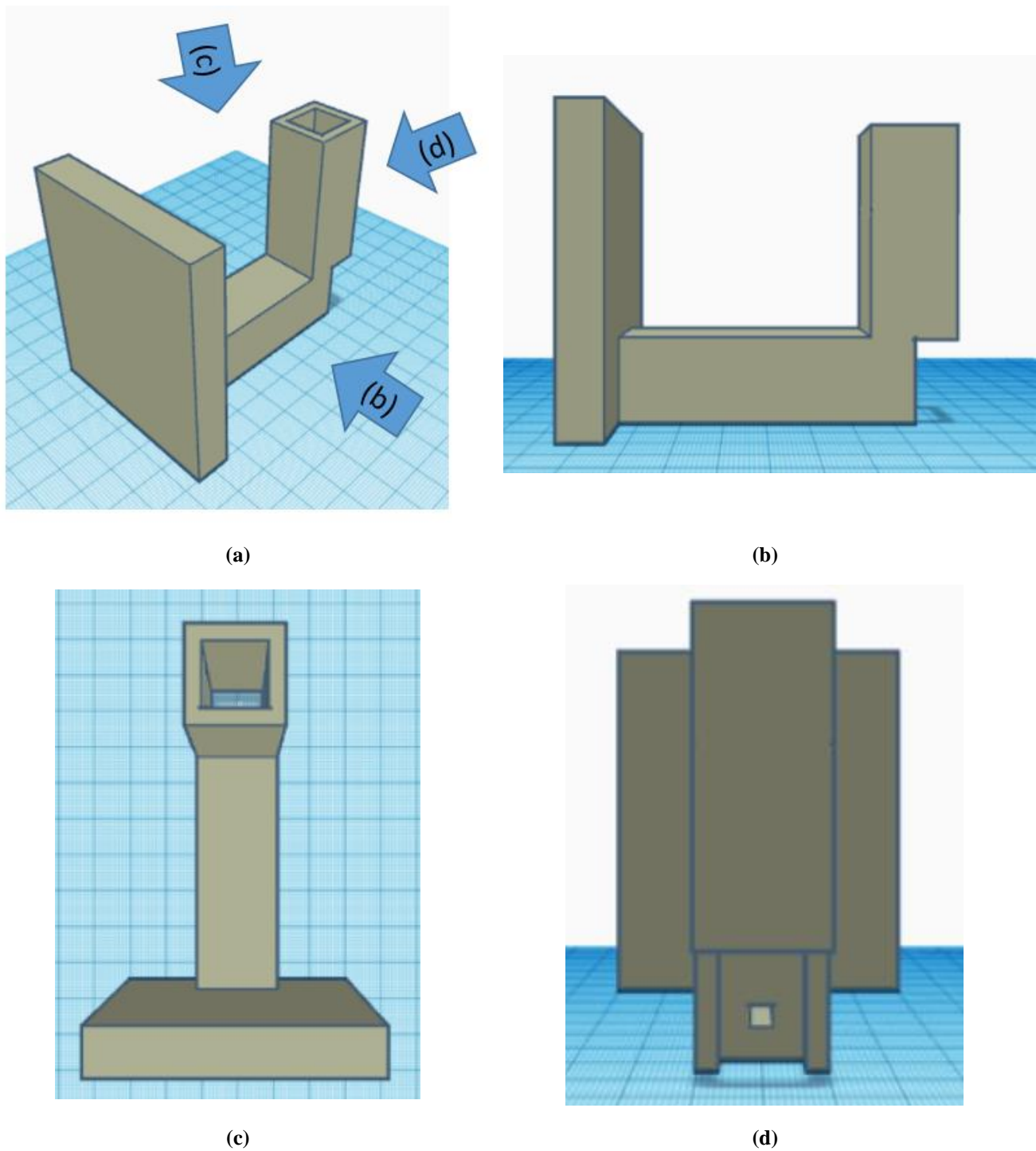


**Figure A1-3 (a) General 3D view and (b) (c) (d) different perspectives of the designed transmitter holder.**

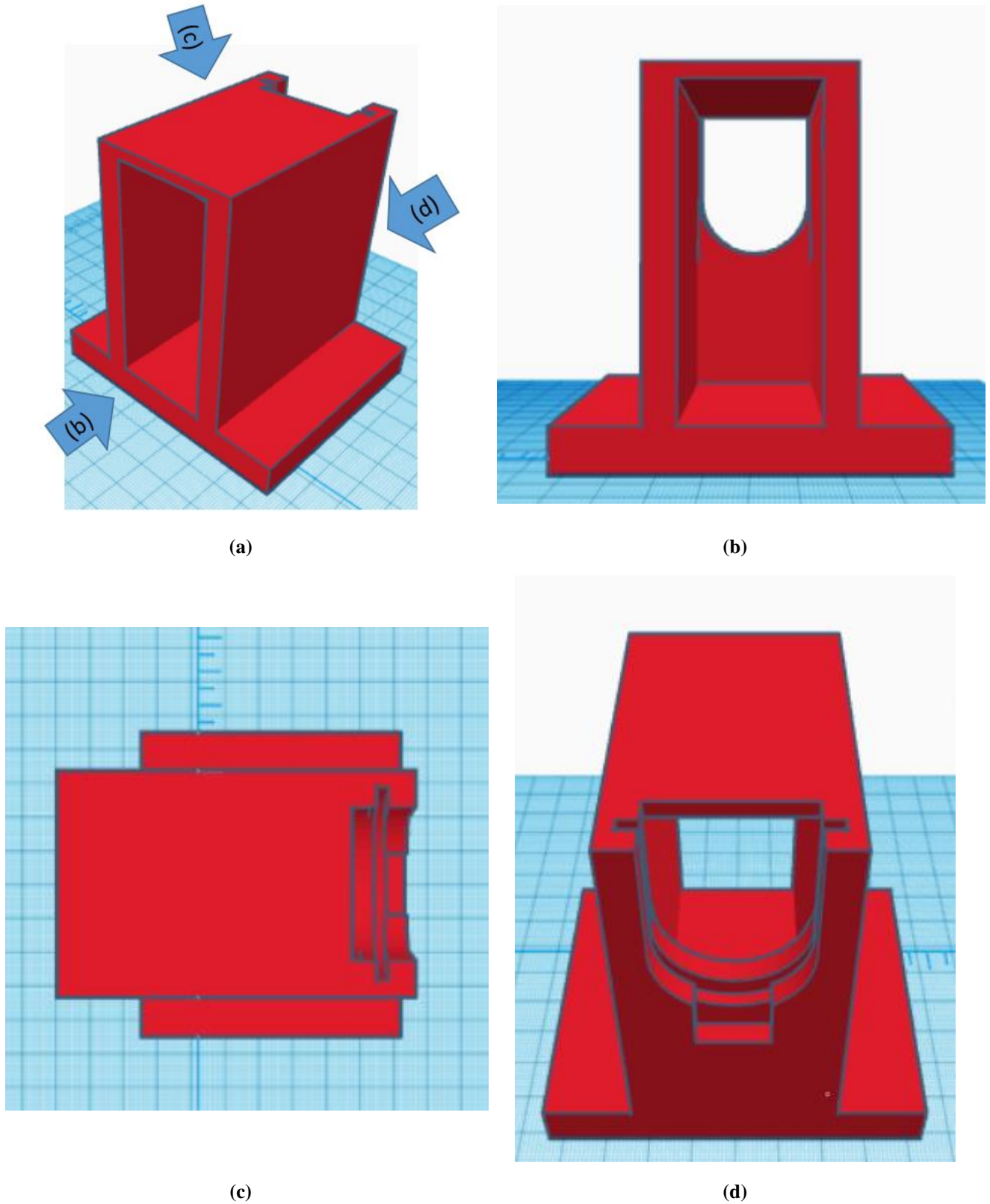


**Figure A1-4 (a) General 3D view and (b) (c) (d) different perspectives of the designed receiver holder.**